

# **Pattern formed by an evaporating Droplet on a Dissolving Substrate**

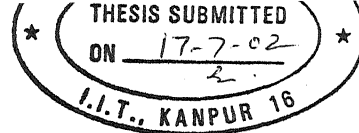
A Thesis Submitted In Partial  
Fulfillment of the Requirements  
For the Degree of  
Master of Technology

By  
**Joydeep Guha**

To the  
Department of Chemical Engineering  
**Indian Institute of Technology**  
**Kanpur**

July, 2002

# CERTIFICATE



**Certified that the work contained in this thesis entitled “ PATTERN FORMED BY AN EVAPORATING DROPLET ON A DISSOLVING SUBSTRATE” by Joydeep Guha, has been carried out under my supervision and that this work has not been submitted elsewhere for a Degree.**

**Dr. Ashutosh Sharma**

**Dept. of Chemical Engg'**

**Indian Institute of Technology**

**Kanpur (India)**

**July 2002**



9 FEB 2003 /CE

पुरुषोत्तम काशीनाथ केनकर पुस्तकालय

भारतीय प्रौद्योगिकी संस्थान कानपुर

अवाप्ति क्र० A-41800



A141800

## **Acknowledgements**

I would like to express my heartiest thanks to my thesis supervisor Dr. Ashutosh Sharma for his guidance and support throughout the progress of this work.

I take this opportunity to express my thanks to all my lab mates who stood by my side at tough times. Special thanks are due to Girdhari and Shrikant, for they are the friends in true sense. I would like to thank my Professors at IIT-K, for their cooperation in the course work.

Finally, I would like to thank my parents and sister for their love, support and encouragement. Everything I have I owe it to them.

## **Abstract**

A fluid droplet on a solid surface though appears to be a simple system for study, involves an intricate mechanism. Despite countless studies, issues about the phenomenon occurring at the contact line, defined as the line beyond which the solid is wet, continue to engage the interest of the researchers. One such phenomenon is the Contact line Pinning. The above system of drop evaporation from a substrate becomes much more complicated when the drop is evaporated on a dissolving substrate. In this work an attempt has been made to qualitatively characterize the problem of drop evaporation on a dissolving substrate. The basis of analyses of the problem is the study of the final pattern of the redistributed solute (polymer in the present case), which is formed when a drop of pure solvent evaporates from the surface of the dissolving substrate. In the study we tried to figure out the governing mechanism, which lead to the ring like pattern of the final redistributed polymer. The experimental conditions have been altered to figure out the governing mechanism. We were able to qualitatively characterize the problem under different experimental conditions. The mechanism of solute transfer to the three phase contact line in an evaporating drop presents a simple yet effective method to form microstructures.

# Contents

## List of Figures

- 1 Introduction & Literature review.....1**
  
- 2 Contact line deposit and Pattern formation in an evaporating drop.....7**
  - 2.1 General system of study.....7
  - 2.2 Contact line deposits in an evaporating drop.....9
  - 2.3 Effect of Localized Evaporation on the transfer .....24  
of solute in an evaporating drop
  - 2.4 Results and Discussions.....34
  
- 3 Pattern formed by an evaporating droplet on a Dissolving substrate.....42**
  - 3.1 System of study.....42
  - 3.2 Solute Redistribution by an evaporating droplet on a dissolving substrate.....43
  - 3.3 Study of Pendant drop evaporating from a dissolving substrate.....52
  - 3.4 Effect of Localized evaporation on the transfer of solute.....59  
when the drop evaporates from a dissolving substrate
  - 3.5 Effect of solvent on the final pattern formation of the.....66  
Redistributed polymer, when the drop of solvent  
Evaporates from the surface of dissolving substrate
  
- 4 Conclusions.....92**

# List of Figures

1.1	Schematic of drop evaporating from nondissolving substrate.	2
1.2	Schematic of drop evaporating from dissolving substrate.	3
2.2	Image of final pattern when a solution of PMMA Dries in an ambient atmosphere.	10
2.3	Image of final pattern when a solution of PMMA Dries in an atmosphere of Nitrogen.	10
2.4	Schematic illustration when the contact line is not pinned, and when the contact line is pinned.	11,12
2.5	Plot of Diameter of water drop Vs time, drying on mica surface.	13
2.6	Plot of diameter of polymer solution drop Vs time on mica and glass substrate.	14,15,16
2.7	Plot of variation height of solution drop Vs time, on mica And glass substrate.	18
2.8	Image of final pattern when drop of PMMA solution Dries in an ambient atmosphere.	19
2.9	Schematic of relevant parameters in the theory of solute transfer.	20
2.10	Diagram showing how point of departure affects the escape Of evaporating molecules.	21
2.11	Schematic of a solution drop covered with a lid at its center.	24
2.12	Image of final pattern showing the effect of localized Evaporation.	26,27,28, 29,30
2.14	Diagram showing the shape of interface after some time In the case of localized evaporation.	32
3.1	Schematic of drop evaporating from a dissolving substrate.	43
3.2	Profile of 6wt% PMMA film.	44
3.3	Image of the final pattern when a drop of toluene evaporates from a PMMA surface.	45
3.4	Enlarged view of the section of the ring in the final Pattern when a drop toluene evaporates from PMMA surface.	46
3.5	Image illustrating the stages in the development of final pattern When a drop of toluene evaporates from a PMMA surface.	47,48
3.6	Schematic diagram illustrating the forces at the contact line.	50
3.7	Schematic illustration of the pendant drop configuration.	52
3.8	Image of the final pattern when a pendant drop evaporates From PMMA surface.	53
3.9	Sectional view of the final pattern at 100x magnification When a pendant drop of toluene evaporates from PMMA film.	54

3.10	Images of the final pattern when a drop of toluene .....55 evaporates from PMMA surface, sessile and pendant drop.	55
3.11	Images of final pattern at 100x magnification when.....56 A sessile and pendant drop evaporates from the PMMA surface.	56
3.12	Resolution of forces at the contact line in the case of .....58 pendant drop.	58
3.12	Image f the final pattern formed in the lid experiment.....61,62 when a drop of toluene evaporates from a PMMA surface.	61,62
3.16	Images of the final pattern when a drop of ethyl acetate,.....69,70,71 Chloroform, toluene and dichloromethane evaporates from the surface of PMMA film.	69,70,71

# Chapter 1

## 1.1 Introduction & literature Review

A fluid droplet on a solid surface though appears to be a simple system for study, involves an intricate mechanism. Despite countless studies, issues about the phenomenon occurring at the contact line, defined as the line beyond which the solid is wet, continue to engage the interest of the researchers. One such phenomenon is the Contact line Pinning [1,2]. While looking through a window on a rainy day, one might be stuck by the fact that droplets, though on a vertical surface, nonetheless defy gravity. The reason behind this phenomenon is the Pinning of the contact line by surface irregularities such as roughness or chemical heterogeneity of the glass surface or the matter of fact any surface on which the drop is evaporating. Another such interesting phenomenon is the residue left when coffee dries on the countertop. The coffee stain is darkest along the perimeter of the stain giving it a ring like appearance. The deposition of coffee solute at the edges, knowing apriori that the coffee solute was uniformly distributed is quite surprising.

Ring like stains are not restricted to the coffee stain or the water droplet evaporating from the window pane, but is a quite general phenomenon of which some of the common place examples are mineral rings left on washed glassware, banded deposits of salt on the sidewalk during winter, and enhanced edges in water color paintings. In fact this is a general phenomenon observed whenever a liquid drop containing solutes evaporates under ambient conditions. The capacity of solute to alter the surface properties of the substrate is well known. However in ring-forming drops the problem acquires a new dimension, as the solutes is deposited at the contact line [3], where it exerts great influence on the motion of the contact line [4].

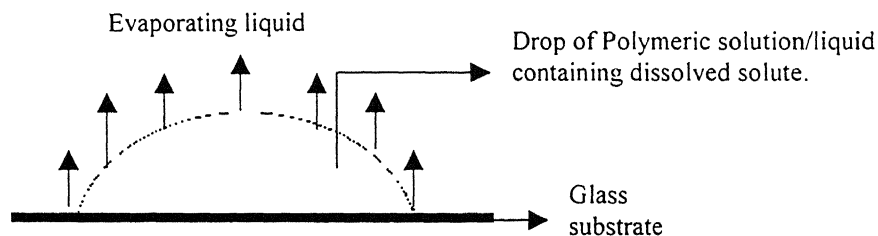


Figure 1.1 Schematics of the evaporating Drop on top of Substrate.

The ring-like patterns are formed when the contact line of the drop on the solid surface is pinned by the local roughness created by particles entrapped there. As soon as solvent loss begins solutes deposit at the three phase contact line, leading to strong anchoring. Another flow pattern in the system that leads to pattern formation is the Bénard Convection. As the drop of liquid evaporates the drops cools at the interface due to adiabatic evaporation, establishing a temperature gradient as a function of depth, as the bulk is at higher temperature. Small perturbations in the surface temperature create gradient in the surface tension. The interface contract toward the high tension regions, establishing a temperature driven Marangoni flow that pulls hot fluid from below the warm regions, reinforcing the instability [5].

The above system of drop evaporation from a substrate becomes much more complicated when the drop is evaporated on a dissolving substrate. In this type of system different competing kinetics comes into play. First being the evaporation of the fluid from the drop, Second is the dissolution kinetics of the substrate in the drop fluid, third is the temperature driven Marangoni flow that pulls the fluid from inside the bulk to the interface, fourth is the advection of the fluid from the bulk to the three phase contact line. The final pattern of the redistributed solute formed after the evaporation of the liquid is the result of the above major competing kinetics. In the present work the system of Dissolving substrate has been investigated qualitatively. Fig 1.2 shows the schematic illustration of a drop evaporating form a dissolving substrate.



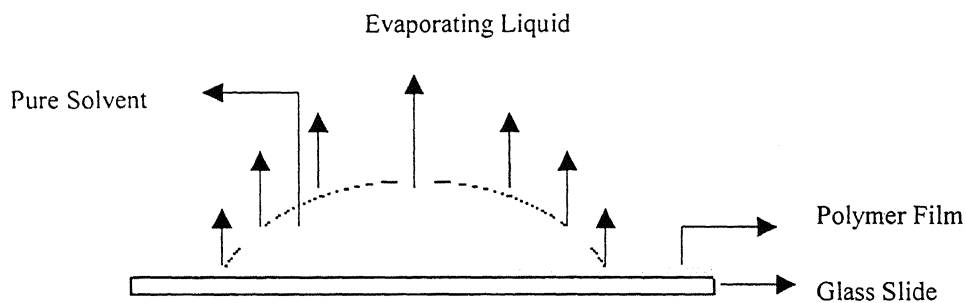


Figure 1.2. Schematics of drop on soluble Substrate.

In the case of dissolving substrate a clean glass slide is spin coated with a polymer solution to a desired thickness. The choice of thickness is governed by the fact that it should not be too small otherwise there is will be depletion of the substrate at the center when the drop dissolves the substrate, nor should it be too thick otherwise the polymer film will peel out from the glass surface. Keeping in view the above factors we have chosen the film thickness to be around 360nm for our study.

Controlling the distribution of solute during drying is vital in many industrial and scientific processes. For examples, paint manufactures use a variety of additives to ensure that the pigment is evenly dispersed and remain so during drying. Protein crystallographers are attempting to use evaporation driven convection to assemble two dimensional protein crystals. In either of these cases segregation effects are undesirable. However in the formation of nanowires [6] or patterning of surface [7] the ring effect can be of a great vantage. Understanding the ring formation process should be of interest to those trying to harness or circumvent these phenomenon. When the drop containing finely divided particles evaporates the particles act as tracers and is deposited in a well-defined macroscopic pattern. Interactions among the particles can be exploited to create local patterns. This phenomenon has been used as a means of organizing particles with dimensions ranging from nanometers to micrometer [5]. Evaporative cooling can be used to form ordered structures with dimensions that can be controlled from about 0.20 to 20  $\mu$  m [8]. Three dimensional ordered structured can be formed by evaporating solutions of a simple coiled-like polymer in a volatile solvent, in the presence of moisture with

forced airflow across the solution surface. A hexagonal array of holes form on the surface of the polymer film. When a solvent less dense than water is used, such as benzene or toluene, the hexagonal array propagates through the film. In contrast, when the solvent is denser than water, such as carbon disulfide, only a single layer of pores is formed and a 3D array is not produced. The process of solute deposition at the three phase contact line, when the solution containing the solute evaporates has been harnessed to produce pure copper line of typical thickness of  $10\mu\text{m}$  and with a resistivity of  $10\mu\Omega\text{cm}$  [9]. In the experiment a solution of copper hexanoate,  $(\text{CH}_2)_4\text{CH}_3$  with  $\text{R}=(\text{CH}_2)_4\text{CH}_3$ , in isopropanol or chloroform, was jetted onto a thin glass foil and reduced to thin metallic form by annealing. Glass capillaries of inner diameter  $100\mu\text{m}$  were used to write liquid lines. The solution viscosity and volume per unit length deposited determine the thickness, width, and number of solid lines formed from a single liquid precursor. Flow visualization studies identified Bénard- Marangoni convection as the mechanism responsible for the formation of multiple solid lines from a single liquid line. This flow pattern traps the majority of solute along the two key boundaries.

The condition under which the drop is evaporating plays a vital role in the formation of the final pattern of the redistributed solute. Very many conditions can be varied which drastically alters the final pattern of the redistributed solute. The drop can be evaporated under saturated atmosphere of the evaporating liquid, thereby reducing the rate of evaporation of the liquid from the liquid air interface. This type of alteration of the ambient condition plays an important role in the case where the substrate dissolves in the liquid drop, which is the present case of study. Further varying the temperature of the substrate alters the final pattern formation of the solute as the rate of evaporation increases, on the other hand increasing the temperature increases the rate of dissolution of the substrate in the liquid drop in case of dissolvable substrate. In this case the two kinetic processes has a competing effect. Another way of playing with the final redistributed pattern of the solute is to vary the exposure area of the drop open to ambient atmosphere (the effect of localized evaporation from the drop surface). One can also saturate the atmosphere with a liquid vapor whose density is higher than the density of the evaporating liquid drop, in this way a three dimensional array of holes can be produced on the final redistributed solute. In fact this has been done with polymeric

solutions containing polyion complex of bilayer forming surfactant evaporated in presence of water vapor [10].

## 1.2 Overview of the present work

The formation of nanostructures is an emerging field of interest and calls in the attention of researchers from diverse background. In recent years innovative stamping and printing techniques have been developed as alternatives to patterning. Polymeric films plays an emerging role in the process as because of some inherent advantage of polymers over other materials such as polymers are easy to handle, they are available in a wide variety having different characteristic properties like photoluminescence, fluorescence, electrical conductivity etc. Polymers are soluble in a variety of organic solvents, to form homogeneous solutions. These solutions can be casted in any forms only bounded by the limitations of imaginations. Polymers can be crosslinked, giving us an excellent tool to freeze the pattern.

Keeping in view the above-mentioned advantages of polymers over other materials, we have chosen polymeric films for our study. The present study involves two types of polymers Polystyrene (PS) commercial grade and Poly-methyl-methacrylate (PMMA) M.wt 1,20,000. In the present work an attempt has been made to qualitatively study the final patterns formed by an evaporating droplet on a Dissolving substrate. The Dissolving substrate is a polymeric film of PS and PMMA on a glass microslide.

In chapter 2, the pattern formed by an evaporating droplet of polymer solution on a non-dissolving substrate i.e. clean glass substrate is presented. This problem is very commonplace, to the extent that it is a direct analogy of the coffee stain problem mentioned earlier. It is a common experience that the residue left when coffee dries on the countertop is typically darkest, and hence most concentrated along the perimeter of the stain giving the deposit a ring like appearance. It seems unbelievable that such a everyday mess holds a promise to the formation of microstructures. This problem has been reported in order to figure out the basic mechanism of solute distribution as the drop of solution containing the solute evaporated. This has been treated as a base case. For the study a 6wt% solution of PMMA in HPLC grade toluene was used as a polymer solution.

Section 2.1 explains the coffee stain problem and results of an analogous experiment done with PS beads in water. This was done to bring out a plausible mechanism. Sec. 2.2 deals with the problem of drop evaporation and solute distribution using 6wt% PMMA in toluene. Sec. 2.3 delves into the problem of localized evaporation and its effect on the final distributed pattern of the solute. Sec. 2.4 is devoted to Results and discussion.

Chapter 3 deals with the problem of dissolving substrate. The problem is quite typical, as many kinetic phenomenons are in competition to produce the final redistributed pattern of the solute. Polymer films of around 360nm thick were prepared by spin coating the polymer solution on clean glass slides. Sec. 3.2 investigates the mechanism of solute transfer, which lead to the final pattern. Sec.3.3 deals with the problem of Pendant drop, and its effect on the final pattern. Sec. 3.4 looks into the effect of localized vaporization from the drop surface on the final pattern. In sec.3.5 the effect of different solvents on the final redistributed pattern is analyzed. Finally in sec 3.6 results are being discussed.

In this study an attempt has been made to characterize qualitatively the problem of pattern formation by evaporating droplet on a dissolving substrate. The mechanism of solute transfer to the three phase contact line in an evaporating drop presents a simple yet effective method to form microstructures. The method of putting the liquid is very flexible since liquid can be drawn in any shape. We think that suitable alteration and proper control of physical and environmental conditions can lead to harnessing this method effectively to create microwells, microchannels and channels of any shape.

## Chapter 2

# Contact Line deposit and pattern formation in an evaporating drop

When a liquid droplet evaporates, flow patterns develop in the liquid drop. These flow patterns are responsible for the transfer of solute in the drop of solution. A common example is the coffee stain, which is left on the countertop when the drop of coffee evaporates. When a polymer solution drop evaporates on top of a glass slide the polymer is transferred to the periphery of the drop or the three phase contact line.

This chapter basically deals with the problem of polymer solution droplet evaporating on top of a glass slide, in presence of  $N_2$ . Results are also given for solution drop drying in ambient condition. Experimental conditions are modified to characterize different dominating mechanism.

## 2.1 General system of study

The general system of study is a polymer solution drop placed on a clean glass slide. With time the solvent evaporates, leaving behind the pattern of the distributed polymer (solute). Polymer solution is 6 wt% PMMA M.wt. 1,20,000 from Aldrich chemicals (USA) in HPLC grade Toluene supplied by E. Merck (India) Ltd. Glass microslide (2.5 x 2.5 cm) is used as substrate on which drop is placed. The drop is evaporated in an atmosphere of pure  $N_2$  and ambient air. In sec. 2.6 drop is evaporated in the presence of water vapor. Figure 2.1 is presented for a clear description of the system.

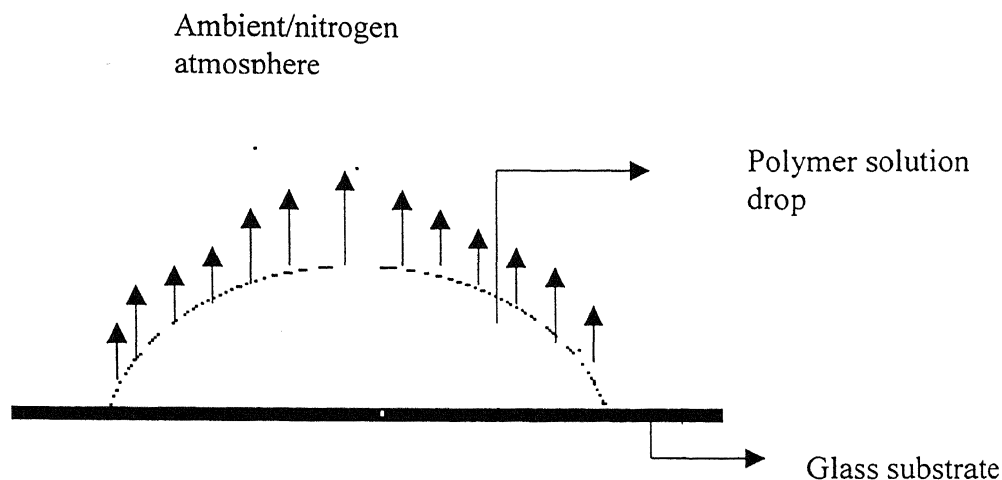


**Figure 2.1 Schematic diagram of a drop on glass slide**

The glass slides used in the experiment were prepared by the following procedure.

1. 2.5 x 2.5 cm pieces are cut out from standard 7.5 x 2.5 cm glass microslides (Bluestar).
2. In the first step, glass slides are rinsed using a glass cleaning detergent, to remove dust, grease, oil etc.
3. Then the slides are rinsed in deionized water.
4. The slides are then rinsed with acetone to remove the surfactant from the cleaning detergent.
5. The slides are then boiled in Trichloroethylene for 15 mins.
6. After that the slides are boiled in Methanol for another 15 mins.
7. Lastly slides are boiled in acetone for next 15 mins.
8. The glass slides are then sonicated in deionized water for a period of 3 mins. This step is repeated three times, and every time the deionized water is changed. This is done to remove any adhered particle.

The slides are then dried using hand held air dryer, kept in a petri dish and stored in a vacuum desiccater until further use.

The glass slides are boiled in three different solvents to remove any organic impurities present. Sonication ensures that the surface is free of any adhered dust particles, which may pin the contact line of the drop. The above cleaning procedure is found suitable for our purpose.

Following instruments has been used in the experiments and analysis.

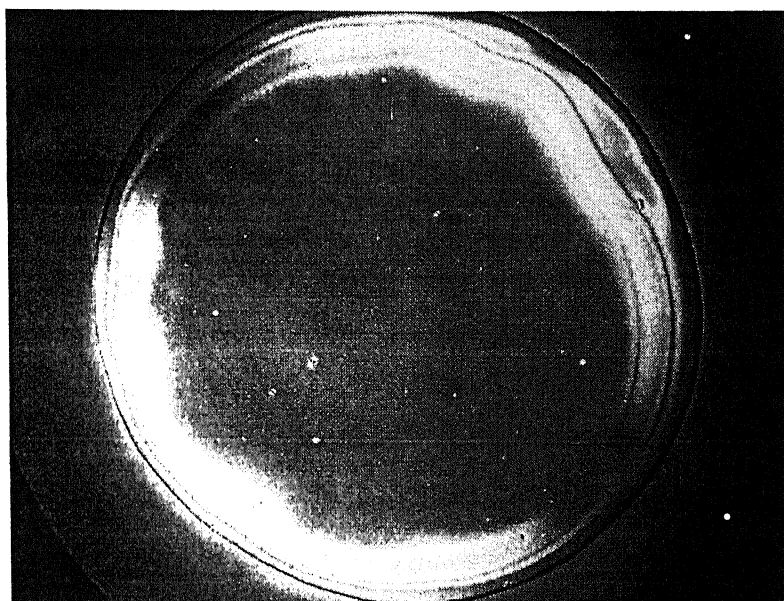
1. Optical Microscope, model No. DMLB 100S, from LEICA Microsystem, Germany.  
The microscope is equipped with both transmitted and reflected light source.
2. Digital camera, model No. COOLPIX 990, from Nikon, Japan.
3. CCD Camera model No. SDC 4304PA, from Samsung Aerospace IND. LTD.
4. Goniometer from Ramé- Hart, Inc, NJ, USA.
5. Profilometer model Alpha-step 100 (Tencor Instruments, CA,USA)

The following software has been used for image capturing and analysis.

1. LEICA Qwin standard Ver. 2.4.
2. Nikon View 3.0.
3. Adobe Photoshop Ver. 5.0LE.
4. MGI Videowave Ver.1.51, VW3013 Eval.
5. ATI Video Player.

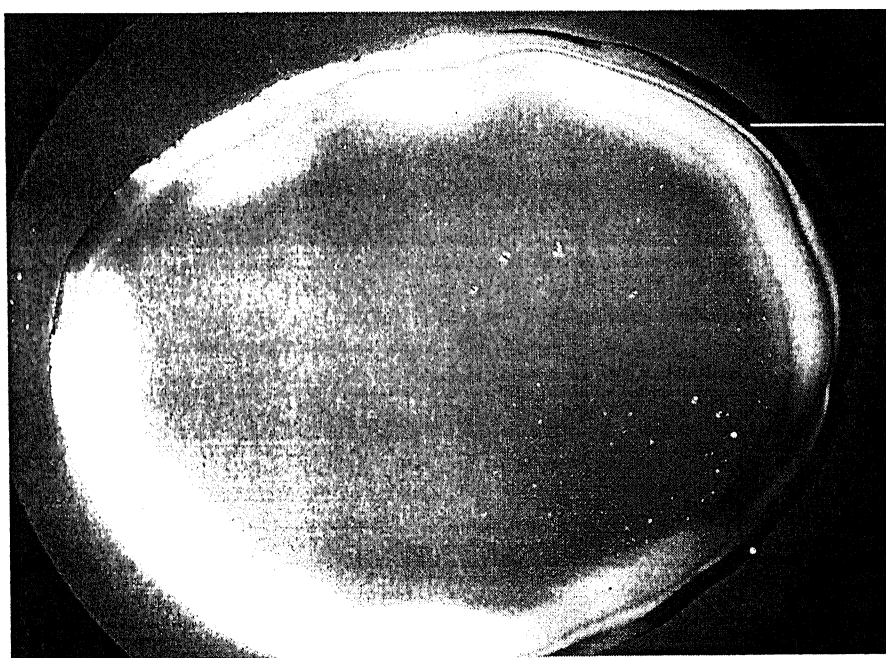
## **2.2 Contact line deposit in an evaporating drop**

When the solution drop dries on the surface of the glass slide, it is observed that the solute is transferred to the periphery or the three phase contact line of the evaporating drop. In the following chapter an attempt has been made to decipher the mechanism lying behind this phenomenon. Fig. 2.2 shows the picture of the final distributed pattern of the solute (polymer in the present case) when the solvent has evaporated from the polymer solution drop. The drop was placed on clean glass slide. The polymer solution is 6wt% PMMA in Toulene. 2 $\mu$ l of solution was placed. The drop was evaporated in an ambient atmosphere at a temperature of 27 $^{\circ}$ C .



→ Ring like deposit of polymer

**Figure 2.2** A Photograph of a dried polymer solution. Polymer solution is 6wt% PMMA in Toluene. The magnification of the picture is 50x. The drop was dried in an ambient atmosphere. Temperature was  $27^{\circ}\text{C}$ . The picture clearly shows the ring like deposit of the polymer at the periphery.



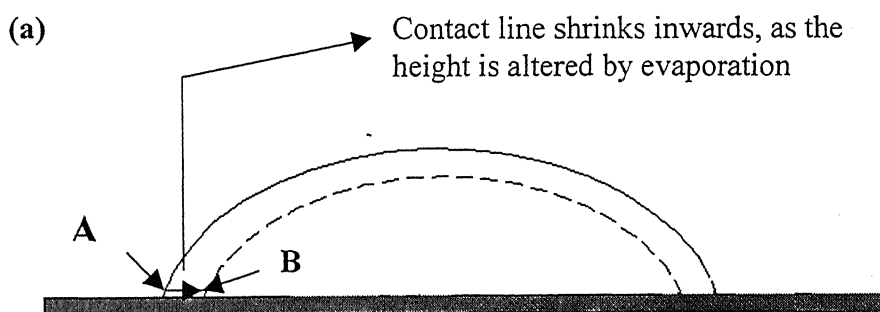
→ Ring Like deposit of Polymer

**Figure 2.3** A Photograph of a dried polymer solution. Polymer solution is 6wt% PMMA in Toluene. The magnification of the picture is 50x. The drop was dried in an atmosphere of nitrogen. Temperature was  $27^{\circ}\text{C}$ . The picture clearly shows the ring like deposit of the polymer at the periphery.

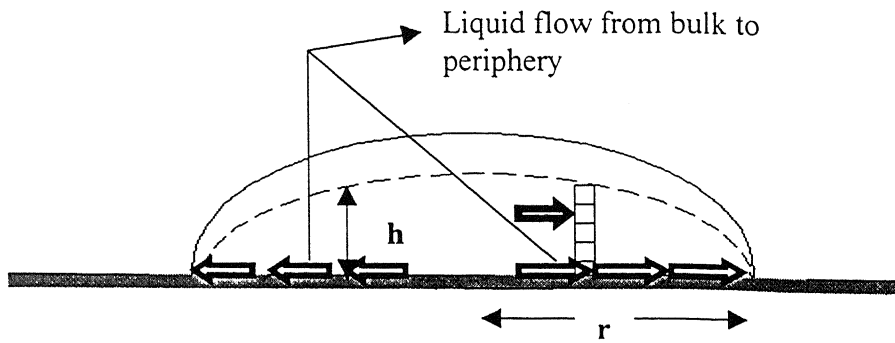


Fig. 2.2 and 2.3 shows the ring like deposit of polymer when the solution drop was dried in an ambient atmosphere and in an atmosphere of pure Nitrogen. From the above two figure it can be noticed that there is not much difference between the two, i.e. the results of the experiment done in an atmosphere of pure nitrogen is similar to that done in an ambient atmosphere.

When the liquid drop evaporates advection current set up, which drives the fluid inside the drop. The phenomenon is due to geometrical constraints. The free surface of the drop constrained by the pinned contact line, squeezes the fluid outwards to compensate for evaporative loss. This phenomenon occurs when the contact line is pinned. Fig 2.4 a) shows the schematically that when the contact line is not pinned, the contact line shrinks inwards as there is fluid loss from the drop due to evaporation. Fig. 2.4 b) illustrate the factor leading to outward flow in a small, thin, dilute, circular drop of fixed radius  $R$ , slowly drying on a solid surface.



**Figure 2.4 a) schematic illustration when the contact line is not pinned. Due to fluid loss from the drop the contact line shrinks towards the center**



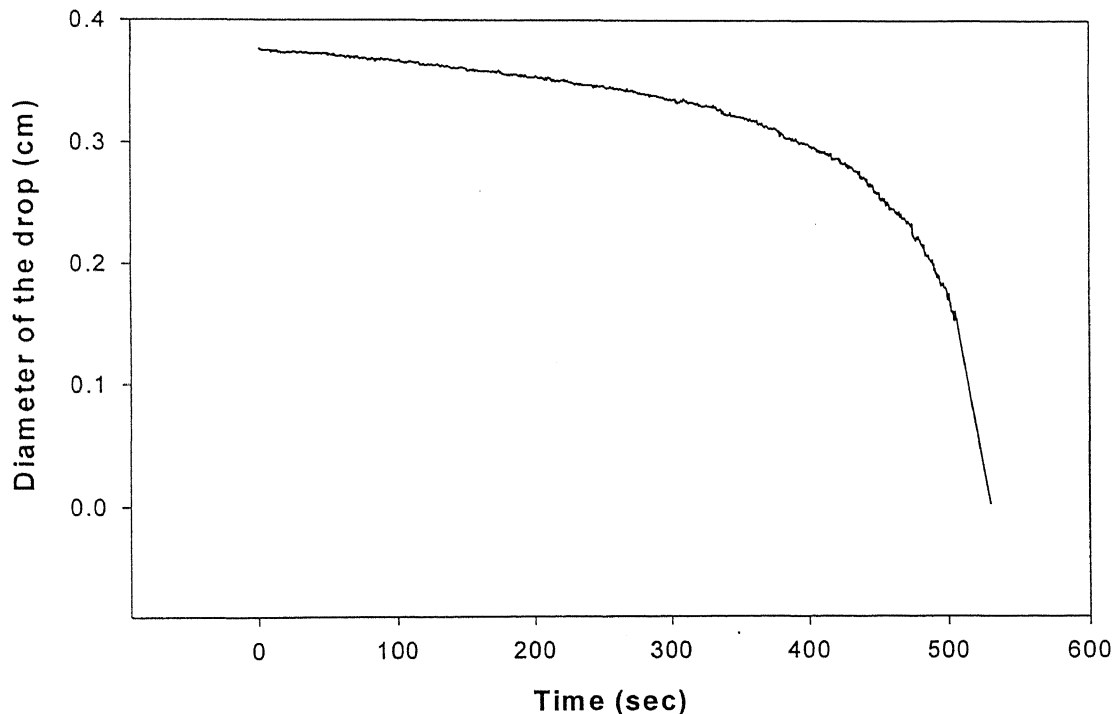
**Figure 2.4 b) schematic illustration of the origin of advection current. Shows the actual motion of the interface, when contact line is pinned.**

The physical idea behind the theory is that a pinned contact line induces an outward, radial flow when there is evaporation from the drop. This is graphically shown in Fig. 2.4(b). The solid line of Fig. 2.4(a) represents the initial position of the air-liquid interface. If the evaporation is spatially uniform and the contact line is not pinned, during some interval of time there will be liquid loss through evaporation and the interface would evolve from the solid line to the dashed line, and the contact line would move from **A** to **B**. However, if the contact line is pinned then there must be a flow that replenishes the liquid that is removed from the edge. The evaporation would alter the height  $h$  of the profile. At the perimeter, all the liquid would be removed and the drop would shrink. But the radius of the drop cannot shrink, as the contact line is pinned. The interface would evolve as shown in Fig. 2.4(b) from the solid line to dashed line. The height profile must maintain the spherical cap as the elasticity of air liquid interface, i.e., the tendency of the interface to minimize its surface area, dictated by surface tension provides the force driving the outward flow of fluid [3]. Thus during the short time  $\Delta t$ , the region shown with horizontal stripes Fig. 2.4(b) must be removed from each point  $r$  of the surface. This is different from the amount removed from that point owing to evaporation. Therefore radial flow must make up for this difference [11].

In the initial phase some preexisting conditions on the substrate anchors the contact line, this permits the ring to start growing and the suspension deposit onto the substrate, near the three phase contact line. The additional growth increases the energy

barrier the contact line must surmount before moving. The phenomenon can very well be described by the term “self pinning”.

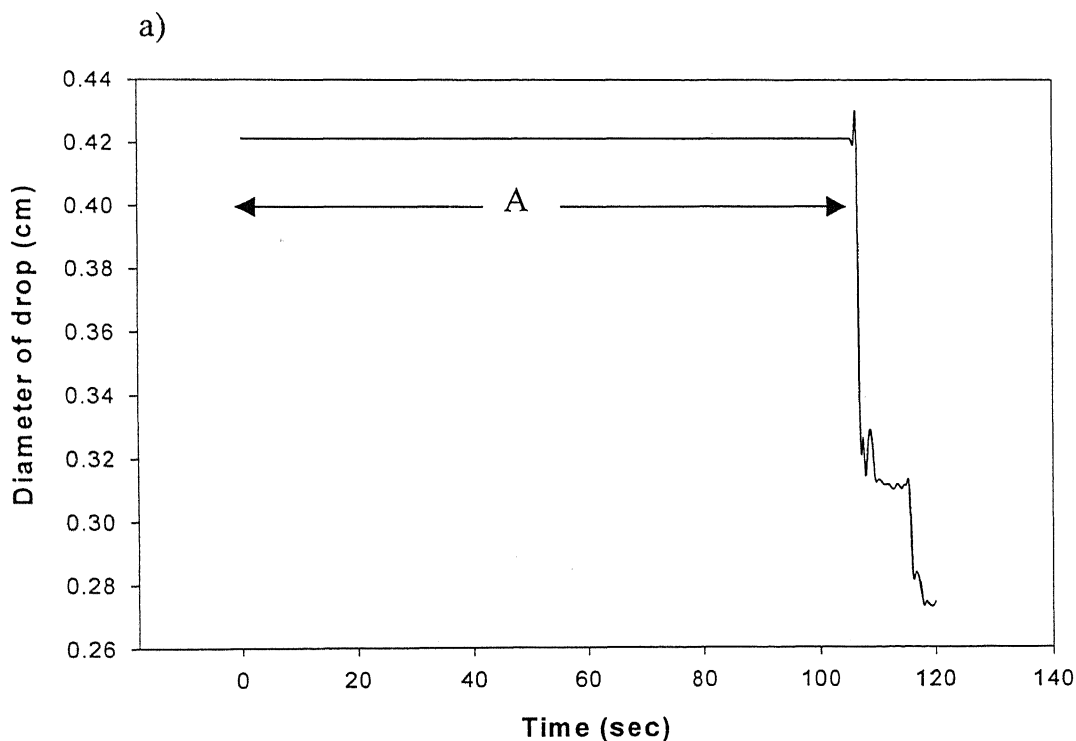
In order to check the hypothesis of self-pinning the effects of solute pinning by heterogeneity of the substrate has been isolated by using a smooth homogeneous substrate. Freshly cleaved mica has been used as a homogeneous substrate. Smoothness of mica substrate is verified by a simple experiment. Theoretically if the substrate is free of any physical heterogeneity i.e. pinning site, then the drop of water placed on the substrate will shrink from initial diameter to practically zero diameter as the drop evaporates. This happens due to the mechanism explained previously through Fig. 2.4(a). A drop of HPLC grade water with an initial volume of  $3\mu\text{l}$  was placed on the mica substrate, and its diameter Vs time is recorded, using a Goniometer. The datas are plotted in Fig 2.5. From the initial diameter of 0.37661cm the diameter shrank continuously to zero diameter.



**Figure 2.5 Plot of diameter of a water drop (cm) drying on mica substrate Vs time. Volume of the drop is  $3\mu\text{l}$ .**

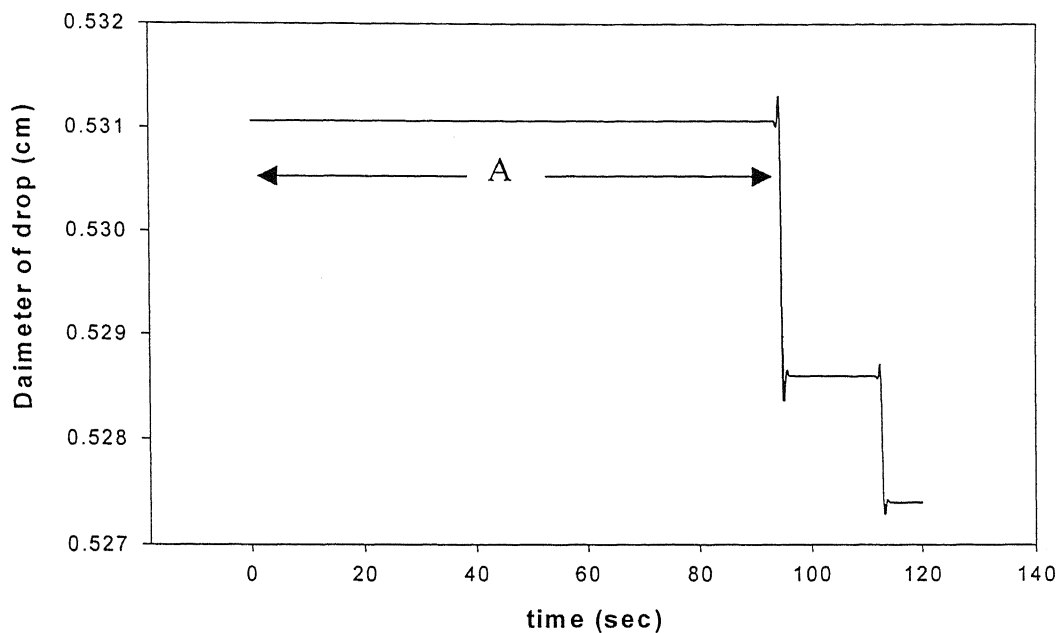
The smoothness of the data is a measure of the smoothness of the substrate.

To validate the claim that self-pinning is responsible for the formation of the ring structure, experiment was done in which drop of polymer solution was placed on the glass and mica substrate. If the contact line is pinned then with evaporation from the drop surface the diameter of drop should practically remain constant and the height should decrease. Data of the radius and height of drop with respect to time is plotted. The drops in the experiment was prepared from 5wt% PS in HPLC grade Toluene and 6wt% PMMA (M.Wt 1,20,000) in HPLC grade Toluene. 5 $\mu$ l of drop was placed on the substrate. Micro-syringe (10 $\mu$ l vol.) was used to form the drops on the substrate. Fig. 2.6 shows the plot of diameter of the drop with respect to time for different polymer and substrate combinations.



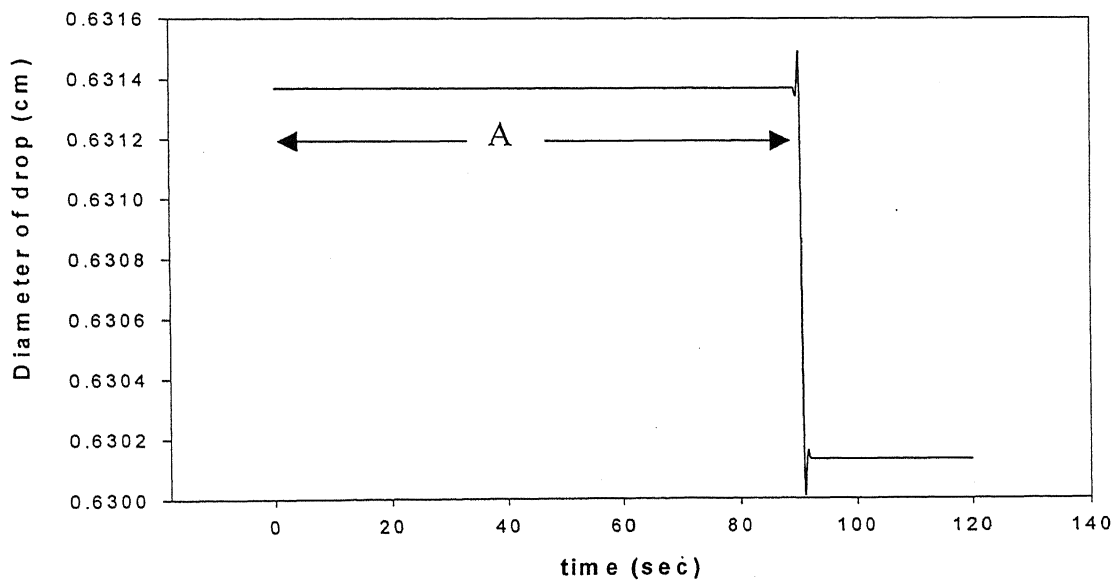
**Figure 2.6 (a) Plot of Diameter of drop Vs time, for 5wt% PS solution in toluene dried on mica**

b)

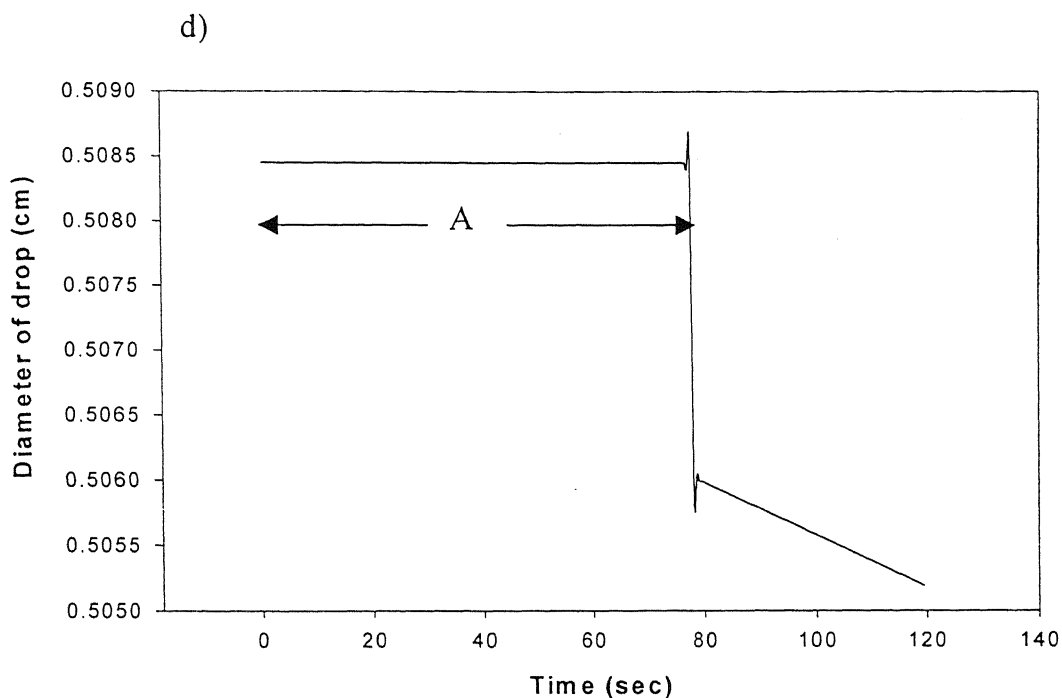


**Figure 2.6(b) Plot of Diameter of drop Vs time, for 5wt% PS in toluene on glass**

c)



**Figure 2.6(c) Plot of Diameter of drop Vs time, for 6wt% PMMA in toluene on mica**



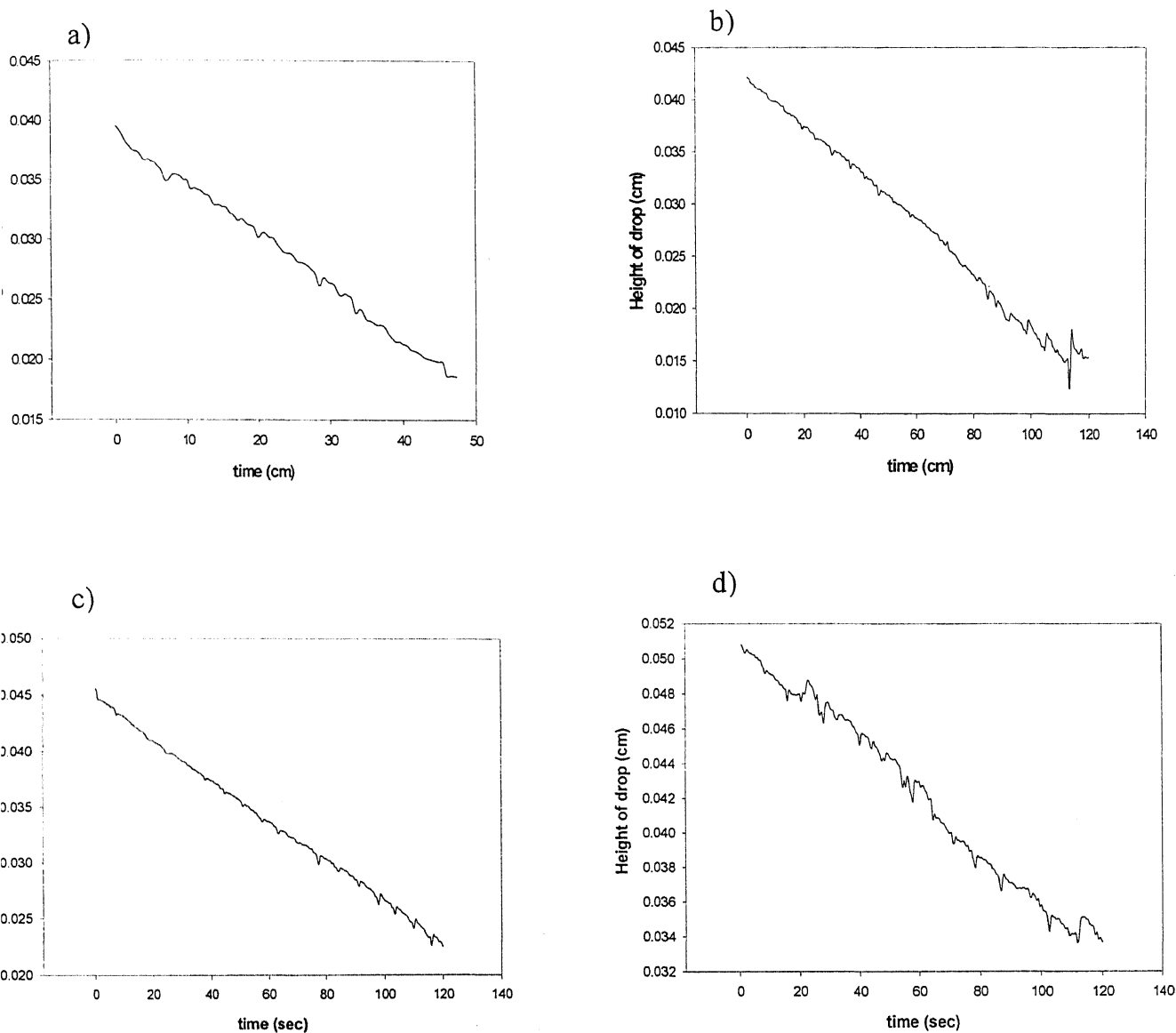
**Figure 2.6(d) Plot of Diameter of drop Vs time, for 6wt%PMMA in toluene on glass**

Fig. 2.6 (a) – (d) shows the plot of diameter of the drop Vs time for two-polymer system PS and PMMA on two different substrate Glass and mica. Drop volume was  $5\mu\text{l}$ . In the above plot i.e. Fig 2.6 (a) –(d) the region A indicates that the Diameter of the drop is constant for the drying period of approximately 100secs. This directly gives the evidence of contact line pinning, because when the contact line is pinned the diameter of the drop cannot change. The contact line pinning is due to the anchoring of the contact line by the initial deposit of the suspension. This can be inferred from the fact that in case of atomically smooth mica the diameter of the drying drop remains constant with time, which indicates the pinning of contact line. We can state this because referring to Fig 2.5, where a drop of pure water evaporates from the mica surface the diameter of the drop continuously shrank to zero with time ( indicating the smoothness of mica surface).

This is the time scale within which most of the solute is deposited at the contact line. The sudden fall of Diameter to a low value is due to the measurement technique of the Goniometer. The Goniometer measures the dimensions of the drop from the

silhouette of the drop as captured by the CCD camera. Initially the camera captures the width of the drop with the pinned contact line, which is constant for some time, but with evaporation the height of the drop decreases and the silhouette of the drop changes. Now in the latter phase of drying when most of the solute has been transferred to the contact line, very small amount of liquid remains inside the drop. The camera could not capture this change of drop dimension as a continuous function in the case when solute deposition is involved. Therefore this discrepancy in the diameter of the drop creeps in. This discrepancy is not noticed when a drop of deionized water evaporates on mica surface Fig 2.5. But we can very safely neglect this discrepancy as most of the solute is transferred to the contact line in the time scale of around 100secs, and within this time frame the diameter of the drop is constant.

As per the mechanism of self-pinning, since the contact line is pinned the evaporation of the liquid reduces the height of the drop profile. We have measured this reduction in the height of the drop profile with time. Figure 2.7 shows these plots of drop height Vs time. Results are presented for PS and PMMA solution drops on mica and glass substrate. These results confirm the mechanism of contact line pinning. Nadkarni and Garoff [12] showed that a single microsphere attached to the surface can pin the contact line. The same process occurs in our case but at a much stronger level, the suspension of polymer jam into the wedge of fluid next to the contact line, preventing the contact line from retracting. A ring is formed during this initial pinned stage. Figure 2.7 shows these plots of drop height Vs time.



**Figure 2.7 Plot of Height of drop profiles Vs time. Drop volume was 5 $\mu$ l. The plot shows the decrease of height of drop profile with evaporation, confirming the mechanism of contact line pinning. (a) 5wt% PS on glass, (b) 5wt% PS on mica, (c) 6wt % PMMA on glass,, (d) 6wt% PMMA on mica**



## 2.2.1 Theory of Solute transfer

The discussion presented in this section is taken from reference [3,11], and it has been included in this work for the sake of explaining the mechanism of solute transfer. The system of study considered in the reference was colloidal 10 $\mu$ m polystyrene microspheres and with solute volume fractions ranging from  $10^{-6}$  to  $10^{-1}$ . The substrate used was glass, mica etc. In our experiments we have used 5wt% of PS in Toluene and 6wt% of PMMA in Toluene. We have used Glass and cleaved mica as our substrate. The results that we got are very similar to the one that has been cited in reference [3,11]. The similarity of the results indicates that ring like deposit form when drop of solution containing solute evaporates. The solute may be microspheres of polymer forming colloidal solution [3,11], or the polymer itself dissolved in the solvent to form a homogeneous polymeric solution, as has been considered in our case. Fig 2.8 shows the result of our experiments.

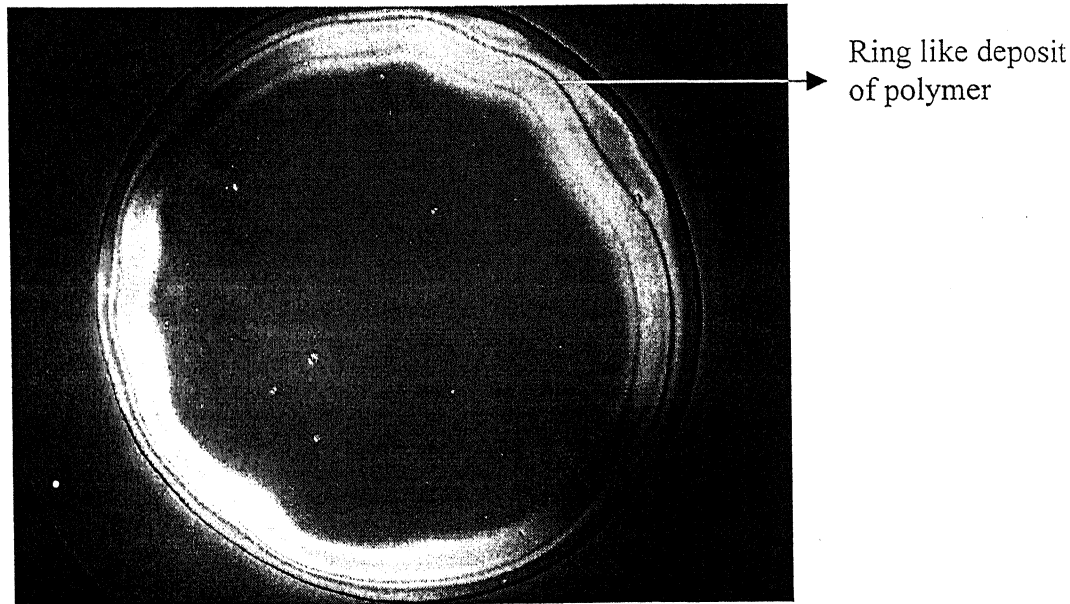


**Figure 2.8** A Photograph of a dried polymer solution. Polymer solution is 6wt% PS in Toluene. The magnification of the picture is 50x. The drop was dried in an ambient atmosphere. Temperature was 27°C. The picture clearly shows the ring like deposit of the polymer at the periphery.

As has been discussed and experimentally proved in sec 2.2, that when a drop of solution evaporates the contact line is pinned. To explain the mechanism of solute transfer the above ideas has been mathematically developed for the case of an axisymmetric drop. . Fig. 2.9 illustrates , the parameters fo rthe theory.

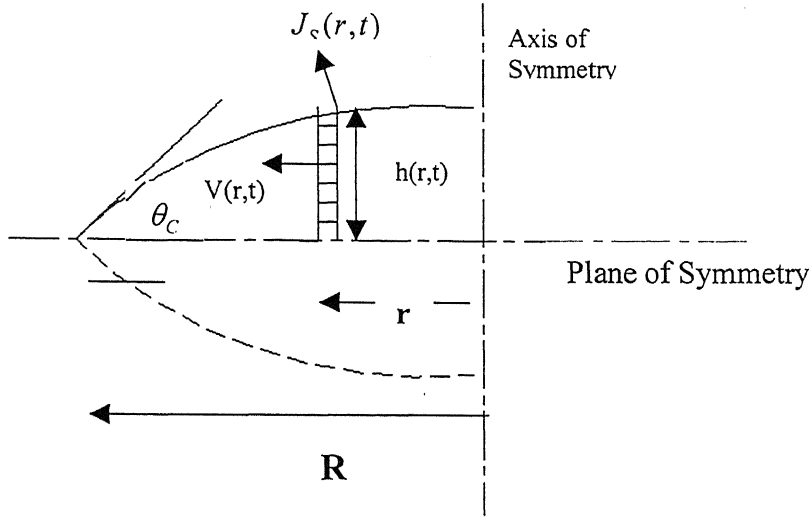


**Figure 2.9 Schematic of relevant parameters for the theory. The contact line is defined as the intersection of the interface with the dashed line denoted as “plane of symmetry”. In experiment the substrate would define the plane of symmetry.  $J(r,t)$  is the evaporation flux.  $V(r,t)$  is the radial velocity of fluid.**

The conservation of fluid determines the relationship between the vertically averaged radial flow of fluid,  $v(r,t)$ , the position of the air-liquid interface,  $h$ , and the rate of mass loss per unit surface area per unit time from the drop by evaporation,  $J_s$ . The rate of change of the amount of fluid in an infinitesimal annular element at a radial distance  $r$  from the center of the drop is equal to the net flux of liquid into the column minus the amount of mass evaporated from the surface of that element. In terms of equations we can write

$$\rho \frac{\partial h}{\partial t} = -\rho \frac{1}{r} \frac{\partial}{\partial r} (r h v) - J_s(r,t) \sqrt{1 + \left(\frac{\partial h}{\partial r}\right)^2} \quad (1)$$

where  $t$  is time and  $\rho$  is the density of the liquid. The above equation is written from the principle of conservation of mass. The above equation can be solved for  $v$  by writing the equation in integral form

$$v(r,t) = -\frac{1}{\rho r h} \int_0^r dr \left( J_s(r,t) \sqrt{1 + \left( \frac{\partial h}{\partial r} \right)^2} + \rho \frac{\partial h}{\partial t} \right) \quad (2)$$

from the above equation it is clear that a nonzero  $v$  arises when there is a mismatch between the local evaporation rate and the rate of change of the interface. From the above equation  $v$  can be calculated knowing  $h(r,t)$ , and  $J$ .

$J_s$ , The evaporative flux from the drop surface depend on whether the rate-limiting step is the transfer rate across the liquid-vapor interface or is the diffusive relaxation of the saturated vapor layer immediately above the drop. In the former case  $J_s$  is constant, while in the latter case,  $J_s$  is strongly enhanced toward the edge of the drop. For the case where the limiting rate is the diffusion of the liquid vapor, the evaporation of the drop rapidly attains a steady state.

The increase of evaporation flux  $J_s$  at the edge is attributed to the greater probability of molecule's escape when leaving from the edge than when leaving from the center of the drop. The statement is explained with the help of a figure, refer Fig 2.10.

A random walk initiated at the center of the drop results in the molecule being reabsorbed

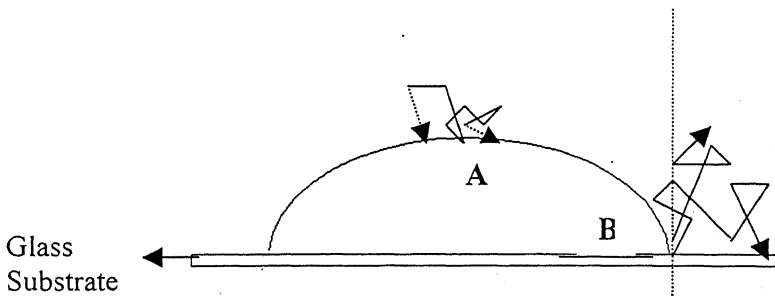


**Figure 2.10 shows how its point of departure affects the probability of escape of an evaporating molecule.**

on the surface of the drop, and there is no escape of the molecule as shown at point A, the reason behind this lies in the fact that when the molecule escapes from the central region of the drop, it experiences the proximity of the same liquid molecules all around it, which has a tendency to attract the escaping molecule, and the escaping molecule falls back into the pool of liquid. On the other hand, when the molecule escapes from the edge, there is much free space available, because the liquid pool is on one side of the vertical line shown by the dashed line. Moreover if the escaped molecule is adsorbed on the substrate, then also the molecule frees itself from the bulk liquid, and there is no chance of returning back to the liquid pool.

The change in volume of the drop must be exactly equal to the evaporation rate. Therefore

$$\frac{dM}{dt} = \rho \frac{d}{dt} \int_0^R dr' 2\pi r' h(r', t) \quad (3)$$

Earlier it was assumed steady state, but  $J_s(r, t)$  is time dependant because of its dependence on the contact angle, which changes during the course of evaporation.

Given the velocity of the fluid inside the drop, the growth of ring can be computed. Assuming constant initial distribution of the solute everywhere in the drop at time  $t=0$ , the time it would take for a packet of fluid to reach the contact line having started at some initial radial distance  $r_0$ , is calculated. Within this time all the solute that lay beyond  $r_0$  becomes part of the ring, therefor the mass of solute in the ring  $m_R(t)$  is

$$m_R(t(r_0)) = 2\pi c_0 \int_{r_0}^R dr' r' h(r', t=0) \quad (4)$$

where  $c_0$  is the mass of solute per unit volume of solution and  $t(r_0)$  is the time it takes to go from  $r=r_0$  at time  $t=0$  to  $r=R$  and can be calculated by integrating  $\frac{dr}{dt} = v(r, t)$  with

the initial condition that  $r(0) = r_0$ . In the treatment vertically averaged velocity is used which implicitly assumes no vertical segregation of solute.

Now the distribution of solute, for which it is assumed that  $c(r)$  is function solely of radius ( $r$ ) (i.e. at a given radial distance the concentration is uniform throughout the liquid column), thus the conservation of solute leads to

$$\frac{\partial}{\partial t}(ch) + \frac{1}{r} \frac{\partial}{\partial r}(rchv) = 0 \quad (5)$$

where  $c$  is assumed to be independent of  $z$ , the vertical distance from the substrate, and diffusion of solute is neglected. The mass in the ring can also be calculated from the difference of the mass of the solute in the drop at  $t = 0$  and the mass of the solute left at a later time.

But in case of dissolving substrate the problem takes a new dimension. In that case the substrate dissolves in the drop with time, and we have to include the vertical segregation of the solute in the drop.

Initially the ring grows as a power law with time. Considering a particle at a distance  $R-r$  from the edge. All the particles that are at equal or lesser distance from the contact line will be swept into the ring by the time the particle reaches the edge so that the ring will increase in mass by  $m_R \sim (R-r)^2$ . Therefore, at early times the ring grows in time as a power law

$$m_R \sim t^{2/(1+\lambda)} \quad (6)$$

The result for the thin drop limit is [3]

$$m_R = m_0 [1 - (1 - t/t_f)^{(1+\lambda)/2}]^{2/(1+\lambda)} \quad (7)$$

where  $m_0$  is the total mass of solute present initially in the drop

## 2.3 Effect of localized evaporation on the transfer of solute in an evaporating drop

In the previous section we discussed the mechanism of solute transfer in an evaporating drop. It was stated on the basis of probabilistic approach, that the rate of evaporation is higher at the edge of the drop than at the center of the drop, and this spatial variation in the rate of evaporation from the surface of the drop is responsible for solute transfer. In this section we check the above-mentioned hypothesis by controlling the exposed surface area of the drop to the atmosphere. The spatial variation in the rate of evaporation on the surface of the drop sets in advection current inside the drop, which drives the solute to the periphery. The main purpose of the experiment is to study the effect controlling the area of evaporation from the drop surface, and to see its effect on the solute transfer based on the final distributed pattern of the solute (polymer in our case).

### 2.3.1 System of study

The system of study comprises of a clean glass slide covered with a covering lid, with a hole in the center of the lid. The diameter of the hole of the covering lid is kept small as compared to the diameter of the drop. Fig 2.11 explains the schematic diagram.

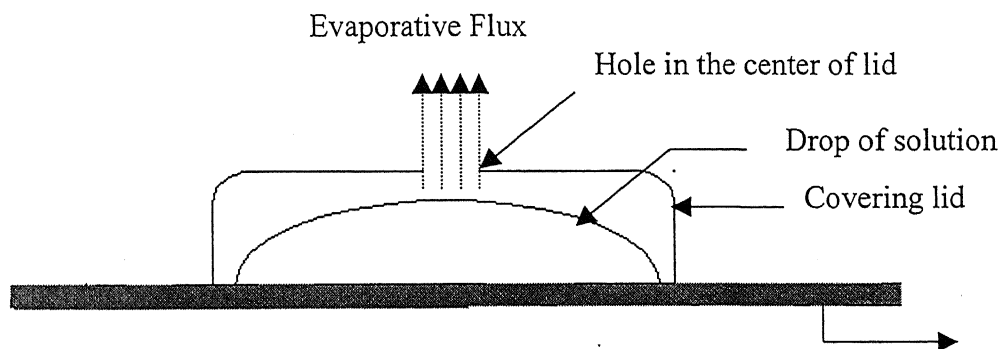


**Figure 2.11 Schematic illustration of a solution drop covered with a lid, having hole at its center. The Diameter of the hole in the lid is small compared to the drop diameter in order to restrict the exposed area of the drop surface.**

Fig 2.11 illustrates the setup of the study. The setup is designed to restrict the evaporative flux to the center of the drop. The drop diameter is intentionally kept small as compared to the diameter of the hole in order to restrict the surface area of evaporation. In the study we have used eight different lids with varying hole diameter at its center. We have varied the hole diameter from 0.5mm to 10mm. The lids are made of hard plastic caps with external diameter 18mm, internal diameter 14mm and height of 3mm. The volume of the drop is 2 $\mu$ l and the diameter of the drop is around 3.4mm.

## 2.3.2 Mechanism involved in Localized Evaporation

In the experiment of Localized evaporation our aim was to see the effect on distributed solute pattern by controlling the area of evaporation from the surface of the drop. This experiment also gives some insight into the original mechanism of solute transfer when the drop is open from all sides. In this experiment the sides are covered with lid, thus restricting the free evaporation from all sides of the drop restricting it mostly to the top portion of the drop.

Fig 2.11 shows that when the drop is covered with lid with a hole at its center, then the evaporation mainly takes place from the center. The evaporative flux  $J_s$  is maximum at the center, and at the edges the evaporation is restricted. We say so because the drop diameter is around 3.4mm and the diameter of the hole on the lid is 0.5mm. Thus the direction of evaporation is concentrated to the center. Theoretically if we increase the hole diameter of the lid, then evaporation takes place also from the edges of the drop, and if we have hole diameter comparable to the diameter of the drop then we should get back the ring pattern in our initial experiments. To verify this we did the experiments with lids having varying (increasing) hole diameter. In the experiments care was taken that the holes are exactly at the center of the lid, which in turn is placed symmetrically on top of the drop, i.e. the hole is exactly at the center of the drop. In our experiments we got the results as has been predicted. We used fixed volume of drop i.e. 2 $\mu$ l, with the drop diameter 3.4mm. The hole diameter of the lid is varied from 0.5, 1.0, 2.0, 3.0, 4.0, 6.0, 8.0, 10.0 mm. In the first case the hole in the lid is very small as compared to the drop,

and in the final cases the hole is large compared to the drop, replicating the ambient condition. As we move from small hole diameter of the lid to the large diameter we got the ring pattern of the solute. Fig 2.12 shows the final pattern of the solute for different hole diameter of the lid. Gray scale profile plots are also presented which confirm the uniformity of the pattern of the distributed solute (polymer).

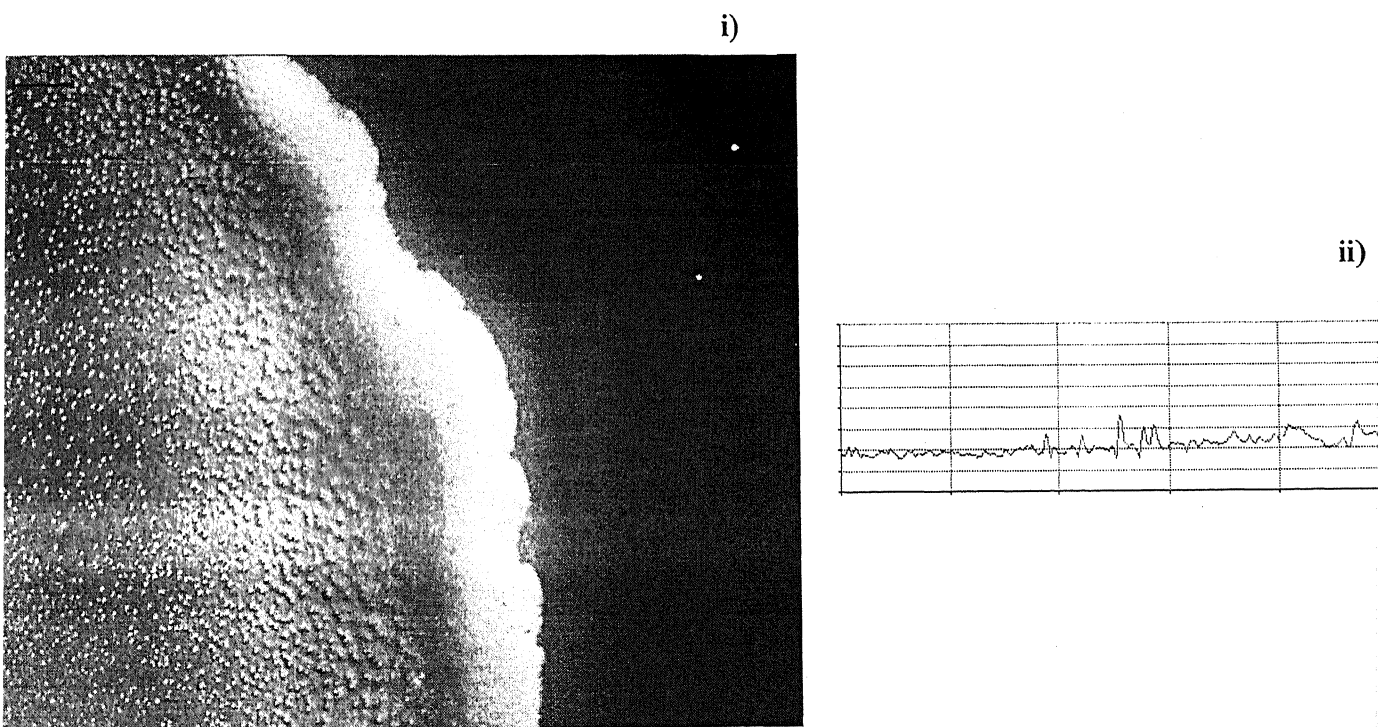
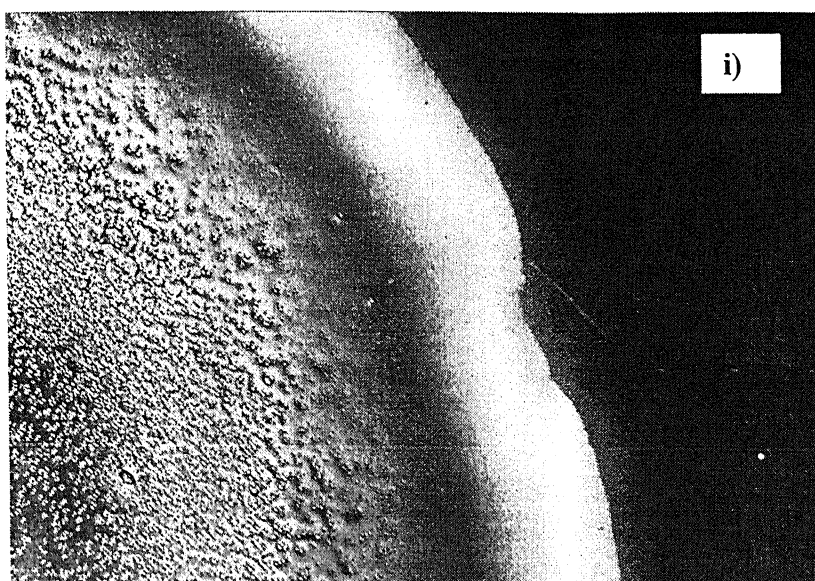


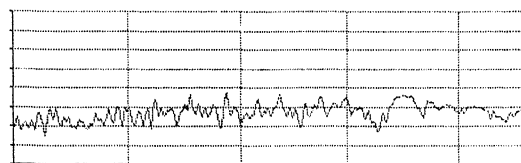
**Figure 2.11a) Digital picture of drop covered with lid with a hole at its center. Drop volume 2 $\mu$ l, drop diameter 3.4mm, temperature of evaporation 27°C. The hole diameter of the lid is 0.5mm. i) Shows the picture, ii) shows the profile plot. The profile plot is the red level of the picture. From the profile it can be inferred that the solute distribution is quite uniform. The picture covers the periphery and the inside of the drop area.**



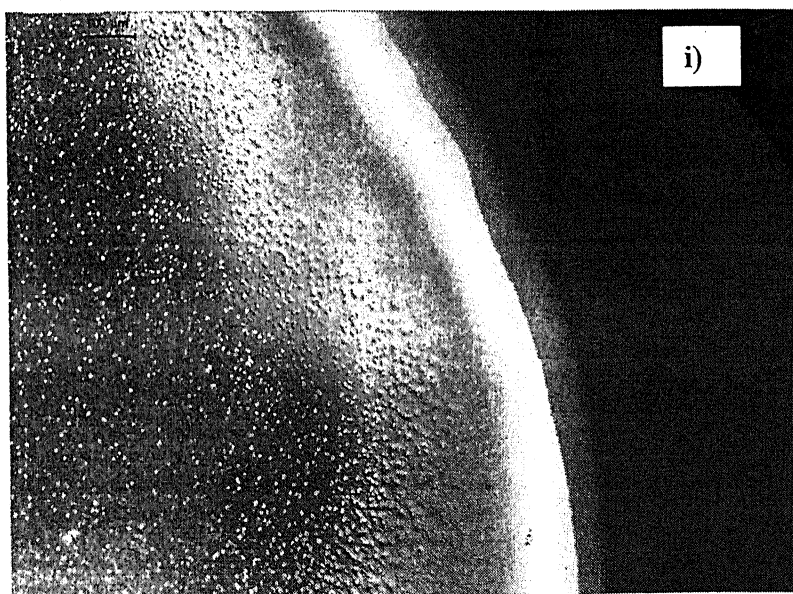
b)



ii)



c)



ii)

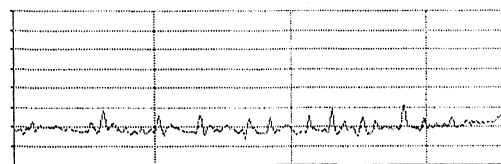
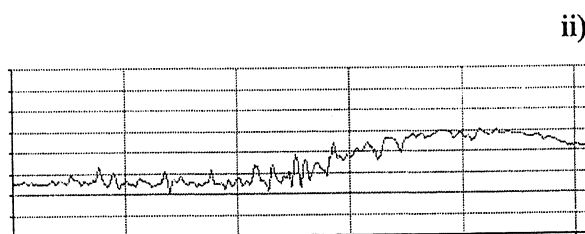
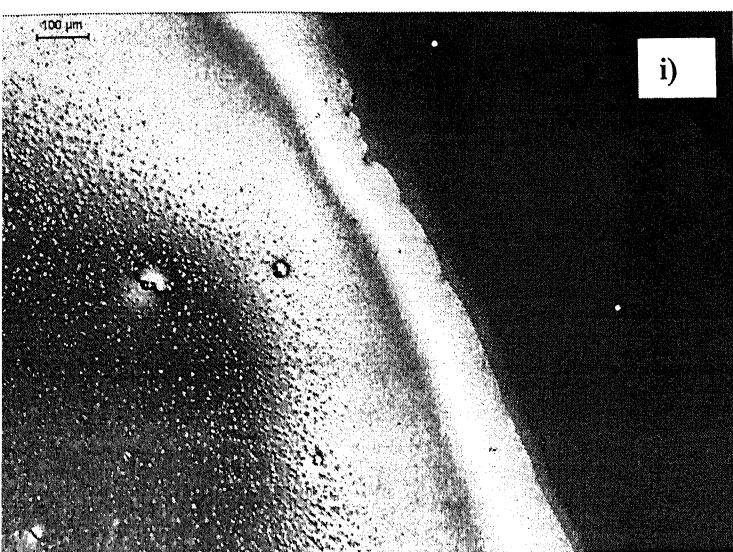


Figure 2.11 b) and c), Digital picture of drop covered with lid with a hole at its center. Drop volume  $2\mu\text{l}$ , drop diameter  $3.4\text{mm}$ , temperature of evaporation  $27^\circ\text{C}$ . The hole diameter of the lid is  $1\text{mm}$  and  $2\text{mm}$  respectively. i) Shows the picture, ii) shows the profile plot. The profile plot is the gray level of the picture.

d)



e)

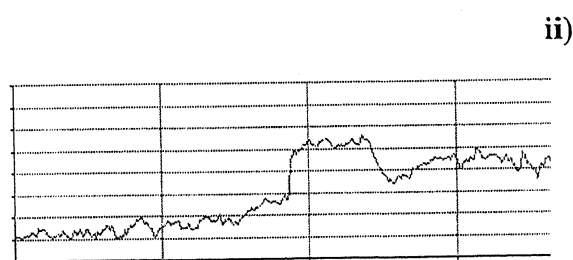
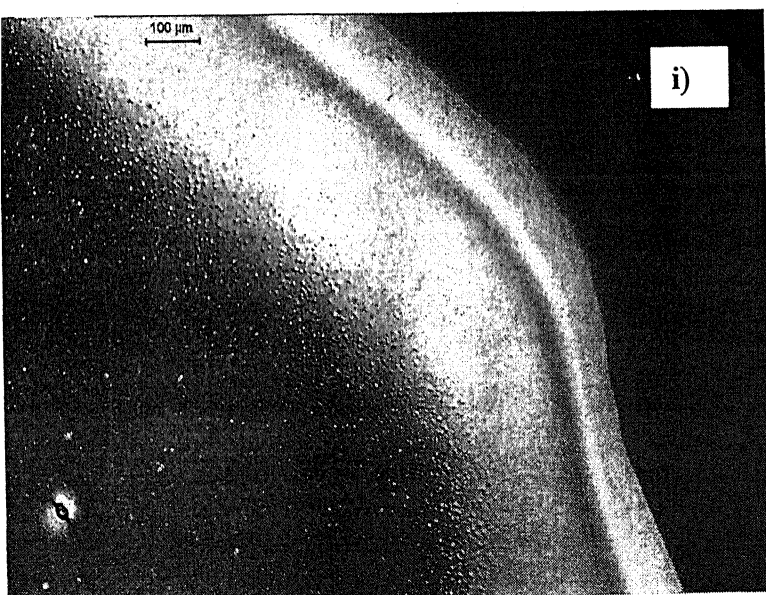
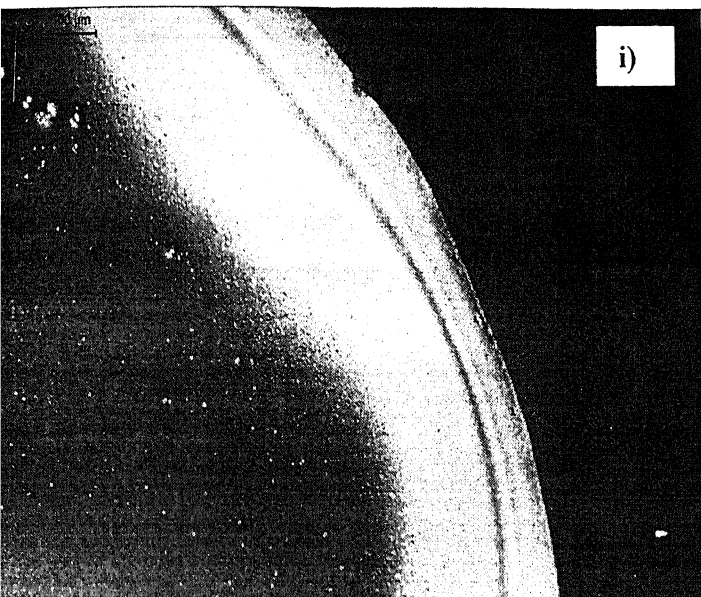
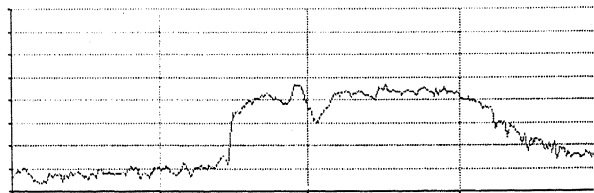


Figure 2.11d) and e), Digital picture of drop covered with lid with a hole at its center. Drop volume  $2\mu\text{l}$ , drop diameter  $3.4\text{mm}$ , temperature of evaporation  $27^\circ\text{C}$ . The hole diameter of the lid is  $3\text{mm}$  and  $4\text{mm}$ . Respectively. i) Shows the picture, ii) shows the profile plot. The profile plot is the gray level of the picture.

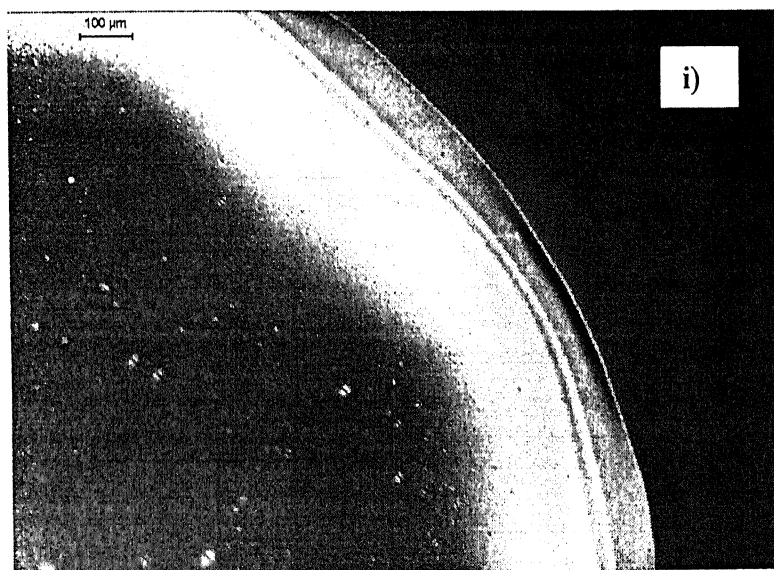
f)



ii)



g)



ii)

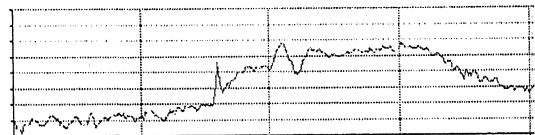
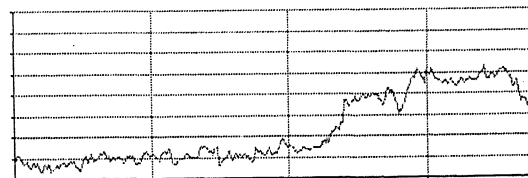
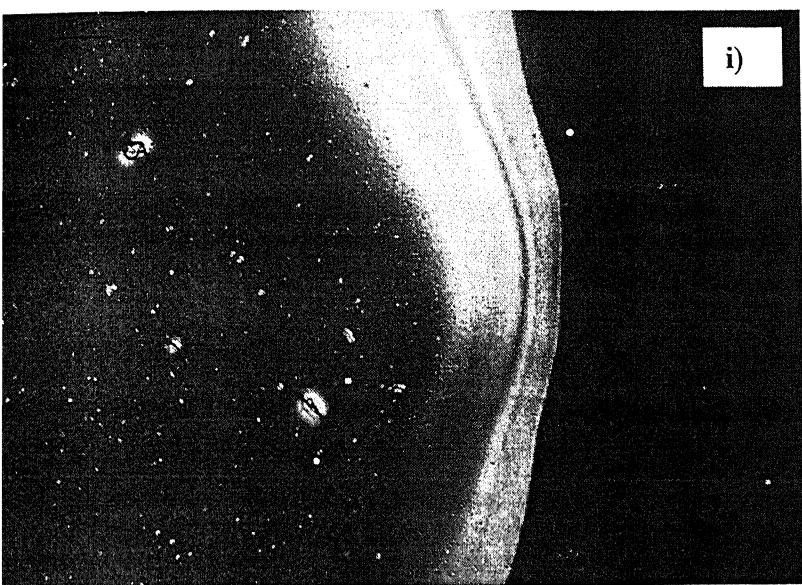
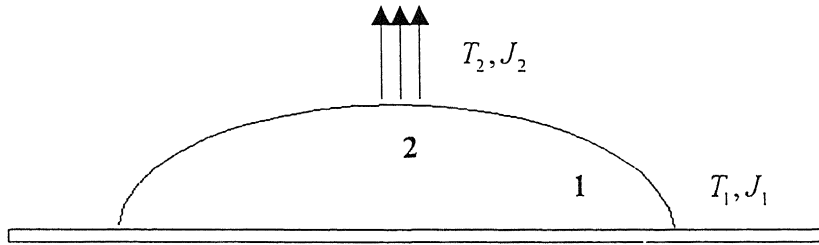


Figure 2.11 f) and g), Digital picture of drop covered with lid with a hole at its center. Drop volume  $2\mu\text{l}$ , drop diameter  $3.4\text{mm}$ , temperature of evaporation  $27^\circ\text{C}$ . The hole diameter of the lid is  $6\text{mm}$  and  $8\text{mm}$  respectively. i) Shows the picture, ii) shows the profile plot. The profile plot is the red level of the picture.



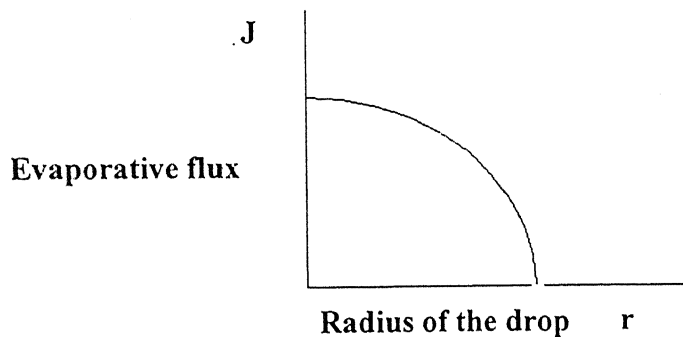
**Figure 2.11 h), Digital picture of drop covered with lid with a hole at its center. Drop volume  $2\mu\text{l}$ , drop diameter  $3.4\text{mm}$ , temperature of evaporation  $27^\circ\text{C}$ . The hole diameter of the lid is  $10\text{mm}$ . i) Shows the picture, ii) shows the profile plot. The profile plot is the red level of the picture.**

Fig 2.11 a) - h) shows the experimental results, along with the gray scale profile. From the profile it is very clear that when the evaporation is taking place from the center, i.e. they hole diameter of the lid is very small as compared to the diameter of the drop, then the deposit is uniform. As we increase the hole diameter of the lid the ring structure starts appearing, as more and more drop area is exposed to atmosphere for evaporation. In Fig 2.11 a), b), c) where the hole diameter is small as compared to the drop diameter the deposit of solute is quite uniform. As the hole diameter of the lid becomes comparable to the diameter of the drop, the solute starts depositing on the periphery as is evident from the gray scale profiles. This can be seen in Fig 2.11 d), e), f), where the lid hole diameter are 3, 4, 6 mm respectively. In Fig 2.11 h) where the lid hole diameter is  $10\text{mm}$ , we noticed the pronounced ring of the solute at the periphery, common to the case when the drop evaporates under open atmosphere. In this case the lid has no influence on the pattern of the deposited solute, because the drop diameter is approximately  $3.4\text{mm}$  smaller than the lid diameter i.e.  $10\text{mm}$ . We present a suitable mechanism which describes the above phenomenon. Refer to Fig 2.12.



**Figure 2.12 Schematic illustration of evaporation from the center of the drop. Point 1 depicts the edge and point 2 depicts the center of the drop.  $T, J$  are the temperature at the point and the evaporative flux from that point respectively.**

Evaporation is restricted to point 2, as the drop is covered with a lid with a hole at its center. Now due to evaporation the fluid loss will be higher at point 2 than at point 1 where there is very limited evaporation. The variation of evaporative flux along the surface is shown in Fig 2.13



**Figure 2.13 Evaporative flux along the surface of the drop. Flux is Highest at the center, and goes to zero at the edges.**

Evaporation is maximum at point 2 and therefore fluid loss is also higher at point 2 than at point 1. As a result after some time the interface will grow as is shown in Fig 2.14



**Figure 2.14 Schematic of the interface after some time. The solid line shows that the due to higher rate the interface will depressed at the center, but due to fluid motion from the edges the spherical shape is maintained shown by the dashed line.**

As shown in the Fig 2.14 the interface will get depressed at the center after some time due to higher evaporation rate, but the surface tension of the interface demands that spherical shape of the drop is maintained, so the fluid will flow from the edges towards the center. This is one of the factors that drive the fluid from the edges to the center of the drop. The Second effect, which plays an important role in the fluid motion, is the Temperature driven Marangoni flow of fluid. As has been stated earlier evaporation is higher at the center i.e. point 2 than at point 1, thus  $J_2$  is higher than  $J_1$ , as a result  $T_2$  will be lower than  $T_1$  due to adiabatic cooling of the surface as a result of evaporation. Now we know that as temperature increases surface tension ( $\gamma$ ) decreases, therefore  $\gamma_2$  will be higher than  $\gamma_1$ .

Fluid has a tendency to flow from regions low surface tension to regions of higher surface tension, which we call as Marangoni flow. Since  $\gamma_2$  is higher than  $\gamma_1$  fluid will flow from point 1 to point 2 i.e. from the edges to the center.

Thus there are two fluid flow mechanism when evaporation is taking place from the center of the drop, first is due to the distortion of the interface which pulls the fluid from the edge to the center, and the second is the temperature driven Marangoni flow, which also drives the fluid from edge to the center. These two fluid flows makes the solution in

the drop to remain in the center, and so the final deposited solute pattern is uniform, rather than the ring structure, which is primarily due to the fluid motion from the center of the drop to the edge of the drop. However pinning of the contact line is always there.

## 2.5 Results and Discussions

When a liquid droplet evaporates, flow patterns develop in the liquid drop. These flow patterns are responsible for the transfer of solute in the drop of solution. When a polymer solution drop evaporates on top of a glass slide the polymer is transferred to the periphery of the drop or the three phase contact line.

Experimental conditions are modified to characterize different dominating mechanism in the process of solute transfer. The general system of study is a polymer solution drop placed on a clean glass slide. With time the solvent evaporates, leaving behind the pattern of the distributed polymer (solute). Polymer solution is 6 wt% PMMA M.wt. 1,20,000 from Aldrich chemicals (USA) in HPLC grade Toluene supplied by E. Merck (India) Ltd. Glass microslide (2.5 x 2.5 cm) is used as substrate on which drop is placed. The drop is evaporated in an atmosphere of pure  $N_2$  and ambient air. Initial drop volume was 2  $\mu$ l

### 2.5.1 Contact line deposit in an evaporating drop

Fig. 2.15 shows the picture of the final distributed pattern of the solute (polymer in the present case) when the solvent has evaporated from the polymer solution drop.

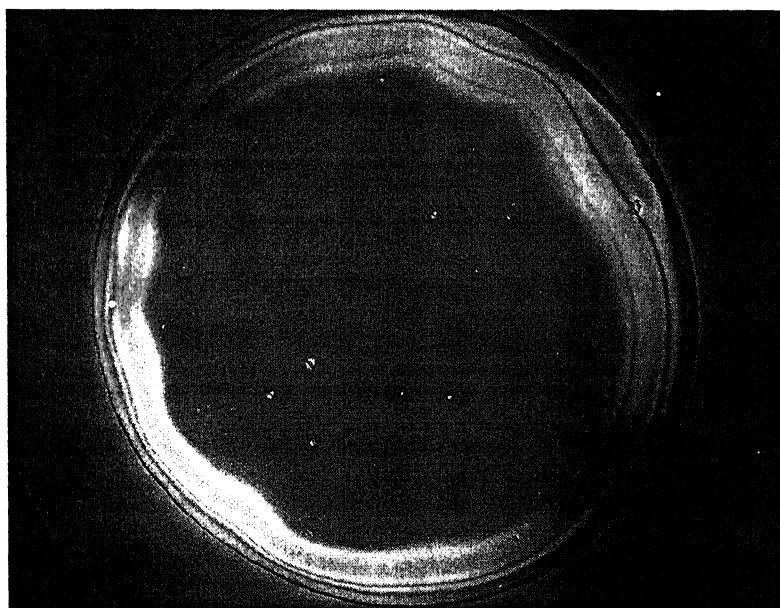


**Figure 2.15** A Photograph of a dried polymer solution. Polymer solution is 6wt% PMMA in Toluene. The magnification of the picture is 50x. The drop was dried in an ambient atmosphere. Temperature of evaporation was 27°C.



Fig. 2.15 shows the ring like deposit of polymer when the solution drop was dried in an ambient atmosphere. When the liquid drop evaporates advection current set up, which drives the fluid inside the drop. The phenomenon is due to geometrical constraints. The free surface of the drop constrained by the pinned contact line, squeezes the fluid outwards to compensate for evaporative loss. Fig. 2.16 illustrate the factor leading to outward flow in a small, thin, dilute, circular drop of fixed radius  $R$ , slowly drying on a solid surface.

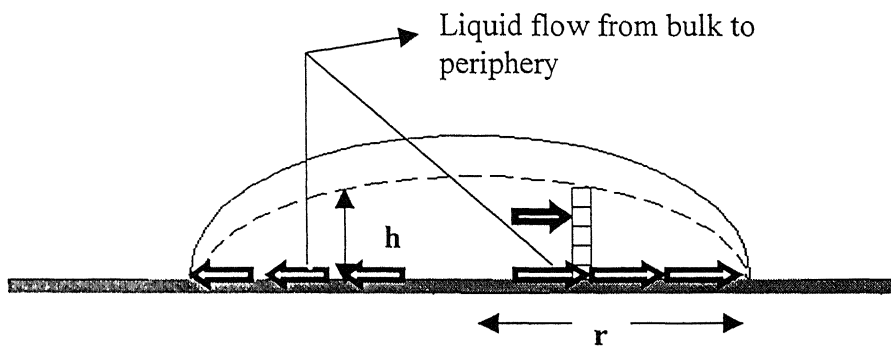


**Figure 2.16 schematic illustration of the origin of advection current. Shows the actual motion of the interface, when contact line is pinned.**

The physical idea behind the theory is that a pinned contact line induces an outward, radial flow when there is evaporation from of the drop. The contact line is pinned in he case of drop solution drop evaporating from the surface. However, if the contact line is pinned then there must be a flow that replenishes the liquid that is removed from the edge. The evaporation would alter the height  $h$  of the profile. At the perimeter, all the liquid would be removed and the drop would shrink. But the radius of the drop cannot shrink, as the contact line is pinned. The height profile must maintain the spherical cap as the elasticity of air liquid interface, i.e., the tendency of the interface to minimize its surface area, dictated by surface tension provides the force driving the outward flow of fluid. Thus during the short time  $\Delta t$ , the region shown with horizontal stripes Fig. 2.16 must be removed from each point  $r$  of the surface. This is different from the amount removed

from that point owing to evaporation. Therefore radial flow must make up for this difference which is responsible for solute transfer from the bulk to the drop edge. In the initial phase some preexisting conditions on the substrate anchors the contact line, this permits the ring to start growing and the suspension deposit onto the substrate, near the three phase contact line. The additional growth increases the energy barrier the contact line must surmount before moving. The phenomenon can very well be described by the term “self pinning”.

The theory of “self pinning” was checked by performing an experiment in which a 3 $\mu$ l drop of HPLC water was evaporated on the surface of freshly cleaved mica. The change in the diameter of the drop Vs time is shown in Fig 2.17.

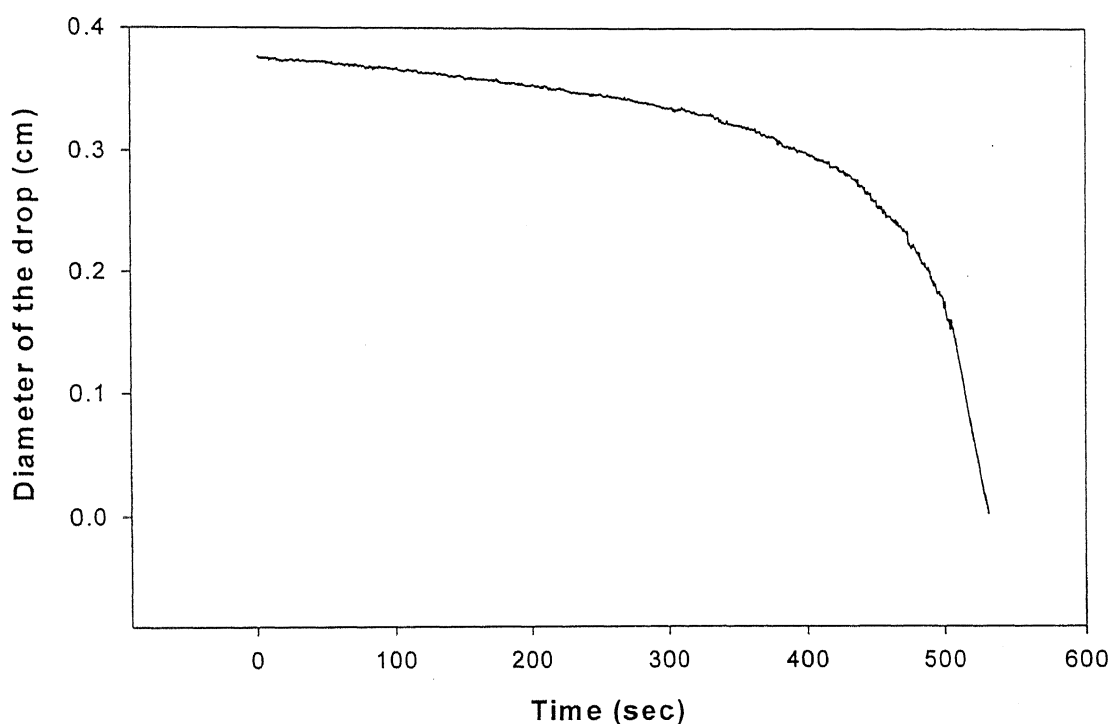


**Figure 2.17 Plot of diameter of a water drop (cm) drying on mica substrate Vs time. Volume of the drop is 3 $\mu$ l.**

The smoothness of the data in Fig 2.17 is a measure of the smoothness of the substrate. Now after confirming the smoothness of the substrate (mica), a drop of 5 $\mu$ l of polymer solution was placed on the freshly cleaved mica surface. The variation of the diameter of the drop is shown in Fig 2.18.

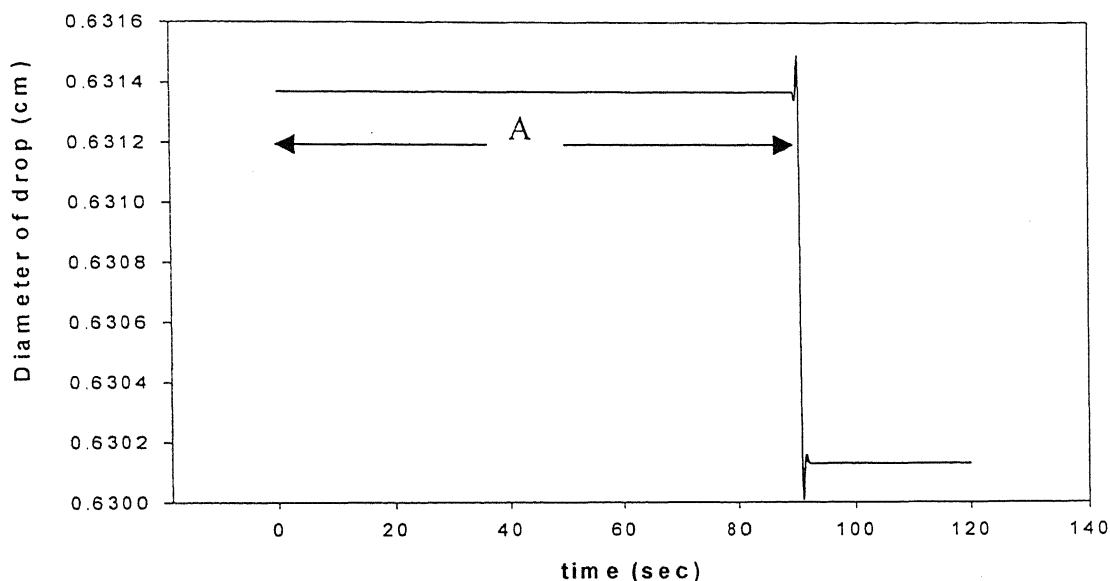


**Figure 2.18 Plot of Diameter of drop Vs time, for 6wt%PMMA in toluene on mica. The temperature of evaporation as 27°C.**

Fig 2.18 the region A indicates that the Diameter of the drop is constant for the drying period of approximately 100secs. This directly gives the evidence of contact line pinning, because when the contact line is pinned the diameter of the drop cannot change. The contact line pinning is due to the anchoring of the contact line by the initial deposit of the suspension. This can be inferred from the fact that in case of atomically smooth mica the diameter of the drying drop remains constant with time, which indicates the pinning of contact line. Now when the contact line is pinned, the height of the drop decreases with evaporation. Experiments were done to verify this fact. Fig 2.19 shows the decrease of height of the drop profile with time, which again indicates the mechanism of self pinning in the theory of solute transfer.

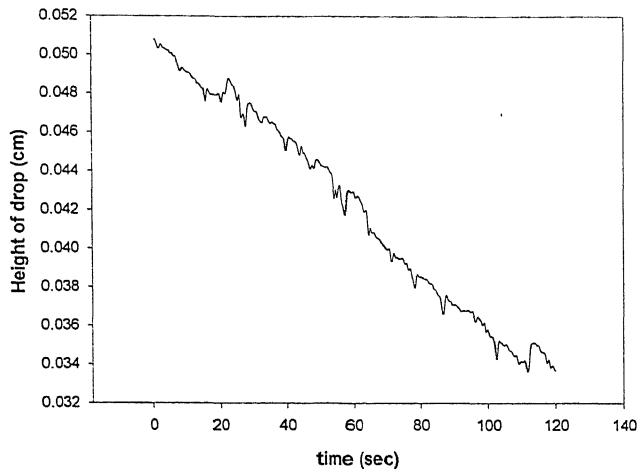


**Figure 2.19 Plot of Height of drop profiles Vs time. Drop volume was 5 $\mu$ l. The plot shows the decrease of height of drop profile with evaporation, confirming the mechanism of contact line pinning. The solution was 6wt% PMMA.**

The results are shown for the case when the substrate was mica. This is done in order to show that self pinning is the dominant mechanism in the theory of solute transfer, because mica surface is atomically smooth.

In the theory of solute transfer within the drop we say that the evaporation rate is higher at the edge of the drop. The increase of evaporation flux  $J_s$  at the edge is attributed to the greater probability of molecule's escape when leaving from the edge than when leaving from the center of the drop.

The change in volume of the drop must be exactly equal to the evaporation rate. Therefore

$$\frac{dM}{dt} = \rho \frac{d}{dt} \int_0^R dr' 2\pi r' h(r', t)$$

Given the velocity of the fluid inside the drop, the growth of ring can be computed. Within a small time interval all the solute that lay beyond a certain radius becomes part of the ring, therefore the mass of solute in the ring  $m_R(t)$  is

$$m_R(t(r_0)) = 2\pi c_0 \int_{r_0}^R dr' r' h(r', t=0)$$

where  $c_0$  is the mass of solute per unit volume of solution and  $t(r_0)$  is the time it takes to go from  $r = r_0$  at time  $t=0$  to  $r = R$  and can be calculated by integrating  $\frac{dr}{dt} = v(r, t)$  with the initial condition that  $r(0) = r_0$ . In the treatment vertically averaged velocity is used which implicitly assumes no vertical segregation of solute.

Now the distribution of solute, for which it is assumed that  $c(r)$  is function solely of radius ( $r$ ) (i.e. at a given radial distance the concentration is uniform throughout the liquid column), thus the conservation of solute leads to

$$\frac{\partial}{\partial t}(ch) + \frac{1}{r} \frac{\partial}{\partial r}(rchv) = 0$$

where  $c$  is assumed to be independent of  $z$ , the vertical distance from the substrate, and diffusion of solute is neglected. The mass in the ring can also be calculated from the difference of the mass of the solute in the drop at  $t = 0$  and the mass of the solute left at a later time.

Initially the ring grows as a power law with time. Considering a particle at a distance  $R-r$  from the edge. All the particles that are at equal or lesser distance from the contact line will be swept into the ring by the time the particle reaches the edge so that the ring will increase in mass by  $m_R \sim (R-r)^2$ . Therefore, at early times the ring grows in time as a power law

$$m_R \sim t^{2/(1+\lambda)}$$

The result for the thin drop limit is [3]

$$m_R = m_0 [1 - (1 - t/t_f)^{(1+\lambda)/2}]^{2/(1+\lambda)}$$

Where  $m_0$  is the total mass of solute present initially in the drop.

Thus it is proposed that in the theory of solute transfer in a solution drop, the self-pinning of the contact line is the predominant mechanism. The rate of evaporation is higher at the edge of the drop as compared to the bulk and at initial time the growth rate of the ring follows the power law.

## **2.5.2 Effect of localized evaporation of the final pattern of the solute.**

It was stated on the basis of probabilistic approach, that the rate of evaporation is higher at the edge of the drop than at the center of the drop, and this spatial variation in the rate of evaporation from the surface of the drop is responsible for solute transfer. The spatial variation in the rate of evaporation on the surface of the drop sets in advection current inside the drop, which drives the solute to the periphery. Controlling the area of evaporation from the drop surface, effects the solute transfer based and the final distributed pattern of the solute (polymer in our case). In the experiments we have used eight different lids with varying hole diameter at its center. We have varied the hole diameter from 0.5mm to 10mm. The volume of the drop is 2 $\mu$ l and the diameter of the drop is around 3.4mm.

Theoretically if we increase the hole diameter of the lid, then evaporation takes place also from the edges of the drop, and if we have hole diameter comparable to the diameter of the drop then we should get back the ring pattern in our initial experiments. The experimental results with lids having varying (increasing) hole diameter verify this hypothesis.

As we increase the hole diameter of the lid the ring structure starts appearing, as more and more drop area is exposed to atmosphere for evaporation. As the hole diameter of the lid becomes comparable to the diameter of the drop, the solute starts depositing on the periphery as is evident from the gray scale profiles. When the lid hole diameter is 10mm, we noticed the pronounced ring of the solute at the periphery, common to the case when the drop evaporates under open atmosphere. In this case the lid has no influence on the pattern of the deposited solute, because the drop diameter is approximately 3.4mm smaller than the lid diameter i.e. 10mm

The interface gets depressed at the center after some time due to higher evaporation rate from the center, but the surface tension of the interface demands that spherical shape of the drop is maintained, so the fluid will flow from the edges towards the center. This is one of the factors that drive the fluid from the edges to the center of the

drop. The Second effect, which plays an important role in the fluid motion, is the Temperature driven Marangoni flow of fluid. Fluid has a tendency to flow from regions low surface tension to regions of higher surface tension, which we call as Marangoni flow. Since Surface tension at the edge is low as compared to the surface tension at the center of the drop, fluid flows from the edge to the center. Thus there are two fluid flow mechanism when evaporation is taking place from the center of the drop, first is due to the distortion of the interface which pulls the fluid from the edge to the center, and the second is the temperature driven Marangoni flow, which also drives the fluid from edge to the center. These two fluid flows makes the solution in the drop to remain in the center, and so the final deposited solute pattern is uniform, rather than the ring structure, which is primarily due to the fluid motion from the center of the drop to the edge of the drop. However pinning of the contact line is always there.

## Chapter 3

# Pattern formed by an evaporating droplet on a Dissolving substrate

The system of drop evaporation from a Dissolving substrate is a very interesting phenomenon. The final pattern is similar to the pattern when the solution drop evaporates on a non-dissolving substrate, though much more complicated kinetic phenomenon are involved in this problem. In this type of system different competing kinetics comes into play. First being the evaporation of the fluid from the drop, which involves mass transfer across the system. Second is the dissolution kinetics of the substrate in the drop fluid, which involves mass transfer within the system. Third is the temperature driven Marangoni flow that pulls the fluid from inside the bulk to the interface, fourth is the advection of the fluid from the bulk to the three phase contact line due to the differential rate of evaporation at the drop edge and at the center of the drop. The final pattern of the redistributed solute formed after the evaporation of the liquid is the result of the above major competing kinetics. In the present work an attempt has been made to qualitatively investigate the system of drop evaporation on dissolving substrate.

### 3.1 System of Study

The present system of study comprises of a dissolving substrate, which is polymeric film that is spin casted on to a glass slide. The polymer solution was prepared by dissolving 6wt% of PMMA (M.wt 1,20,000) in HPLC grade Toluene. The polymer solution is then spin coated on clean glass slides at a speed of around 1830 rpm. The thickness of the polymeric film is around 360nm. The film thickness is quite large (i.e. the film is not thin film). The reason behind this is to exclude the end effects, i.e. we wanted to study the effect of drop evaporation on dissolving substrate, and wanted the whole substrate to be dissolving. More over the dissolving substrate should extend to infinity in one direction. As compared to the length scale of the final pattern the thickness of the drop is quite



adequate. Secondly if we have very thick polymer films then the problem of films cracking and peeling of film arises. Thus the film thickness of the order of 300 – 400 nm was found to be quite suitable. Fig 3.1 gives the schematic of the setup.

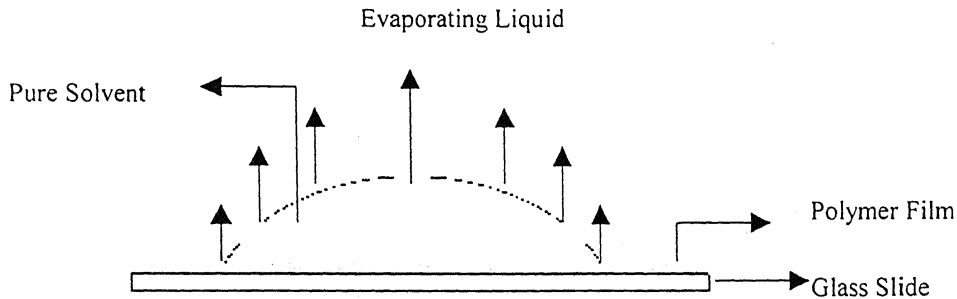
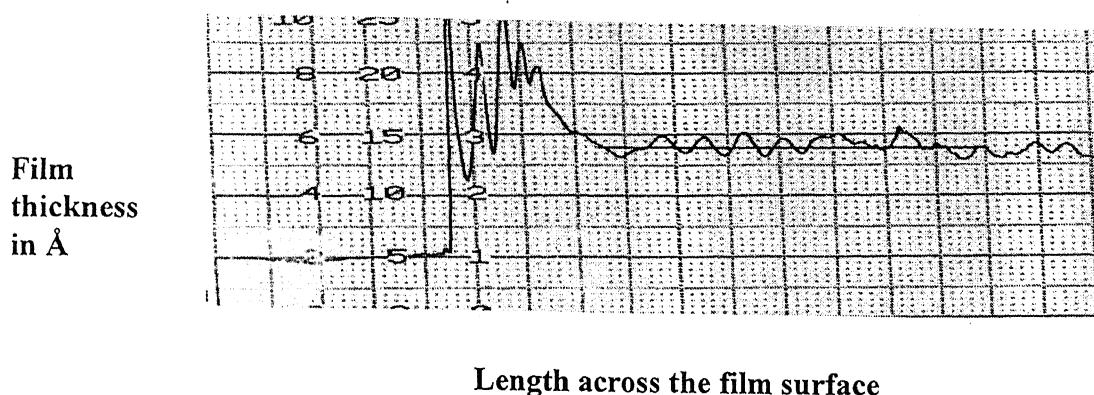


Figure 3.1 Schematics of drop on soluble Substrate.

## 3.2 Solute redistribution by an evaporating droplet on a dissolving substrate

In this section we present the study of the final pattern formed when a drop of pure solvent evaporates on a dissolving substrate. The problem is very different from the one presented in chapter 2. In this case the drop of liquid is a pure solvent of the polymeric film. With time the fluid evaporates from the interface of the drop, and at the same time the polymer film is dissolving in the drop. Initially when we put a drop of liquid (which is a solvent for the polymer) on a polymer film the drop spreads, due to the positive spreading coefficient of the solvent on the polymer. The balance of the forces and contact angle restricts the spreading of the drop to a certain contact angle. Once the drop stops spreading the three phase contact line is pinned.

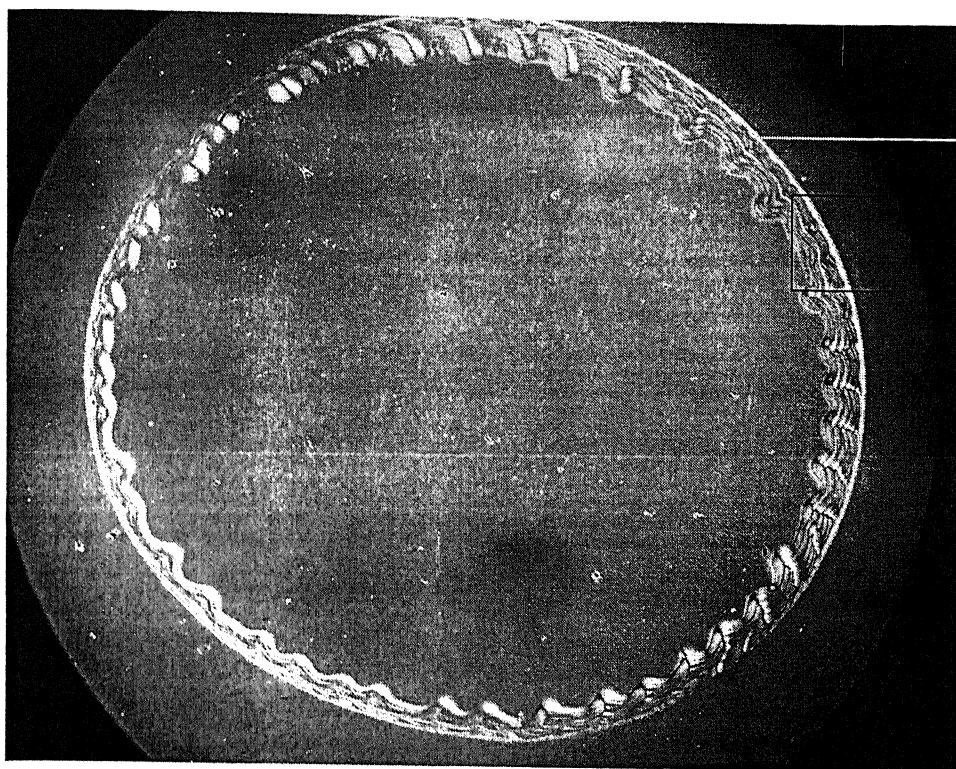
The pinning of the contact line is due to the physical heterogeneity of the polymer film, and the initial deposit of the polymer at the contact line as discussed in chapter 2. Fig 3.2 shows the surface profile of the polymer film. The profile is measured using a Dektak Profilometer in which a stylus travels over a portion of the sample recording the profile. Stylus size used was  $5\mu\text{m}$  radius and the scan distance is 3mm.



**Figure 3.2 profile of the polymer film. The film thickness is around 360nm. Each block measures  $2000\text{\AA}$**

From Fig 3.2 it is clear that the film has physical heterogeneity, which helps in the anchoring of the contact line, once the spreading of the drop stops. The heterogeneity arises during the drying process when the film is spin coated.

Now when we put a drop a pure solvent, toluene in this case on the polymer film then we observe a ring structure. Fig 3.3 shows the digital image of the final pattern of the redistributed solute when the drops evaporate on the dissolving substrate.



Ring structure of the polymer

**Figure 3.3 Digital image of the final pattern of the redistributed polymer, when a sessile drop is placed on the polymer film. Diameter of the drop approximately 2.273mm Polymer solution is 6wt% of PMMA in toluene, film thickness is around 360nm. The drop was evaporated in an ambient atmosphere. Temperature is 27°C. The image is taken at 50x magnification.**

Fig 3.3 shows the ring final pattern of the redistributed polymer, after the drops evaporates from the dissolving substrate. From the figure it is clear that the ring structure is very undulating. The undulations of the contact line are due to the Rayleigh like instability of the contact line. By taking a close look at the contact line we could see, that the ring width consists of striated pattern. Fig 3.4 gives a close up view of the ring structure. In Fig 3.4 the magnification is 100x.



**Figure 3.4** Enlarged image of the square section of the ring structure of Fig 3.3. The image is taken at 100x magnification. The image shows the striation along the ring width and regular ridges.

In Fig 3.4 we could observe the regular striation pattern and regular ridge formation. The structures are formed due to the instabilities of the contact line and the stick slip motion. We suggest the following mechanism behind these structures.

When the drop of pure solvent is placed on the polymer film, it spreads upto the maximum diameter as governed by the balance of the forces at the three phase contact line. After maximum spreading the contact line gets pinned. At the bottom layer, the solvent dissolves the polymer, and forms a solution which gets pinned there by pinning of the contact line, and solidifies to form the initial ring. This process is very fast as the

thickness of the liquid film at the contact line is very small, and therefore the emulsion in this part freezes out to form the initial ring. This ring provides the initial anchoring of the contact line. As has been discussed in Sec.2.2, in an evaporating drop the rate of evaporation is higher at the contact line than at the bulk. This leads to the flow of fluid from the bulk to the contact line. The liquid front at the periphery experiences Rayleigh-like instability and takes the undulating form. The contact line then depins and retracts and experiences a similar instability. The thickness of the fluid film is small near the three-phase contact line and thus the undulated pattern caused by the instability gets frozen down. The regular striation observed in Fig 3.4 is due to the depinning of the contact line, and the ridges observed in the same figure are due to the undulations of the contact line, which get frozen out due to the presence of polymer in the emulsion at the three-phase contact line.

Fig 3.5 shows the stages in the development of the final pattern as the drop evaporates from the dissolving substrate. The images are shown at different times until the final pattern is formed.

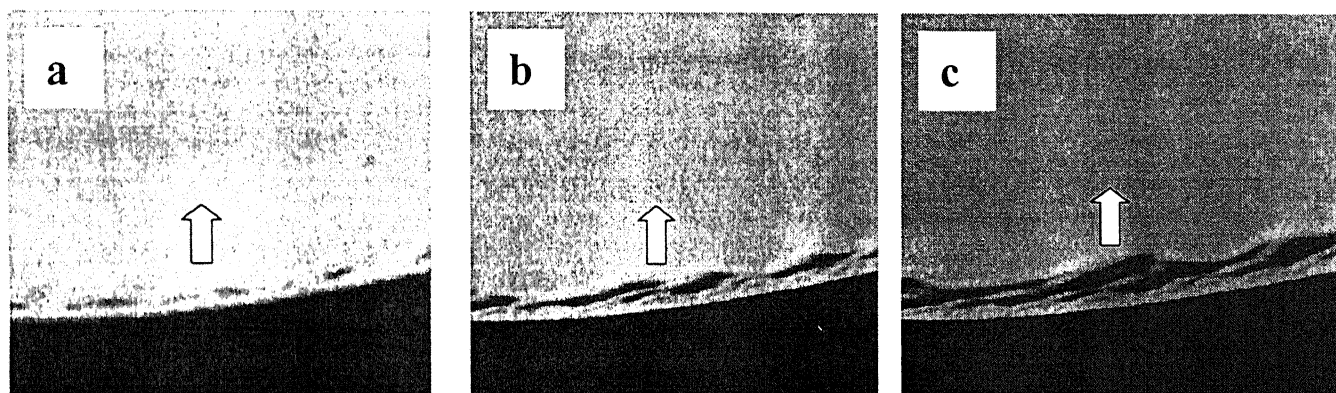


**Figure 3.5** a), b), c) illustrates the stages in the development in the final pattern, at  $t=2, 4, 6$  sec respectively, when the drop evaporates from the dissolving substrate. The Pictures are taken with an optical microscope, with magnification 50x. The solid arrow shows the direction of the retracting edge. The image sequence shows the instability of the contact line.

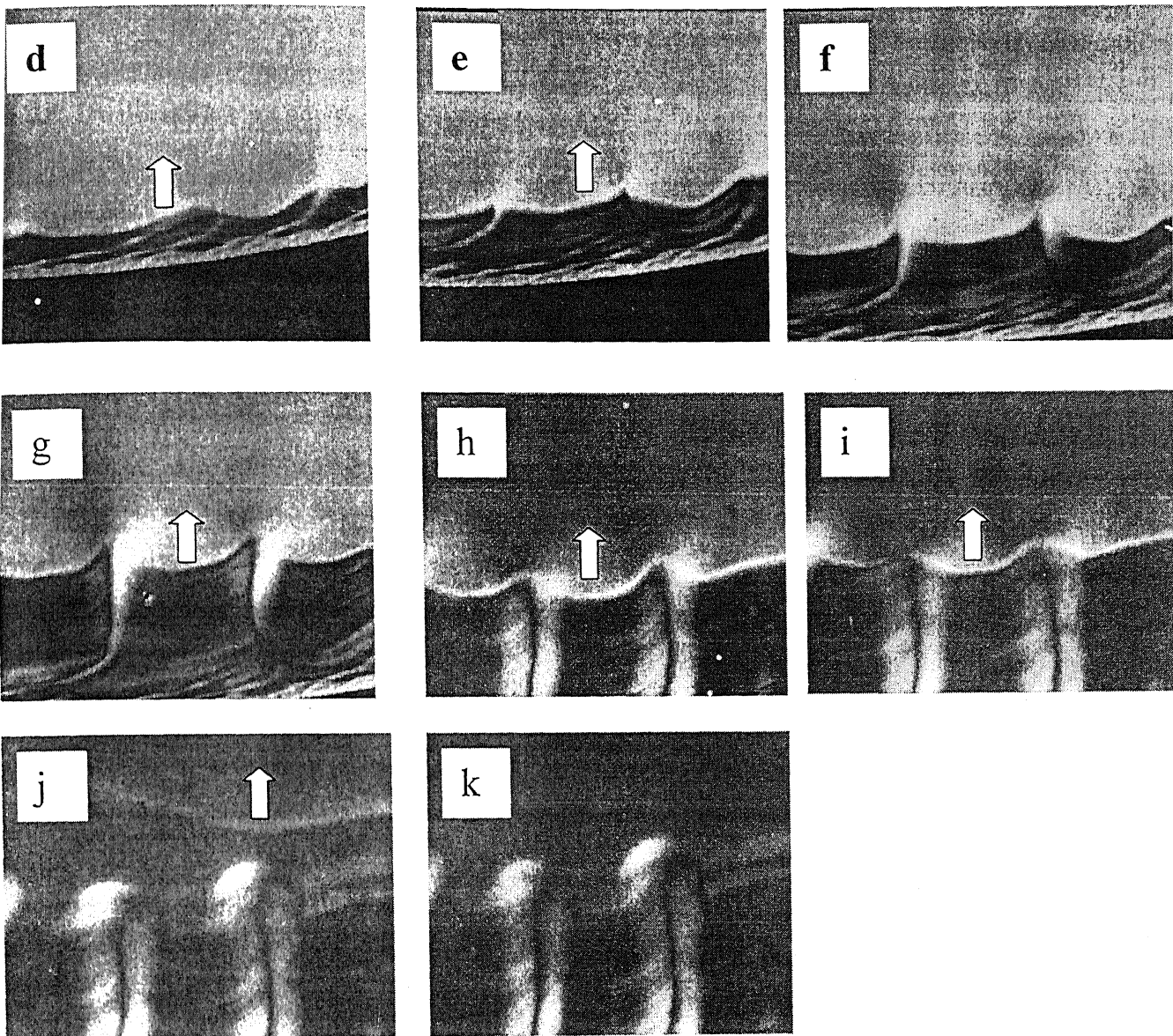


Figure 3.5 d), e), f), g), h), i), j), k) illustrates the stages in the development in the final pattern, at  $t=8, 10, 12, 14, 20, 23, 24, 25$  secs respectively, when the drop evaporates from the dissolving substrate. The Pictures are taken with an optical microscope, with magnification 50x. The solid arrows shows the direction of the retracting edge. The image sequence shows the instability of the contact line.



Fig 3.5 show the sequence in the formation of the final pattern of the redistributed pattern. The solid arrows show the direction of the retracting fluid front. Two fluid motions are taking place in this phenomenon. First is the motion of fluid from the bulk of the drop to the periphery, due to the differential rate of evaporation at the periphery and the bulk. Second is the retracting of the contact line due to depinning. The first fluid motion bring the polymer from the bulk of the drop to the three phase contact line, and deposit it there, and the second fluid motion deposit the polymer in a regular striated pattern as observed in Fig 3.4

The image sequence of Fig 3.5 verify that the regular striation and the ridge observed in Fig 3.4 is due to the instability of the fluid edge which is coming from the bulk to the periphery. By careful observation of the images in Fig 3.5 we notice that the outer boundary of the ring is smooth, and only the inner boundary is wavy. Now the question arises as to why this discrepancy occurs? We think that the following phenomenon is behind this observation.

When a drop is placed on the polymer film, the bottom layer the fluid dissolves the polymer, and since the film thickness is very small at the boundary ( i.e. near the three phase contact line) the fluid evaporates instantaneously freezing the pattern. This may be the sort of initial demarcation. Since the volume of fluid present in the outermost boundary is very small, the emulsion form is very thick, as a result it does not experiences the instability. Now the wavy nature of the inner boundary is due the instability of the fluid edge( front) which is coming from the bulk to the periphery, where the amount of fluid is higher and the emulsion is quite thin as a result the fluid edge experiences the instability. The image sequences of Fig 3.5 suggest a similar phenomenon. Finally in the last stage, i.e. in the inner layer, due to the force constraints the contact line cannot depin any more, and the undulations grow into large shapes, and gets freezed up as the solvent evaporates, The remaining fluid on the surface which contain very low per cent of polymer (or no polymer, we can't say for sure as we could not measure the polymer concentration on film surface) evaporates out as shown in Fig 3.5 (w).

### 3.2.1 Mechanism of Depinning of the contact line

The mechanism suggested in this section is not general, and is restricted to the case where pinning of contact line is the predominant mechanism. Moreover this mechanism shall not hold when the fluid is slipping. Fig 3.6 gives the schematic illustration of the forces acting on the contact line.

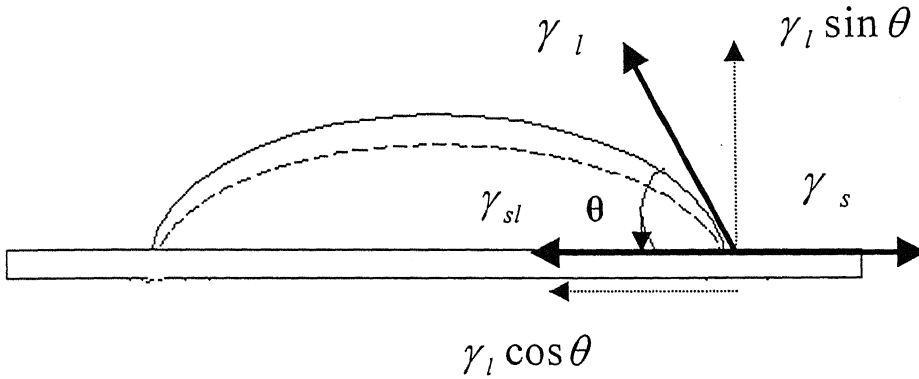


Figure 3.6 Schematic illustration of the forces acting at the contact line.

Fig 3.6 shows the balance of forces at the three phase contact line, where

$\gamma_l$  is the Fluid interfacial energy.

$\gamma_s$  is the interfacial energy of the substrate.

$\gamma_{sl}$  is the interfacial energy at the fluid and substrate contact.

$\gamma_l \sin \theta$  is the vertical component of the interfacial energy of the fluid.



$\gamma_l \cos \theta$  is the horizontal component of the interfacial energy of the fluid.

$\theta$  is the contact angle of the fluid on the substrate.

The above mentioned interfacial energies are related through Young's equation given by

$$\gamma_l \cos \theta + \gamma_{sl} = \gamma_s$$

For the given system of fluid and polymer substrate the interfacial energies are constants, the only varying parameter is the contact angle ( $\theta$ ), and that to when the contact line is pinned. The reason is that when the contact line is pinned, as the fluid evaporates from the drop, the interface takes the shape as shown by the dashed line, thus decreasing the contact angle.

Now we know that the function  $\cos \theta$  is a decreasing function, i.e. as  $\theta$  decreases the function  $\cos \theta$  increases. As the fluid evaporates from the drop the contact angle ( $\theta$ ) decreases as a result of which the function  $\cos \theta$  increases there by increasing the force component  $\gamma_l \cos \theta$ . Now with decreasing  $\theta$  the function  $\gamma_l \sin \theta$  decreases.

As the other forces are constants for a given system the increase of  $\gamma_l \cos \theta$  component and decrease of  $\gamma_l \sin \theta$  component causes the contact line to get uprooted from its initial position and retract inwards.

At a certain position the contact line stops retracting and gets fixed up when the forces at the contact line are balanced as governed by the Young's equation at a certain contact angle  $\theta$ . This position of the contact line is maintained for some time during which the polymer is deposited at that position, and again as fluid evaporates the contact angle decreases and the same phenomenon occurs there by depinning the contact line. This phenomenon of balance and disbalance of forces at the contact line continues causing pinning and depinning of the contact line, which gives striated pattern in the ring.

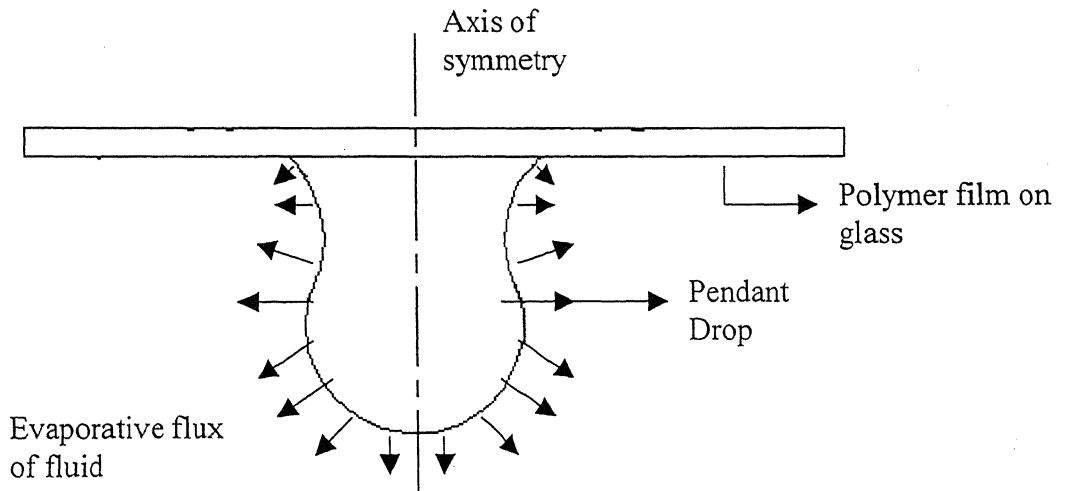
गुरुप्रोत्तम काशीनाथ केजकर पुस्तकालय

भारतीय प्रौद्योगिकी संस्थान कानपुर

अवधि क्र० A-14180C

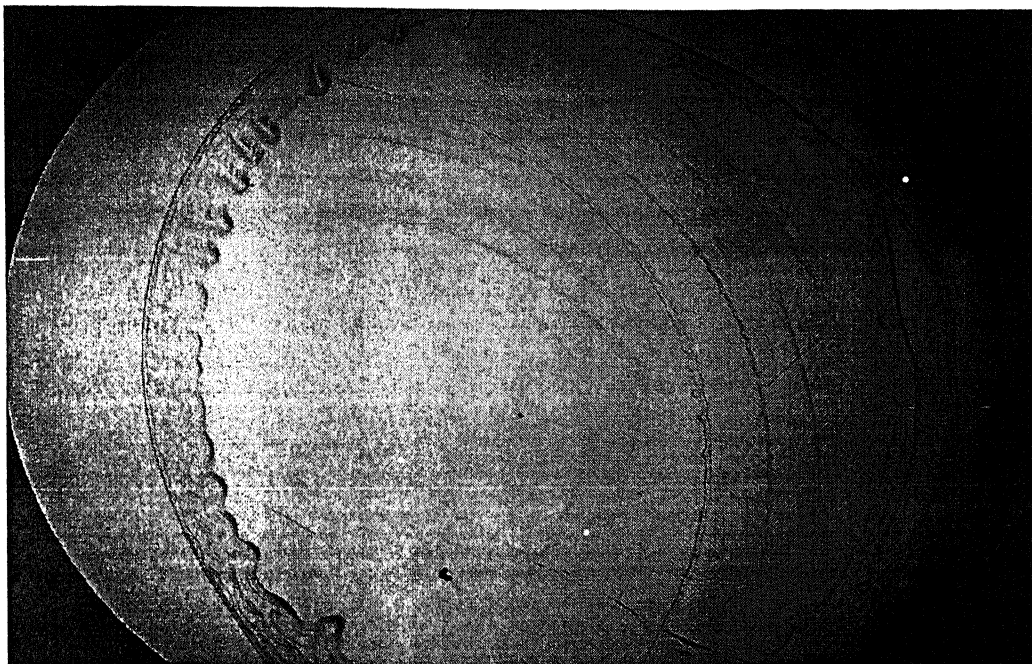
### 3.3 Study of Pendant drop evaporating from a dissolving substrate

In this section we studied the effect of pendant drop on the final redistributed pattern of the polymer, when the pendant drop evaporates from a dissolving substrate. The dissolving substrate is a PMMA film (Mwt. 1,20,000) of thickness 360nm approximately. The pendant drop volume is  $2\mu\text{l}$ , and the initial drop diameter is 3.4mm approximately. The polymer was prepared by spin coating the polymer solution on the glass substrate. Fig 3.6 illustrates the configuration of the pendant drop.



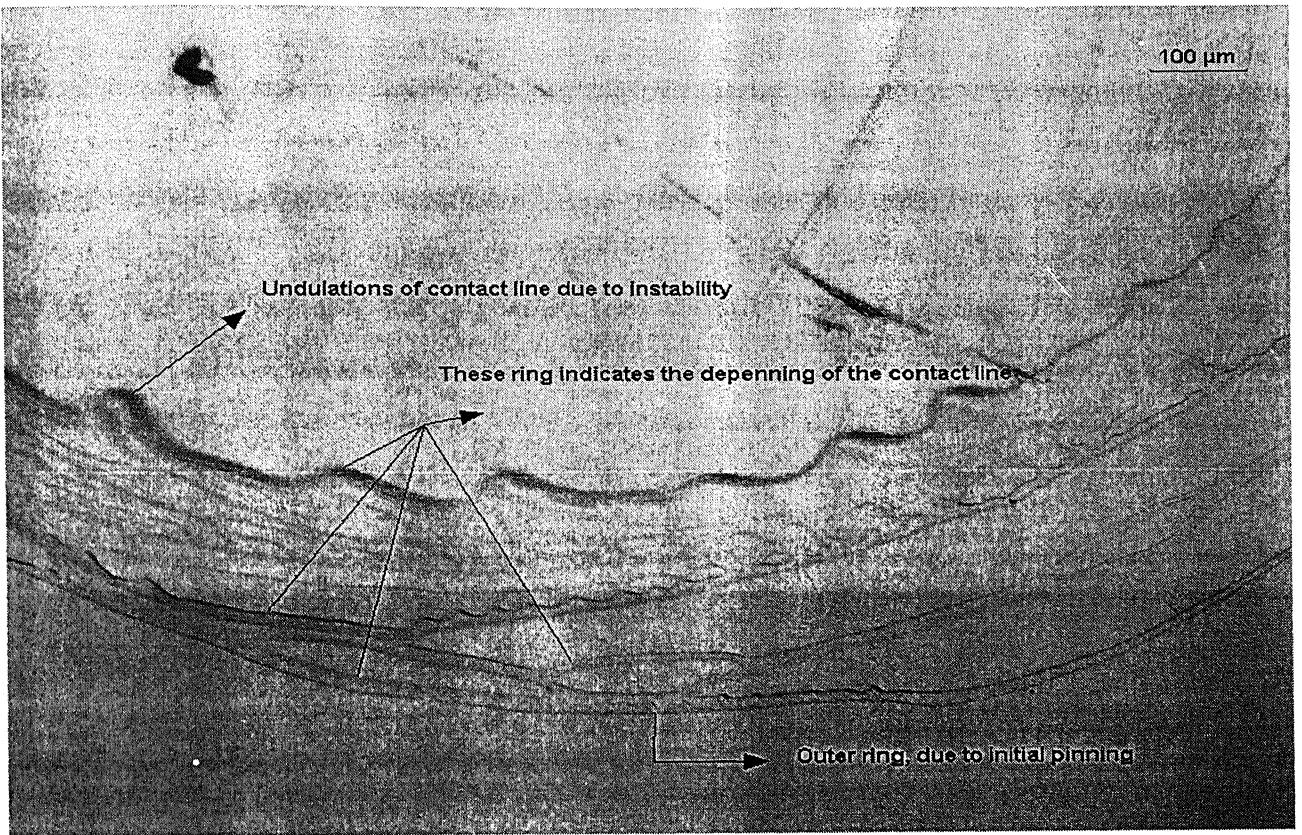
**Figure 3.7 Schematic illustration of the pendant drop**

Fig 3.7 shows the image of the final pattern of the redistributed polymer when the pendant drop evaporates from the surface of a dissolving substrate.



**Figure 3.8** Image of the final pattern of the polymer film, taken at 50x magnification, taken with a digital camera. Drop volume is 0.5 $\mu$ l, and the initial drop diameter is 4.24mm approx, as measured from the pinned edge of the final redistributed pattern. Temperature of evaporation is 27°C.

From Fig 3.8 Depinning of the contact line is clearly visible. Fig 3.9 shows the sectional view of the final pattern, which clearly indicates depinning of the contact line, and the length scale of depinning is large, as compared to the sessile drop. In case of the sessile drop the striation of the final pattern is regular and compact, and occurs in a single band. Moreover in the case of a sessile drop the area within the drop is free from the concentric rings where as in the case of pendant drop the concentric rings are present within the drop area there by indicating the process of pinning and depinning in the course of evaporation.



**Figure 3.9** Sectional view of the final pattern of the redistributed polymer. Magnification is 50x. Drop volume 0.5 $\mu$ l, and initial drop diameter is 4.24mm. The image shows the initial pinned contact line, the movement of contact line due to depinning, and the undulations of the contact line due to instability. The numbered lines in the image give the distance, which

The measurement of the marked line shown in Fig 3.9 is presented as follows.

Object	Distance ( $\mu$ m)
1	85.29
2	84.45
3	28.70
4	90.05
5	91.65
6	36.95
7	30.47
8	42.04
9	35.26
10	21.01

From Fig 3.9 it is observed that the distance that the contact line moves after depinning is large, and is not constant, as indicated by the table above. Moreover the contact line depins in a random manner, enclosing areas of different shape and size. This may be due to the instability of the contact line, otherwise if the contact line depins in a stable fashion then the final pattern would form concentric rings. Fig 3.10 shows the image of the final pattern developed when a sessile and a pendant drop evaporate from the surface of a dissolving substrate. In both the cases the initial drop volume is  $2\mu\text{l}$  of solvent. The drops were evaporated in an ambient condition at a temperature of  $27^\circ\text{C}$ .

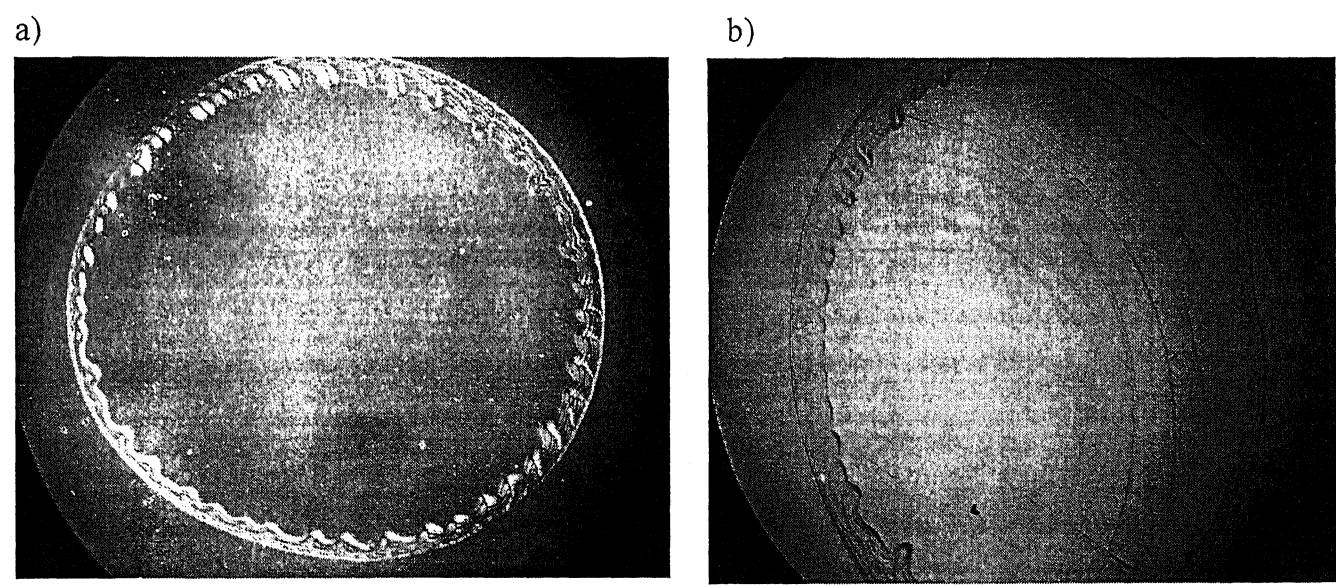


**Fig 3.10 Images of the final pattern formed when a) sessile and b) pendant drops evaporate from the surface of a dissolving substrate. The initial drop volume is same in both the cases i.e.  $2\mu\text{l}$ . The drop was evaporated under ambient condition of  $27^\circ\text{C}$ .**

From Fig 3.10 a) – b) we can clearly observe that in case of pendant drop pinning and deppining of the contact line is very predominant. The initial band of striated rings near the periphery of the drop is common in both the cases. The only difference is the formation of concentric rings in the case of pendant drop. We try to describe the above-observed phenomenon as follows. In the case of pendant drop the gravity has an opposing influence as compared to the sessile drop (refer Fig 3.7). In the case of sessile drop the drop sits on top of the substrate and the gravity has the role of pinning, where as in the case of pendant drop (Fig 3.7 ) the gravity pulls the liquid down and this has a

depinning effect. Due to this effect we observe concentric rings with large spacing between them in the case of pendant drop as compared to the sessile drop, where there are few concentric rings in the form of a band near the periphery of the drop. Fig 3.11 shows the images of the sessile and the pendant drop which were used to measure the spacing between the concentric rings in both the cases.

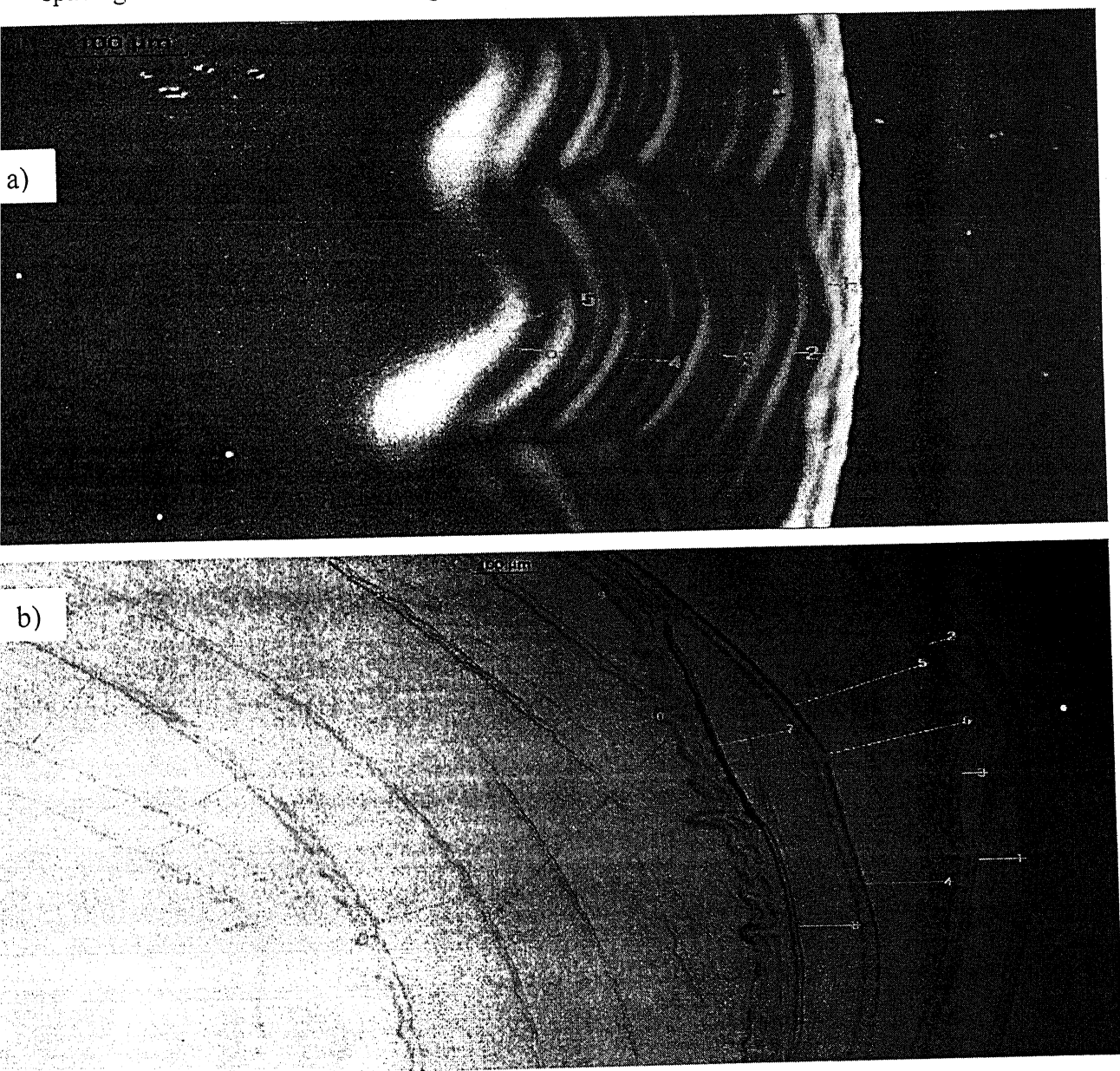


Figure 3.11 images of the final pattern formed when a) sessile magnification 100x, and b) pendant drop magnification 50x, evaporates. The images show the distance measured between the concentric rings. The magnification of the image is 50x



The marked distances shown in Fig 3.11 is presented below.

a) for sessile drop

Object	Distance ( $\mu\text{m}$ )
1	25.17
2	23.69
3	33.05
4	53.72
5	25.13
6	40.34

b) for pendant drop

Object	Distance( $\mu\text{m}$ )
1	67.99
2	45.84
3	38.43
4	133.02
5	218.52
6	225.81
7	124.06
8	93.11
9	89.29
10	133.52
11	117.22
12	125.73
13	161.40
14	113.35
15	75.44
16	42.96
17	103.22
18	175.04

Now as stated in sec 3.2.1 depinning occurs due to misbalance of forces at the contact line. The inward force pulling the contact line  $\gamma_l \cos \theta$  increases with decreasing contact angle  $\theta_c$ . For the sessile drop the inward force pulls the contact line where as the gravity has a stabilizing effect therefore the contact line retracts a very small distance and again gets pinned by the solute deposition, refer to data for Fig 3.11 a) for the distance moved by the contact line after depinning. This is the reason, why the contact line forms a

concentric striated pattern confined to the periphery of the drop edge in the form of a band.

In the case of the pendant drop in addition to the inward force  $\gamma_l \cos \theta$  at the contact line, the gravity is also pulling the contact line.

Fig 3.12 shows the resolution of the force at the contact line in case of a pendant drop.

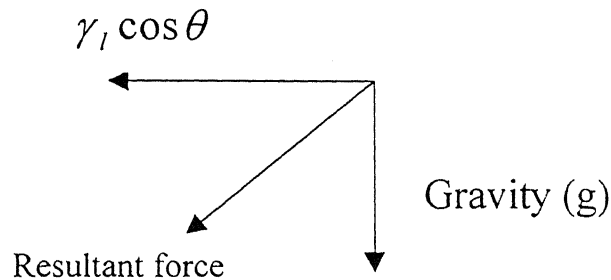


Figure 3.12 resolution of forces at the contact line in the case of pendant drop

The above diagram shows that the resultant force, which pulls the contact line in the case of pendant drop, is much stronger than the force, which pulls the contact, line in the case of a sessile drop. Therefore the contact line moves a greater distance between depinning and subsequent pinning in the case of a pendant drop.

Thus we can say that gravity favors pinning in the case of sessile drop and it favors depinning in the case of pendant drop.



### 3.4 Effect of localized evaporation on the transfer of solute in an evaporating drop

In this section we look into the effect of controlling the exposed surface area of the drop to the atmosphere on the final redistributed pattern of the polymer. The spatial variation in the rate of evaporation on the surface of the drop sets in advection current inside the drop, which drives the solute to the periphery. The main purpose of the experiment is to study the effect controlling the area of evaporation from the drop surface, and to see its effect on the solute dissolution and transfer based on the final redistributed pattern of the solute (polymer in our case).

#### 3.4.1 System of study

The system of study comprises of a clean glass slide covered with a covering lid, with a hole in the center of the lid. The diameter of the hole of the covering lid is kept small as compared to the diameter of the drop. Fig 3.12 explains the schematic diagram.

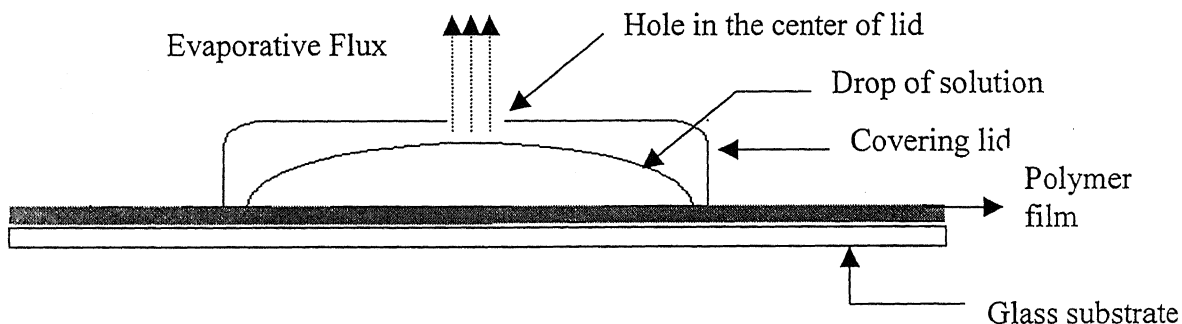


**Figure 3.12 Schematic illustration of a solution drop covered with a lid, having hole at its center. The Diameter of the hole in the lid is small compared to the drop diameter in order to restrict the exposed area of the drop**

Fig 3.12 illustrates the setup of the study. The setup is designed to restrict the evaporative flux to the center of the drop. The drop diameter is intentionally kept small as compared to the diameter of the hole in order to restrict the surface area of evaporation. In the study we have used eight different lids with varying hole diameter at its center. We have varied

the hole diameter from 0.5mm to 10mm. The lids are made of hard plastic caps with external diameter 18mm, internal diameter 14mm and height of 3mm. The volume of the drop is 2 $\mu$ l and the diameter of the drop is around 3.4mm.

### 3.4.2 Mechanism involved in Localized Evaporation

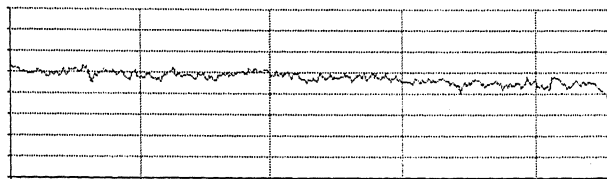
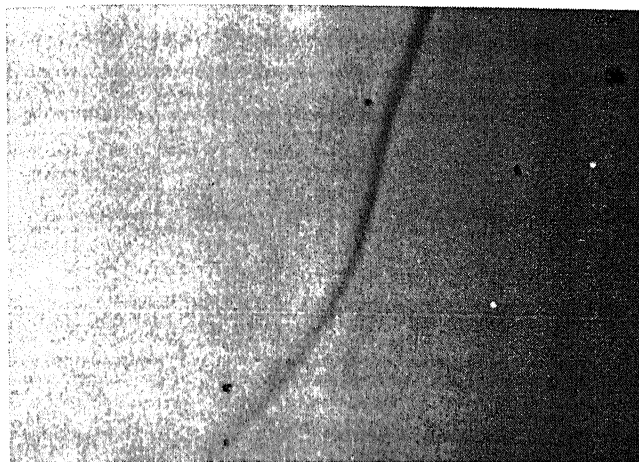
In the experiment of Localized evaporation our aim was to see the effect of controlling the evaporation rate on the surface of the drop on the dissolution of polymer and the mechanism of solute transfer.

Referring to Fig 3.12 shows that when the drop is covered with lid with a hole at its center, then the evaporation mainly takes place from the center. The evaporative flux  $J_s$  is maximum at the center, and at the edges the evaporation is restricted. We say so because the initial drop diameter is around 3.4mm and the diameter of the hole on the lid is 0.5mm. Thus the evaporation is concentrated to the center. As the rate of evaporation is decreased to a appreciable degree, the drop spreads on the polymer surface due to the compatibility of the solvent with the polymer. Theoretically if we increase the hole diameter of the lid, then evaporation takes place also from the edges, and if we have hole diameter larger than the diameter of the drop then we should get back the ring pattern. To verify this we did the experiments with lids having varying (increasing) hole diameter. In the experiments care was taken that the holes are exactly at the center of the lid, which in turn is placed symmetrically on top of the drop, i.e. the hole is exactly at the center of the drop.

In our experiments we got the results as has been predicted by the theory. We used fixed volume of drop i.e. 2 $\mu$ l, with the initial drop diameter 3.4mm. the hole diameter of the lid was varied from 0.5, 1.0, 2.0, 3.0, 4.0, 6.0, 8.0, 10.0 mm. In the first case the hole in the lid is very small as compared to the drop, and in the final case the hole is large compared to the drop diameter, replicating the ambient condition. As we move from small hole diameter of the lid to the large diameter we got the ring pattern of the solute. Fig 2.12 shows the final pattern of the solute for different hole diameter of the

lid. Gray scale profile plots are also presented which confirm the uniformity of the pattern.

a) i)



ii)

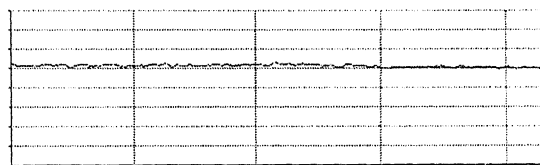
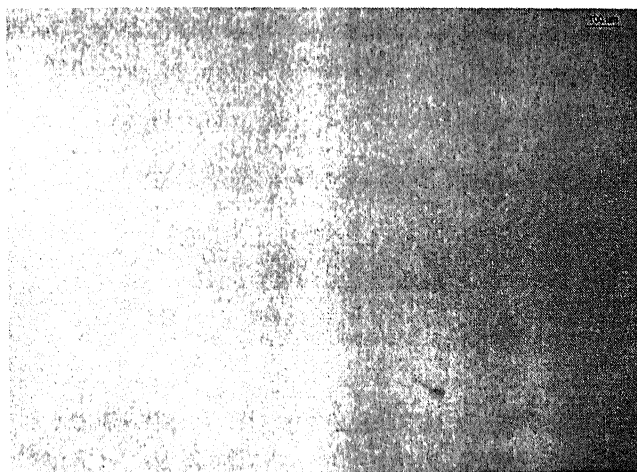
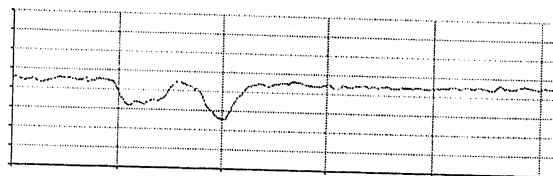
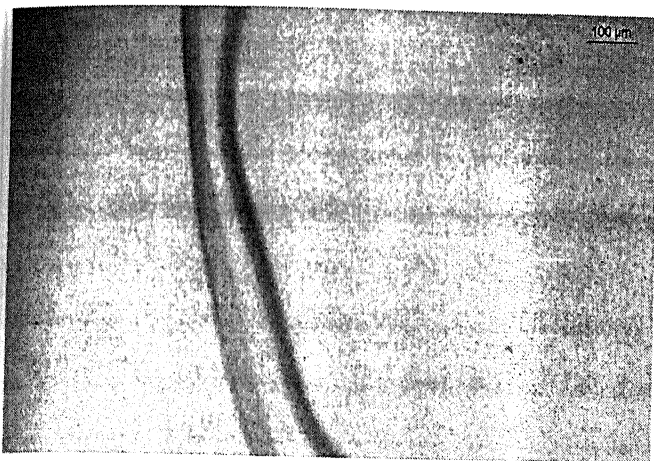


**Figure 3.13 a) Digital image of drop covered with lid with a hole at its center. Drop volume 2 $\mu$ l, drop diameter 3.4mm, temperature of evaporation 27°C. The hole diameter of the lid is 0.5mm. i) Shows the image at the periphery, ii) shows the image at the center. The profile plots are to the right of the image. The profile plots are the light intensities( gray level). From the profile it can be inferred that the solute distribution is quite uniform at the periphery and at the center. The image covers the periphery and the inside of the drop area.**

b)



c)

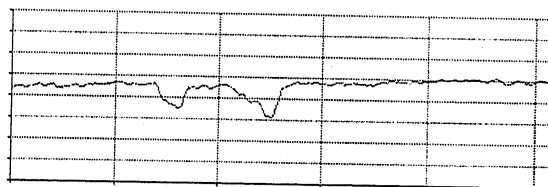
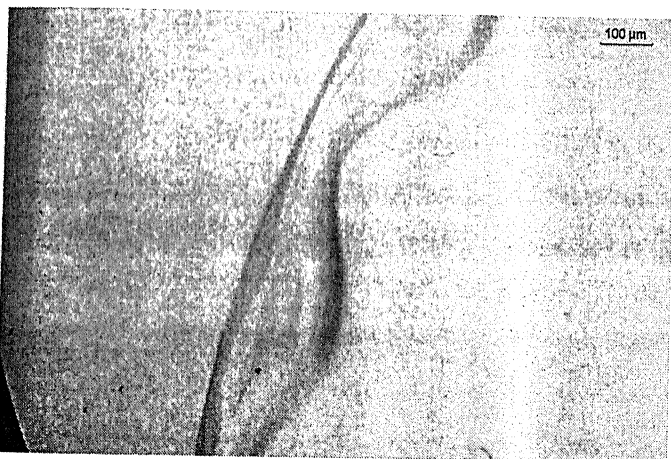


**Figure 3.13 b), c) Digital image of drop covered with lid with a hole at its center. Drop volume  $2\mu\text{l}$ , drop diameter  $3.4\text{mm}$ , temperature of evaporation  $27^\circ\text{C}$ . The hole diameter of the lid is b)  $8\text{mm}$  and c)  $10\text{mm}$**

The profile plots are to the right of the image. The profile plots are the light intensities (gray level). From the profile it can be inferred that the solute is aggregating at the periphery as we increase the hole diameter of the lid. The image covers the periphery and the inside of the drop area.

Fig 3.13 a) - c) shows the experimental results, along with the gray scale profile. In Fig 3.13 a,ii) image of the center of the drop has been showed in order to confirm that whether there are some pattern formation of the polymer at the center of the drop due to the effect of localized evaporation. By observing the images of the Fig 3.13 a,ii), we can

conclude that the polymer is distributed uniformly within the drop area, as we confine the area of evaporation.

From the profile it is very clear that when the evaporation is taking place from the center, i.e. the hole diameter of the lid is very small as compared to the diameter of the drop, then the deposit of the polymer within the drop area is uniform. As we increase the hole diameter of the lid the ring structure starts appearing as, more and more drop area is exposed to atmosphere for evaporation. In Fig 3.13 a), where the hole diameter is small as compared to the diameter of the drop, the deposit of solute is quite uniform. As the hole diameter of the lid becomes comparable to the diameter of the drop, the solute starts depositing on the periphery as is evident from the gray scale profiles. This can be seen in Fig 3.13 b), c) where the lid hole diameter are 8 and 10 mm respectively. In Fig 3.13 c) where the lid hole diameter is 10mm, we noticed the pronounced ring of the solute at the periphery, common to the case when the drop evaporates under open atmosphere. In this case the lid has no influence on the pattern of the deposited solute, because the drop diameter is approximately 3.4mm smaller than the lid diameter i.e. 10mm. We present a suitable mechanism which describes the above phenomenon. Refer to Fig 3.14.

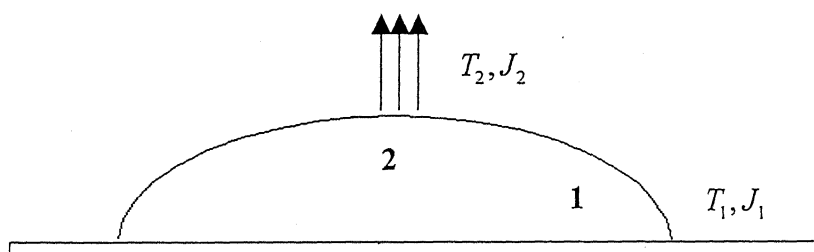


**Figure 3.14 Schematic illustration of evaporation from the center of the drop. Point 1 depicts the edge and point 2 depicts the center of the drop.  $T, J$  are the temperature at the point and the evaporative flux from that point respectively.**

Evaporation is restricted to point 2, shown in Fig 3.14, as the drop is covered with a lid with a hole at its center. Now due to evaporation the fluid loss will be higher at point 2 than at point 1 where there is very limited evaporation. The variation of evaporative flux along the surface is shown in Fig 3.14

Evaporation is maximum at point 2 and therefore fluid loss is also higher at point 2 than at point 1. As a result after some time the interface will grow as is shown in Fig 3.15



**Figure 3.15 Schematic of the interface after some time. The solid line shows that the due to higher rate the interface will depressed at the center, but due to fluid motion from the edges the spherical shape is maintained shown by the dashed line.**

As shown in the Fig 3.15 the interface will get depressed at the center after some time due to higher evaporation rate, but the surface tension of the interface demands that spherical shape of the drop is maintained, so the fluid will flow from the edges towards the center. This is one of the factors that drive the fluid from the edges to the center of the drop.

Second effect, which plays an important role, is the Temperature driven Marangoni flow of fluid. As has been stated earlier evaporation is higher at the center i.e. point 2 than at point 1, thus  $J_2$  is higher than  $J_1$ , as a result  $T_2$  will be lower than  $T_1$  due to adiabatic cooling of the surface as a result of evaporation. Now we know that as temperature increases surface tension ( $\gamma$ ) decreases, therefore  $\gamma_2$  will be higher than  $\gamma_1$ . Fluid has a tendency to flow from regions low surface tension to regions of higher surface tension, which we call as Marangoni flow. Since  $\gamma_2$  is higher than  $\gamma_1$ , fluid will flow from point 1 to point 2 i.e. from the edges to the center.

Thus there are two fluid flow mechanism when evaporation is taking place from the center of the drop, first fluid motion is due to the distortion of the interface which pulls

### 3.5 Effect of solvent on the final pattern formation of the redistributed polymer, when the solvent drop evaporates from the surface of the dissolving substrate

In this section we have looked into the problem of solvents effects on the final pattern formation. The system of study remains the same as earlier i.e a drop of solvent is placed on the polymer film of PMMA which is spin casted onto a clean glass slide. The volume of the drop was 2 $\mu$ l. The polymer film thickness is around 360nm. In the study we have used four different solvents. The solvents and some of its properties have been listed in the following table.

Table 1.

Solvent	Vapor Pressure(Pa) @25°C	B.P (°C)	Density (g/ml) @30°C	Viscosity (Centistokes) @30°C
Dichloromethane	$5.6 \times 10^4$	39.75	1.317 (@25°C)	0.44(@20°C)
Chloroform	$2.57 \times 10^4$	61.15	1.4706	0.514
Ethyl Acetate	$1.24 \times 10^4$	77.11	0.88851	0.400
Toluene	$4.27 \times 10^3$	110.62	0.85769	0.526

From the vapor pressure data we can say that the order of volatility of the solvents from more volatile to less volatile is Dichloromethane > Chloroform > Ethyl Acetate > Toluene. The more is the volatility of the solvent the higher shall be the rate of evaporation of the drop, lowering the time scale within which the polymer dissolves in the polymer. As explained in chapter 2 that the rate of evaporation is higher at the edge (periphery) of the drop than at the center of the drop. Due to higher volatility the rate of evaporation shall be enhanced thereby leading to the higher rate of depletion of fluid from the edge of the drop. This effect shall draw in fluid from the bulk at a much higher rate in case of a volatile solvent as compared to a less volatile solvent. Now as the rate of the fluid flow increases from bulk to the edge, the Kinetic energy of the fluid front increases thereby making it more viable to the instability. Before analyzing the effect of

solvent on the final pattern of the polymer a brief discussion on the solubility of polymer is presented.

### 3.5.1 Solubility of polymer in solvent

The solubility of various polymers in various solvents is largely determined by its chemical structure. As a rule structural similarity favors solubility. In terms of the above mentioned facts this means that the solubility of a given polymer in a given solvent is favored if the solubility parameter of the polymer and the solvent are equal. Besides the chemical structure, also the physical state of a polymer is important for its solubility properties. Crystalline polymers are relatively insoluble and often dissolves at temperatures slightly below their crystalline melting point. As a general rule the solubility decreases as the molecular mass of the solute increases. In 1936 Hildebrand proposed the square root of the cohesive energy density as a parameter identifying the behavior of specific solvents. In 1949 he proposed the term solubility parameter and the symbol  $\delta$ .

The cohesive energy  $E_{coh}$  of a substance in a condensed state is defined as the increase in the internal energy  $U$  per mole of substance if all the intermolecular forces are eliminated.

$$\text{The cohesive energy} \equiv E_{coh} = \Delta U \quad (\text{dimensions: J/mol})$$

$$\text{Cohesive energy density } e_{coh} = \frac{E_{coh}}{V} \quad (\text{at 298 K}) \quad (\text{dimensions: J/cm}^3)$$

$V$  = specific volume

$$\text{And solubility parameter } \delta = \left( \frac{E_{coh}}{V} \right)^{1/2} = e_{coh}^{1/2} \quad (\text{at 298 K}) \quad (\text{dimensions: J}^{1/2}/\text{cm}^{3/2})$$

The thermodynamic criteria of solubility are based on the free energy of mixing  $\Delta G_M$ .

Two substance are mutually soluble if  $\Delta G_M$  value is negative. By defination

$$\delta(\text{J}^{1/2}/\text{cm}^{3/2}) \quad \Delta G_M = \Delta H_M - T\Delta S_M$$



where

$\Delta H_M$  = enthalpy of mixing.

$\Delta G_M$  = entropy of mixing.

As  $\Delta S_M$  is generally positive, there is a certain limiting positive value of  $\Delta H_M$  below which dissolution is possible. According to Hildebrand, the enthalpy of mixing can be calculated by

$$\Delta h_M = \phi_1 \phi_2 (\delta_1 - \delta_2)^2$$

where

$\Delta h_M$  = enthalpy of mixing per unit volume.

$\phi_1$  and  $\phi_2$  = volume fractions of component 1 and 2.

$\delta_1$  and  $\delta_2$  = solubility of components 1 and 2.

From the above equations,  $\Delta h_M = 0$ , if  $\delta_1 = \delta_2$ , so that two substance with equal solubility parameters should be mutually soluble due to negative entropy factor. As a difference between  $\delta_1$  and  $\delta_2$  increases the tendency towards dissolution decreases.

Therefore as a requirement for the solubility of a polymer P in solvent S, the quantity  $(\delta_p - \delta_s)^2$  has to be small, as small as possible. The solubility interaction parameter of the polymer used and the solvent is presented in Table 2.

Table 2.

Polymer	$\delta(J^{1/2} / cm^{3/2})$
PMMA	18.6 – 26.2

Solvents	$\delta(J^{1/2} / cm^{3/2})$
Dichloromethane	19.9
Chloroform	18.9-19
Ethyl Acetate	18.6
Toluene	18.2-18.3

Table 3. shows the parameter of solubility  $(\delta_p - \delta_s)^2$  of PMMA with different solvents.

Table 3.

Polymer (PMMA)	$(\delta_p - \delta_s)^2$
Dichloromethane	1.69
Chloroform	0.09
Ethyl Acetate	0
Toluene	0.16

From Table 3. It is clear that PMMA is most compatible with Ethyl Acetate. The decreasing order of solubility of PMMA in solvents are Ethyl Acetate > Chloroform > Toluene > Dichloromethane. Thus for a given time scale within which the drop will evaporate from the polymer surface Ethyl Acetate will dissolve the maximum amount of PMMA and Dichloromethane will dissolve the minimum amount of PMMA.

Fig 3.16 shows the digital image of the final pattern of the redistributed polymer, when the drop of different solvents are put on the polymer film and allowed to evaporate.

a)

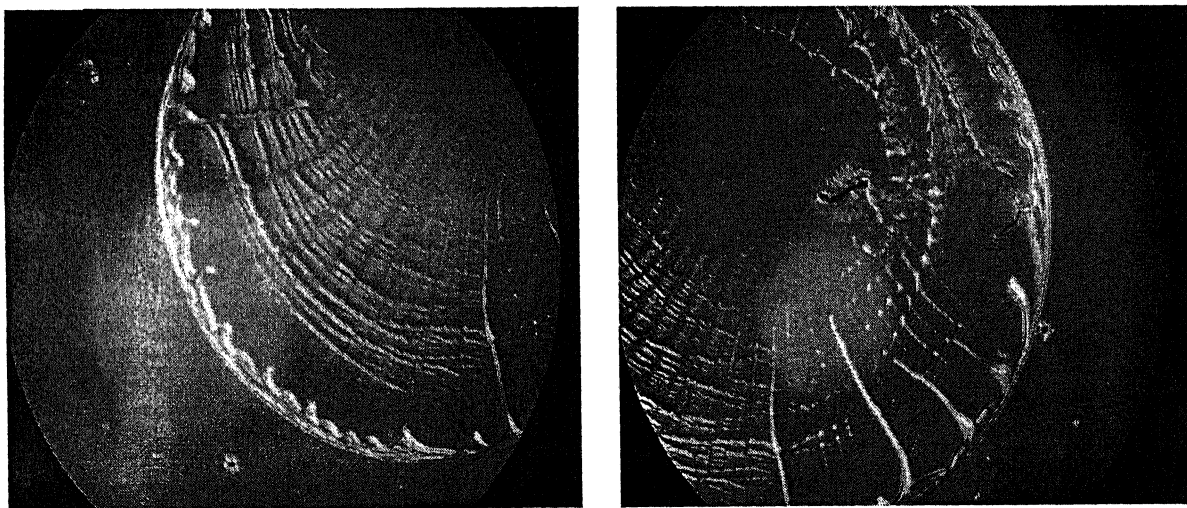


Figure 3.16 a) Digital image of the final pattern of solute when a 2µl drop of Ethyl Acetate evaporates from the surface of the PMMA film. Film thickness is 360nm approximately. Drop was evaporated under ambient condition of 27 °C. Magnification of image is 50x.

b)

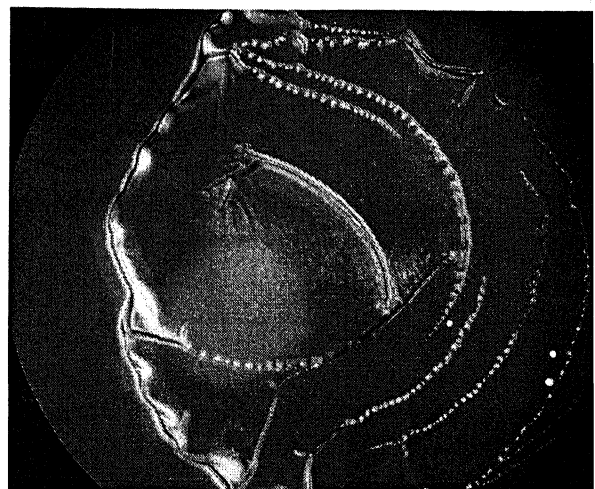
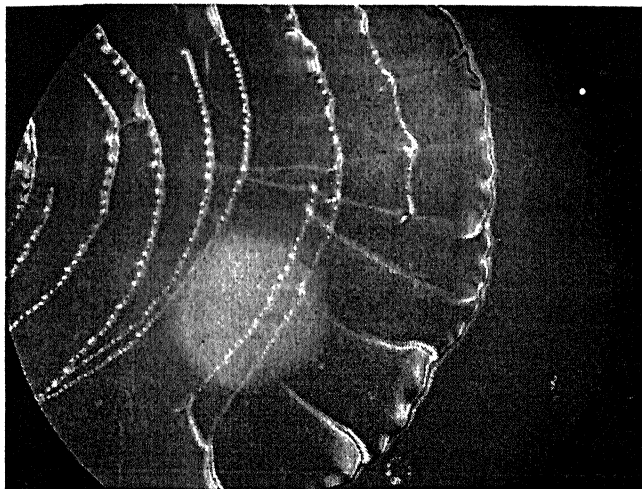


Figure 3.16 b) Digital image of the final pattern of solute when a 2 $\mu$ l drop of Chloroform evaporates from the surface of the PMMA film. Film thickness is 360nm approximately. Drop was evaporated under ambient condition of 27 °C. Magnification of image is 50x.

c)

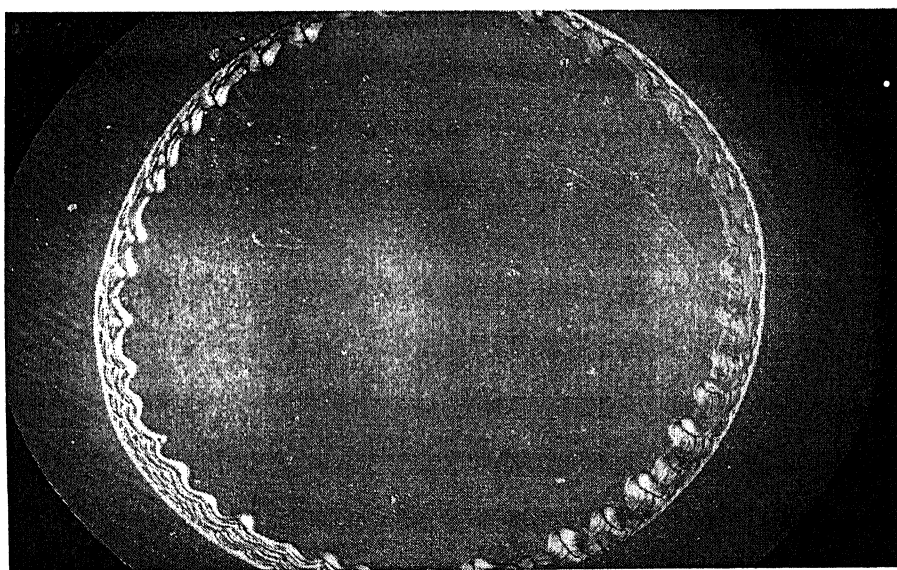


Figure 3.16 c) Digital image of the final pattern of solute when a 2 $\mu$ l drop of Toluene evaporates from the surface of the PMMA film. Film thickness is 360nm approximately. Drop was evaporated under ambient condition of 27 °C. Magnification of image is 50x.

d)

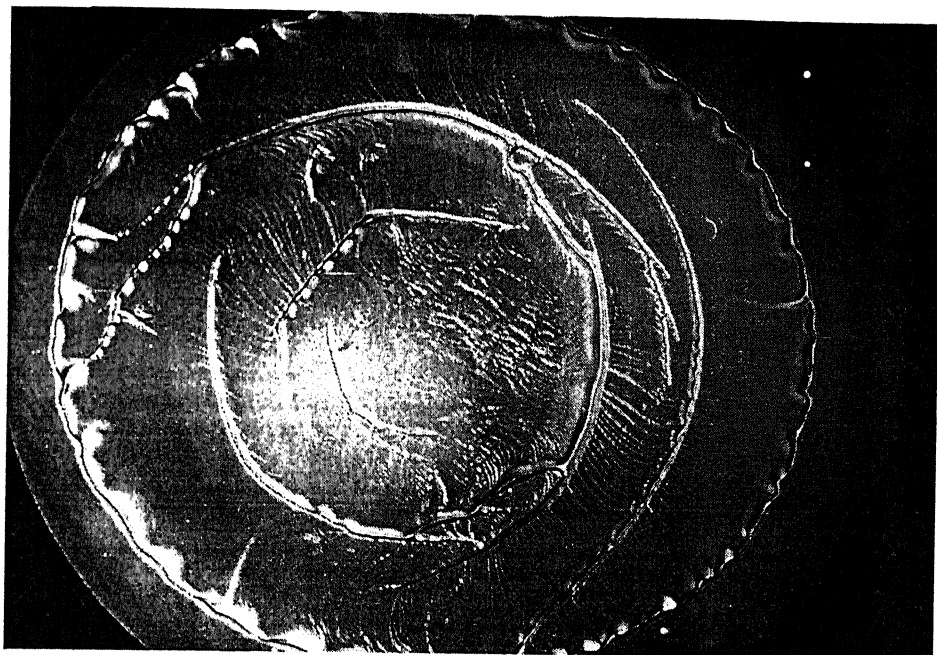


Figure 3.16 d) Digital image of the final pattern of solute when a 2 $\mu$ l drop of Dichloromethane evaporates from the surface of the PMMA film. Film thickness is 360nm approximately. Drop was evaporated under ambient condition of 27 °C. Magnification of image is 50x

Fig 3.16 a) – d) shows the image of the final pattern when the drops of different solvents evaporates from the polymer film. The decreasing orders of volatility of the solvents are.

Dichloromethane > Chloroform > Ethyl Acetate > Toluene.

And the decreasing order of solubility of PMMA in the solvents are

Ethyl Acetate > Chloroform > Toluene > Dichloromethane

That means that Dichloromethane is the most volatile solvent among the one used, and the solubility of PMMA is maximum in Ethyl Acetate and minimum in Dichloromethane

From the Fig 3.16 a) – d) it is observed that with increasing solubility of the PMMA in the solvent the number of concentric rings within the drop also increases, indicating the repeatability of pinning and depinning process. This is quite evident from the images in Fig 3.16 a) – d) where pattern formed due to the evaporation of different solvents is shown. PMMA has maximum solubility in ethyl acetate followed by chloroform, toluene and dichloromethane. Now as the solubility of the polymer in a solvent decreases the number of concentric rings also decreases, which is evident from

the images in Fig 3.16 a) through c) for the case of ethyl acetate, chloroform, and toluene respectively. It is also observed that instability of contact line increases with decreasing solubility of the polymer in the solvent drop. This may be due to the reason, that with decreasing solubility of the polymer in the solvent, the polymer suspension formed is less dense and more easily takes the form of instability ( i.e. undulation pattern). The denser suspension of polymer resists taking the form of instability.

From Fig 3.16 c) we observe that when a drop of toluene evaporates, the concentric rings are restricted to the drop edge in the form of a band, and within the drop area the distribution of polymer is quite smooth. As we compare the pattern formed when the drop of toluene evaporates and when a drop of dichloromethane evaporates ( Fig 3.16 c) and d) respectively), we observe that although the solubility of PMMA is higher in toluene as compared to dichloromethane, the number of concentric rings within the drop area is higher in the case of dichloromethane, where as in the case of toluene there are no concentric rings within the drop area. This observation goes against our previous understanding, where we said that with decreasing solubility of the polymer in the solvent the number of concentric rings within the drop area decreases. This contradiction may arise due to the fact, that in the volatility series dichloromethane is most volatile and toluene is the least volatile solvent used. The number of undulations indicating the instability of the contact line also decreases for the case of dichloromethane Fig 3.16d) as compared to toluene Fig 3.16 c). We have measured the number of undulations in the outer most ring of the final pattern for a specific length in the case of toluene and dichloromethane.

# Number of undulations is 6 for a length of  $1119.6\mu\text{m}$  along the outermost ring in the case of toluene .

# Number of undulations is 3 for a length of  $1119.8\mu\text{m}$  along the outermost ring in the case of dichloromethane.

Fig 3.17 shows the image where we had measured the number of undulations for the case of toluene and dichloromethane respectively.

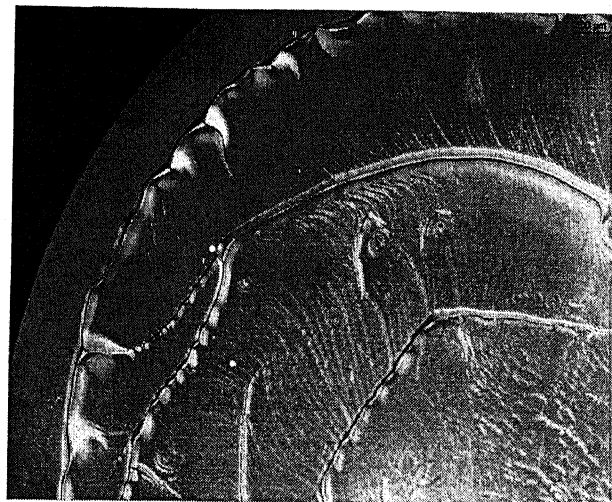
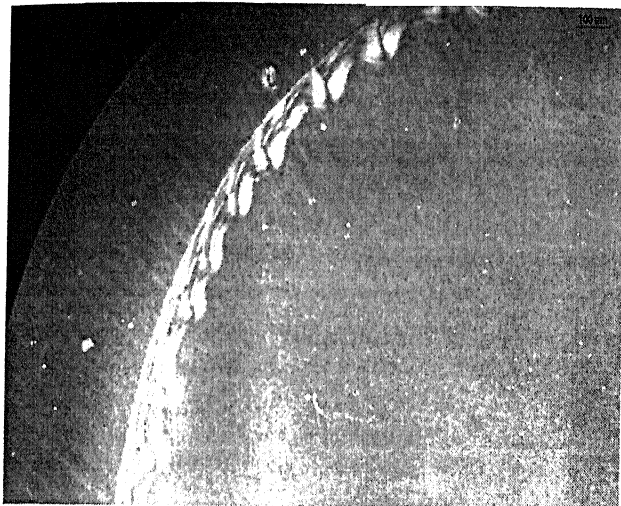


**Fig 3.17 Image showing the measured length along the outer ring for the case of a) toluene b) dichloromethane. The magnification of the image is 50x.**

Now with increasing solubility of the polymer in the solvent the gap between the concentric rings within the drop area decreases, suggesting that the distance the contact line travels between depinning and subsequent pinning is minimum when the solubility of polymer is more.

Fig 3.18 presents the images and the distance between the consecutive concentric rings, for the different cases of solvent drops.

a)

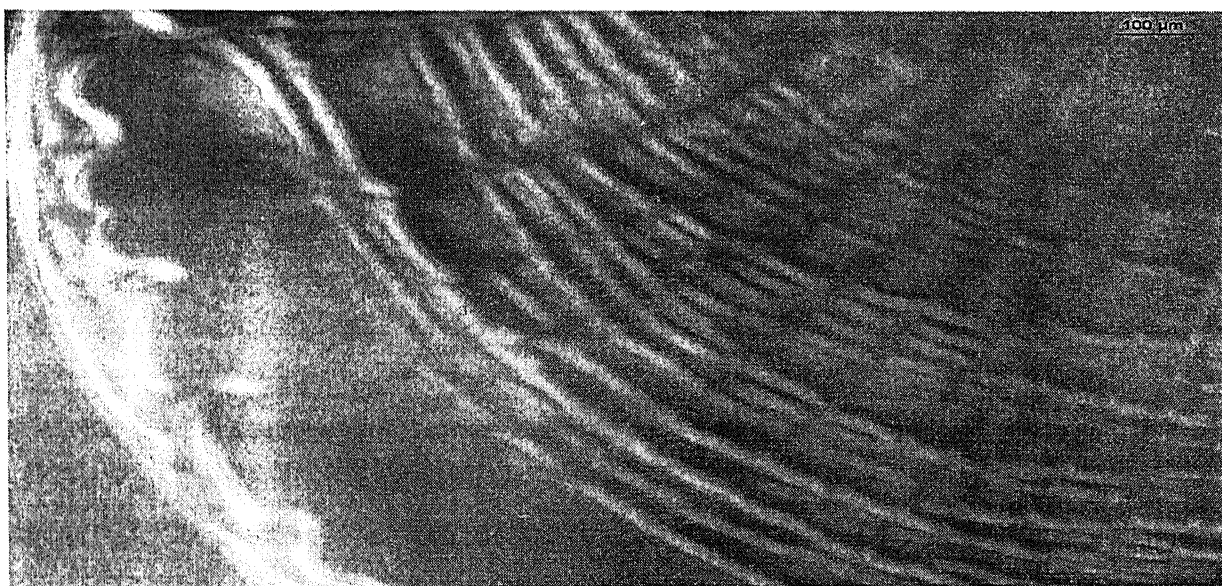


**Fig 3.18 a) image of final pattern when a drop of ethyl acetate evaporates, showing the distance between the concentric rings, magnification is 50x**





**Fig 3.18 b) image of final pattern when a drop of chloroform evaporates, showing the distance between the concentric rings, magnification is 50x**

c)

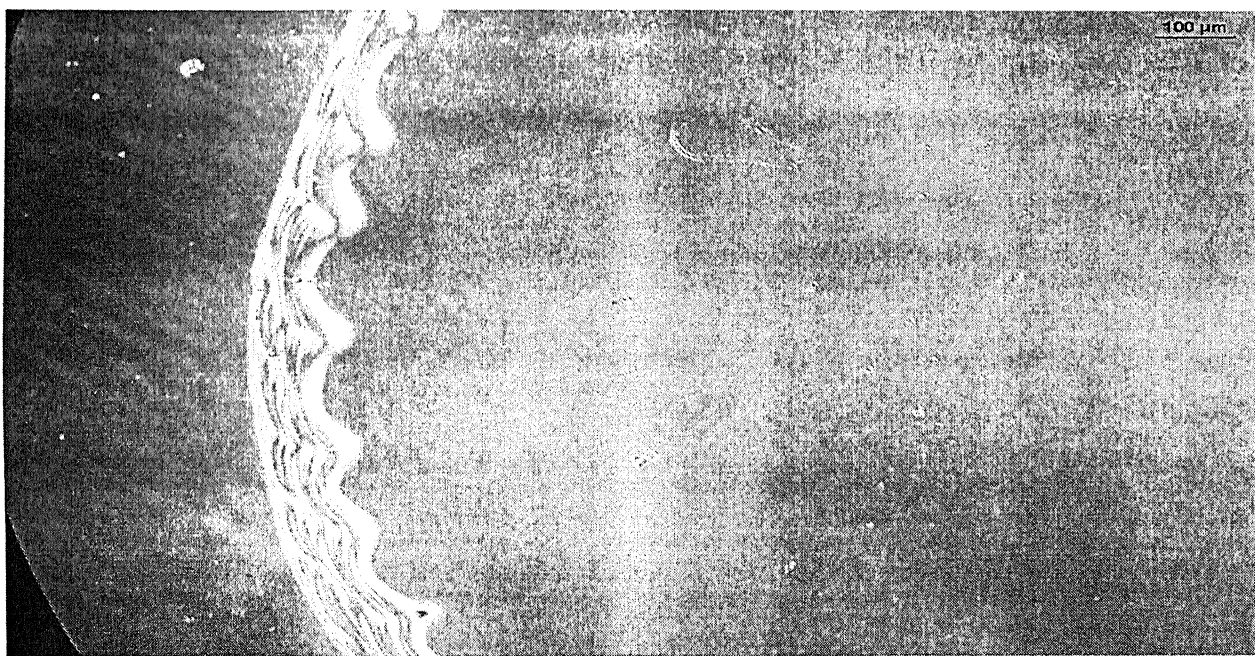


**Fig 3.18 c) image of final pattern when a drop of toluene evaporates, showing the distance between the concentric rings, magnification is 50x**

d)

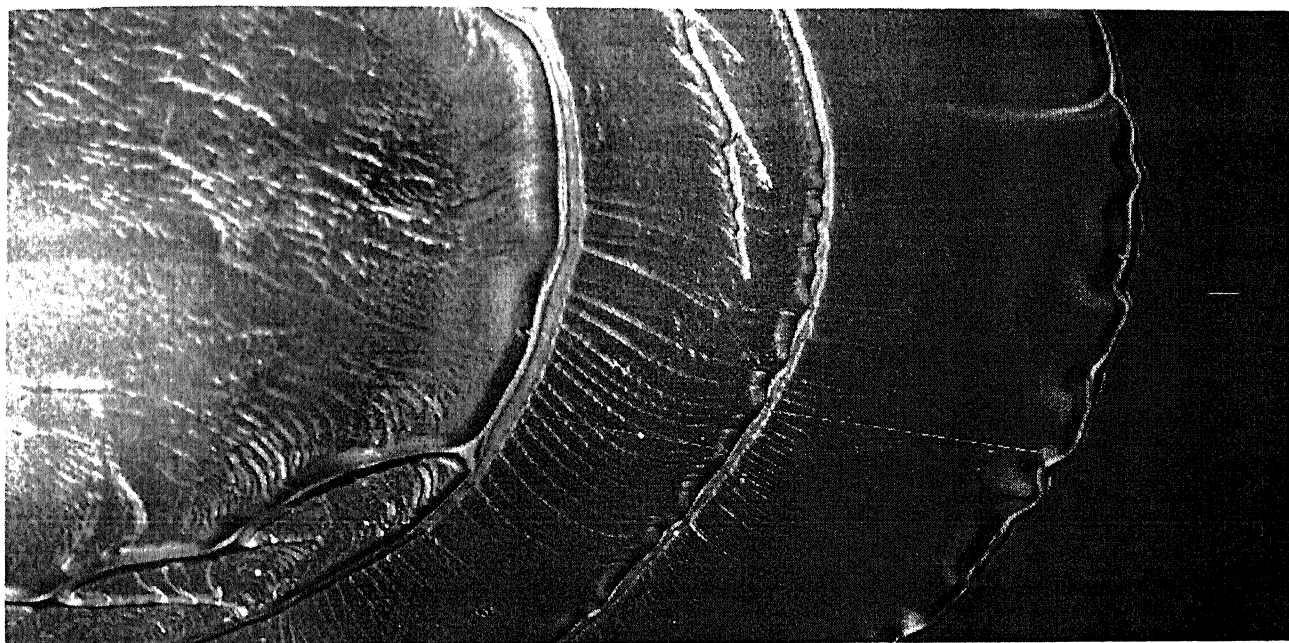


Fig 3.18 d) image of final pattern when a drop of dichloromethane evaporates, showing the distance between the concentric rings, magnification is 50x

The distance of the numbered line in Fig 3.18 a) – d) is presented as under.

Figure 3.18 a)

Object	Distance( $\mu\text{m}$ )
1	34.38
2	33.05
3	56.88
4	40.58
5	41.41
6	27.89
7	15.99
8	32.82
9	35.75
10	31.18
11	19.88
12	21.97
13	17.80
14	16.85
15	21.01
16	18.93
17	21.97

For the case of ethyl acetate the number of undulations is 8 for a specific length of 1125.74 $\mu\text{m}$ , along the outer ring.



**Figure 3.18 b)**

Object	Distance
--------	----------

1	725.14
---	--------

2	80.44
---	-------

3	361.40
---	--------

4	69.23
---	-------

5	59.71
---	-------

For the case of chloroform the number of undulations is 6 for a specific length of 1127.4 $\mu$ m, along the outer ring

**Figure 3.18 c)**

Object	Distance
--------	----------

1	14.78
---	-------

2	8.87
---	------

3	20.69
---	-------

4	13.30
---	-------

For the case of toluene the number of undulations is 7 for a specific length of 1126.8  $\mu$ m, along the outer ring.

**Figure 3.18 d)**

Object	Distance
--------	----------

1	362.95
---	--------

2	258.11
---	--------

3	102.44
---	--------

For the case of dichloromethane the number of undulations is 6 for a specific length of 1127.6  $\mu$ m, along the outer ring.

The above data verify that with increasing solubility the distance between the concentric rings decreases. The number of undulations in along the outer ring is also given alongside the data.

The above observations can be explained as follows. In sec 3.2.1 we had stated that the depinning of contact line depends upon the balance of forces at the three phase contact line. Depinning occurs when the force pulling the contact line increases, as the contact angle ( $\theta_c$ ) decreases. Now if the suspension of the polymer is thick (highly dense) which is due to higher solubility, than the contact lien resists the inward pulling force and the distance traveled by the contact line between depinning and subsequent

pinning is less. Now the density of the polymer suspension in the drop of solvent can be increased by two methods.

- i) Polymer is highly soluble in the solvent.
- ii) If the polymer solubility in the solvent is moderate and the drop of solvent spends enough time on top of the substrate.

The above two points help in explaining our observations. Now the solubility of PMMA in ethyl acetate is higher than chloroform, which in turn is higher than toluene. Thus the suspension of polymer formed in the case of ethyl acetate drop is quite thick as compared to chloroform, followed by toluene for a given time scale. Therefore in the case of ethyl acetate (Fig 3.16 a)) the distance moved by the contact line between depinning and subsequent pinning is low, and the concentric rings are more closely spaced, where as the spacing of the concentric ring increases in the case of chloroform (Fig 3.16 b)) and for toluene the rings are restricted near the periphery in the form of a band.

Since dichloromethane is more volatile than toluene, the time scale for the evaporation of the drop is low for dichloromethane as compared to toluene. Thus in case of dichloromethane the solution formed is less dense as compared to the one formed with toluene and therefore the distance traveled by the contact line between depinning and subsequent pinning is larger in the case of dichloromethane as compared to toluene.

## **3.6 Results and Discussions**

### **3.6.1 Pattern formed by an evaporating droplet on a Dissolving substrate**

The system of drop evaporation from a Dissolving substrate is a very interesting phenomenon. The final pattern is similar to the pattern when the solution drop evaporates on a non-dissolving substrate, though much more complicated kinetic phenomenon are involved in this problem. In this type of system different competing kinetics comes into play. First being the evaporation of the fluid from the drop, which involves mass transfer across the system. Second is the dissolution kinetics of the substrate in the drop fluid, which involves mass transfer within the system. Third is the temperature driven Marangoni flow that pulls the fluid from inside the bulk to the interface, fourth is the advection of the fluid from the bulk to the three phase contact line due to the differential rate of evaporation at the drop edge and at the center of the drop. The final pattern of the redistributed solute formed after the evaporation of the liquid is the result of the above major competing kinetics. The present system of study comprises of a dissolving substrate, which is polymeric film that is spin casted on to a glass slide. The polymer solution was prepared by dissolving 6wt% of PMMA (M.wt 1,20,000) in HPLC grade Toluene. The polymer solution is then spin coated on clean glass slides at a speed of around 1830 rpm. The thickness of the polymeric film is around 360nm. In this case the drop of liquid is a pure solvent of the polymeric film.

With time the fluid evaporates from the interface of the drop, and at the same time the polymer film is dissolving in the drop. When a drop of liquid (which is a solvent for the polymer) on a polymer film the drop spreads, due to the positive spreading coefficient of the solvent on the polymer. The balance of the forces and contact angle restricts the spreading of the drop to a certain contact angle. Once the drop stops spreading the three phase contact line is pinned. The pinning of the contact line is due to the physical heterogeneity of the polymer film. When the drop of pure solvent is placed on the polymer film, it spreads upto the maximum diameter as governed by the balance of

the forces at the three phase contact line. After maximum spreading the contact line gets pinned. At the bottom layer, the solvent dissolves the polymer, and forms a solution which gets pinned there by pinning of the contact line, and solidifies to form the initial ring. This process is very fast as the thickness of the liquid film at the contact line is very small, and therefore the emulsion in this part freezes out to form the initial ring. This ring provides the initial anchoring of the contact line. As has been discussed in Sec.2.2, in an evaporating drop the rate of evaporation is higher at the contact line than at the bulk. This leads to the flow of fluid from the bulk to the contact line. The liquid front at the periphery experiences Rayleigh like instability and takes the undulating form. The contact line then depins and retracts and experiences a similar instability. The thickness of the fluid film is small near the three phase contact line and thus the undulated pattern caused by the instability gets freeze down. The regular striation observed in the band of ring is due to the depinning of the contact line, and the ridges observed in the same figure is due to the undulations of the contact line, which gets freeze out due to presence of polymer in the emulsion at the three phase contact line.

Fig 3.5 chapter 3, shows the stages in the development of the final pattern as the drop evaporates from the dissolving substrate. The images are shown at different times until the final pattern is formed. In the case of drop evaporation two fluid motions are taking place. First is the motion of fluid from the bulk of the drop to the periphery, due to the differential rate of evaporation at the periphery and the bulk. Second is the retracting of the contact line due to depinning. The first fluid motion brings the polymer from the bulk of the drop to the three phase contact line, and deposits it there, and the second fluid motion deposits the polymer in a regular striated pattern as observed.

The image sequence of Fig 3.5 chapter 3, verifies that the regular striation and the ridge observed in Fig 3.4 is due to the instability of the fluid edge which is coming from the bulk to the periphery. It is noticed that the outer boundary of the ring is smooth, and only the inner boundary is wavy. The following phenomenon is behind this discrepancy. When a drop is placed on the polymer film, the bottom layer the fluid dissolves the polymer, and since the film thickness is very small at the boundary (i.e. near the three phase contact line) the fluid evaporates instantaneously freezing the pattern. This may be the sort of initial demarcation. Since the volume of fluid present in the outermost boundary is

very small, the emulsion form is very thick, as a result it does not experiences the instability. Now the wavy nature of the inner boundary is due the instability of the fluid edge( front) which is coming from the bulk to the periphery, where the amount of fluid is higher and the emulsion is quite thin as a result the fluid edge experiences the instability. The image sequences of Fig 3.5 chapter3, suggest a similar phenomenon. Finally in the last stage, i.e. in the inner layer, due to the force constraints the contact line cannot depin any more, and the undulations grow into large shapes, and gets freezed up as the solvent evaporates, The remaining fluid on the surface which contain very low per cent of polymer (or no polymer, we can't say for sure as we could not measure the polymer concentration on film surface) evaporates out.

Thus the governing mechanism is the self-pinning of the contact line due to which the final redistributed pattern is formed. Because of higher rate of evaporation at the edge of the drop as compared to the bulk, bringing draws the fluid to the edge of the drop, there by bringing the dissolved solute to the edge of the drop. The dissolved polymer gets solidified at the edge, due to evaporation of the solvent. The striated pattern and the undulations observed in the final pattern is due to the depinning and subsequent pinning of the contact line and the rayleigh like instability of the fluid front coming from the bulk respectively.

### **3.6.2 Study of Pendant drop evaporating from a dissolving substrate**

The effect of pendant drop configuration affects the final redistributed pattern of the polymer, when the pendant drop evaporates from a dissolving substrate. The dissolving substrate is a PMMA film (Mwt. 1,20,000) of thickness 360nm approximately. The pendant drop volume is 2 $\mu$ l, and the initial drop diameter is 3.4mm approximately.

From image of the final pattern of the solute in the case of pendant drop configuration depinning of the contact line is clearly visible. Fig 3.20 shows the comparative image of the final pattern in the case of a sessile and a pendant drop. In both the cases the initial

drop volume is  $2\mu\text{l}$  of solvent. The drops were evaporated in an ambient condition at a temperature of  $27^\circ\text{C}$ .

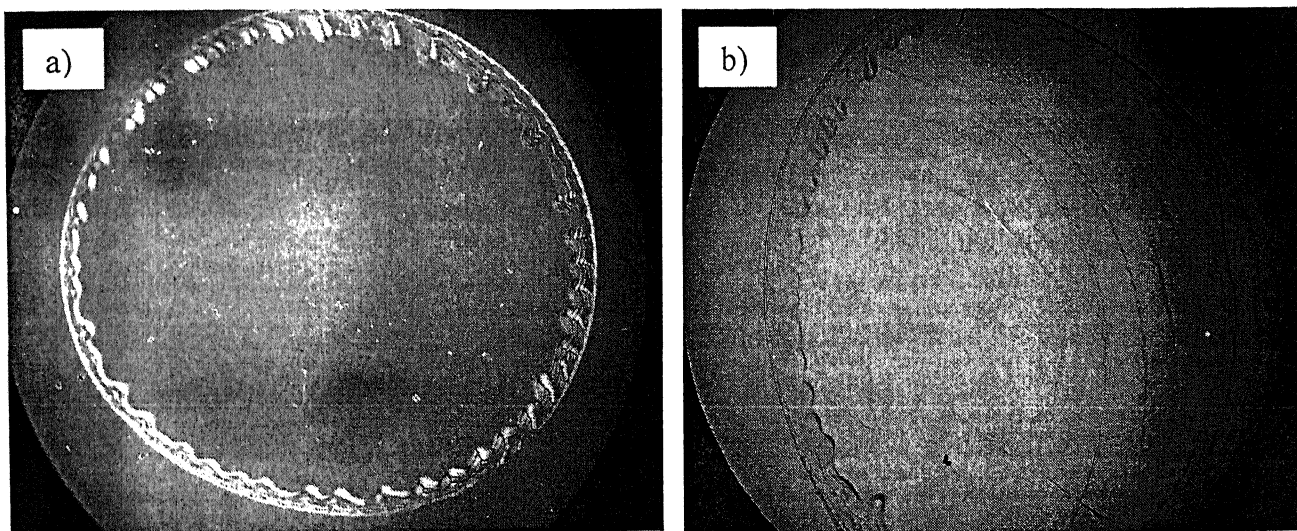


**Fig 3.19 Images of the final pattern formed when a) sessile and b) pendant drops evaporate from the surface of a dissolving substrate. The initial drop volume is same in both the cases i.e.  $2\mu\text{l}$ . The drop was evaporated under ambient condition of  $27^\circ\text{C}$ .**

From Fig 3.19 a) – b) clearly shows that in case of pendant drop pinning and deppining of the contact line is very predominant. The initial band of striated rings near the periphery of the drop is common in both the cases. The only difference is the formation of concentric rings in the case of pendant drop. We try to describe the above-observed phenomenon as follows.

In the case of pendant drop the gravity has an opposing influence as compared to the sessile drop. In the case of sessile drop the drop sits on top of the substrate and the gravity has the role of pinning, where as in the case of pendant drop, the gravity pulls the liquid down and this has a depinning effect.

Due to this effect we observe concentric rings with large spacing between them in the case of pendant drop as compared to the sessile drop, where there are few concentric rings in the form of a band near the periphery of the drop. Fig 3.21 shows the images of the sessile and the pendant drop which were used to measure the spacing between the concentric rings in both the cases.

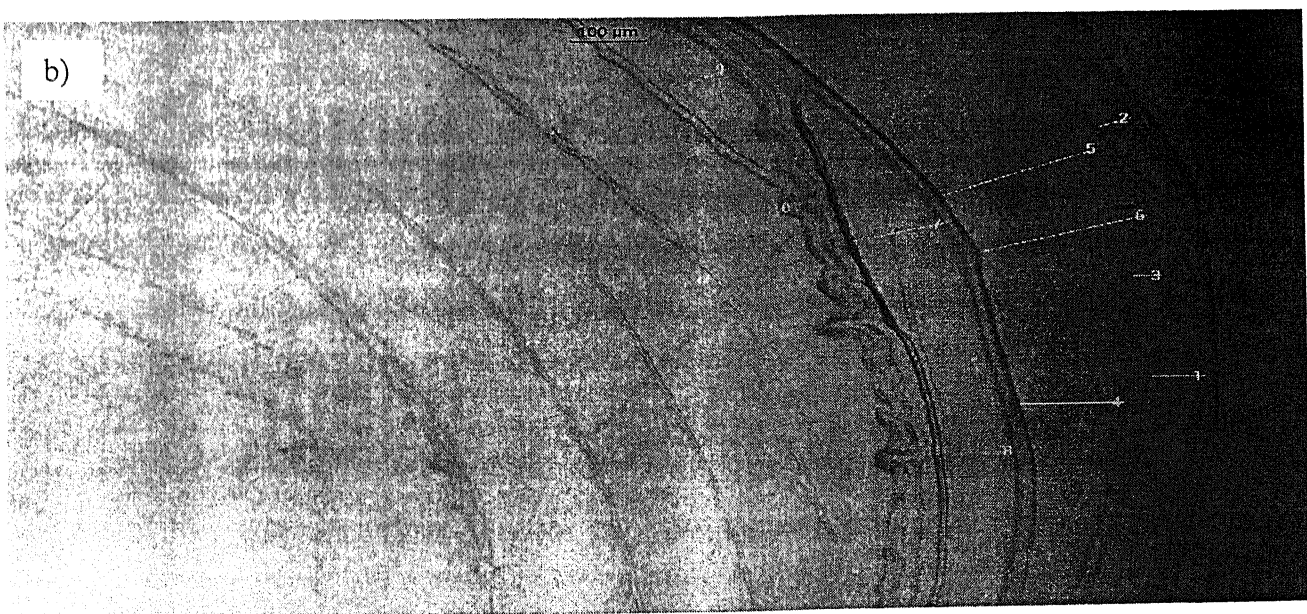
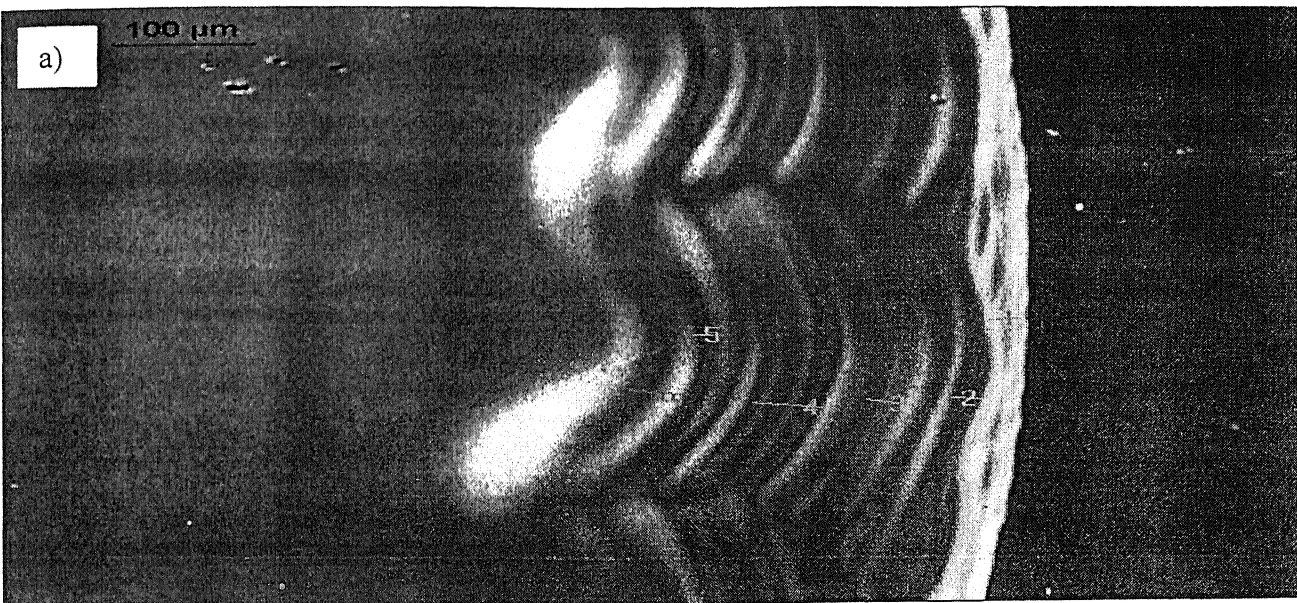


Figure 3.20 images of the final pattern formed when a) sessile magnification 100x. b) Pendant drop magnification 50x. The images show the distance measured between the concentric rings.

The marked distances shown in Fig 3.21 is presented below.

a) for sessile drop

Object	Distance ( $\mu\text{m}$ )
1	25.17
2	23.69
3	33.05
4	53.72
5	25.13
6	40.34

b) for pendant drop

Object	Distance( $\mu\text{m}$ )
1	67.99
2	45.84
3	38.43
4	133.02
5	218.52
6	225.81
7	124.06
8	93.11
9	89.29
10	133.52
11	117.22
12	125.73
13	161.40
14	113.35
15	75.44
16	42.96
17	103.22
18	175.04

Now as stated in sec 3.2.1 depinning occurs due to misbalance of forces at the contact line. The inward force pulling the contact line  $\gamma_l \cos \theta$  increases with decreasing contact angle  $\theta_c$ . For the sessile drop the inward force pulls the contact line where as the gravity has a stabilizing effect therefore the contact line retracts a very small distance and again gets pinned by the solute deposition, refer to data for Fig 3.20 a) for the distance moved by the contact line after depinning. This is the reason, why the contact line forms a concentric striated pattern confined to the periphery of the drop edge in the form of a band. In the case of the pendant drop in addition to the inward force  $\gamma_l \cos \theta$  at the



contact line, the gravity is also pulling the contact line. The force which the contact line in the case of pendant drop, is much stronger than the force, which pulls the contact, line in the case of a sessile drop. Therefore the contact line moves a greater distance between depinning and subsequent pinning in the case of a pendant drop.

Thus we can say that gravity favors pinning in the case of sessile drop and it favors depinning in the case of pendant drop.

### **3.6.3 Effect of localized evaporation on the transfer of solute in an evaporating drop**

The system of study comprises of a clean glass slide covered with a covering lid, with a hole in the center of the lid. The diameter of the hole of the covering lid is kept small as compared to the diameter of the drop. Theoretically if we increase the hole diameter of the lid, then evaporation takes place from the edges of the drop, and if we have hole diameter larger than the diameter of the drop then we should get back the ring pattern. In our experiments we got the results as has been predicted by the theory. We used fixed volume of drop i.e. 2 $\mu$ l, with the initial drop diameter 3.4mm. The hole diameter of the lid was varied from 0.5, 1.0, 2.0, 3.0, 4.0, 6.0, 8.0, 10.0 mm. In the first case the hole in the lid is very small as compared to the drop, and in the final case the hole is large compared to the drop diameter, replicating the ambient condition.

Thus there are two fluid flow mechanism when evaporation is taking place from the center of the drop, first fluid motion is due to the distortion of the interface which pulls the fluid from the edge to the center, and the second is the temperature driven Marangoni flow, which also drives the fluid from edge to the center. These two fluid flows makes the solution in the drop to remain in the center, and so when the solvent evaporates the solute is uniformly distributed throughout the drop, rather than the ring structure which is primarily due to the fluid motion from the center of the drop to the edge (periphery) of the drop. However pinning of the contact line is always there.

### 3.6.4 Effect of solvent on the final pattern formation of the redistributed polymer

The system of study remains the same as earlier i.e a drop of solvent is placed on the polymer film of PMMA which is spin casted onto a clean glass slide. The volume of the drop was 2 $\mu$ l. The polymer film thickness is around 360nm. In the study we have used four different solvents. From the vapor pressure data order of volatility of the solvents is Dichloromethane > Chloroform > Ethyl Acetate > Toluene.

On the basis on polymer (PMMA) solvent interaction parameter the decreasing order of solubility of PMMA in solvents are Ethyl Acetate > Chloroform > Toluene > Dichloromethane.

That means that Dichloromethane is the most volatile solvent among the one used, and the solubility of PMMA is maximum in Ethyl Acetate and minimum in Dichloromethane. It is observed that with increasing solubility of the PMMA in the solvent the number of concentric rings within the drop also increases, indicating the repeatability of pinning and depinning process. PMMA has maximum solubility in ethyl acetate followed by chloroform, toluene and dichloromethane. Now as the solubility of the polymer in a solvent decreases the number of concentric rings also decreases. It is also observed that instability of contact line increases with decreasing solubility of the polymer in the solvent drop. This may be due to the reason, that with decreasing solubility of the polymer in the solvent, the polymer suspension formed is less dense and more easily takes the form of instability ( i.e. undulation pattern). The denser suspension of polymer resists taking the form of instability.

As we compare the pattern formed when the drop of toluene evaporates and when a drop of dichloromethane evaporates we observe that although the solubility of PMMA is higher in toluene as compared to dichloromethane, the number of concentric rings within the drop area is higher in the case of dichloromethane, where as in the case of toluene there are no concentric rings within the drop area. This observation goes against our previous understanding, where we said that with decreasing solubility of the polymer in the solvent the number of concentric rings within the drop area decreases. This

contradiction may arise due to the fact, that in the volatility series dichloromethane is most volatile and toluene is the least volatile solvent used. The number of undulations indicating the instability of the contact line also decreases for the case of dichloromethane. We have measured the number of undulations in the outer most ring of the final pattern for a specific length in the case of toluene and dichloromethane.

# Number of undulations is 6 for a length of  $1119.6\mu\text{m}$  along the outermost ring in the case of toluene .

# Number of undulations is 3 for a length of  $1119.8\mu\text{m}$  along the outermost ring in the case of dichloromethane.

Fig 3.23 shows the image where we had measured the number of undulations for the case of toluene and dichloromethane respectively.

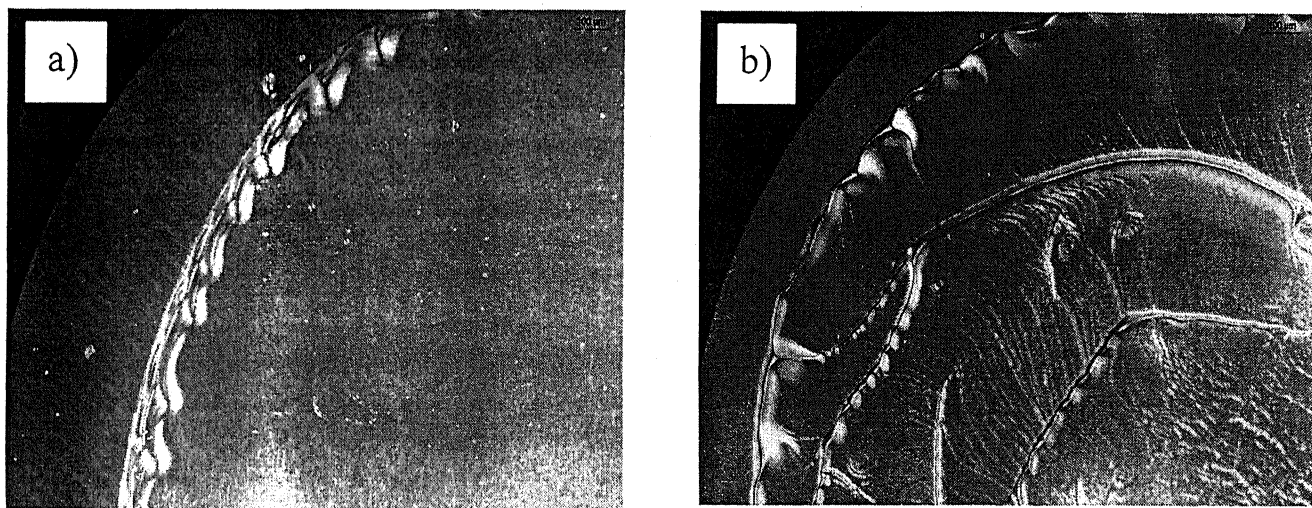


**Fig 3.21 Image showing the measured length along the outer ring for the case of a) toluene b) dichloromethane. The magnification of the image is 50x.**

Now with increasing solubility of the polymer in the solvent the gap between the concentric rings within the drop area decreases, suggesting that the distance the contact

line travels between depinning and subsequent pinning is minimum when the solubility of polymer is more.

Fig 3.24 presents the images and the distance between the consecutive concentric rings, for the different cases of solvent drops.

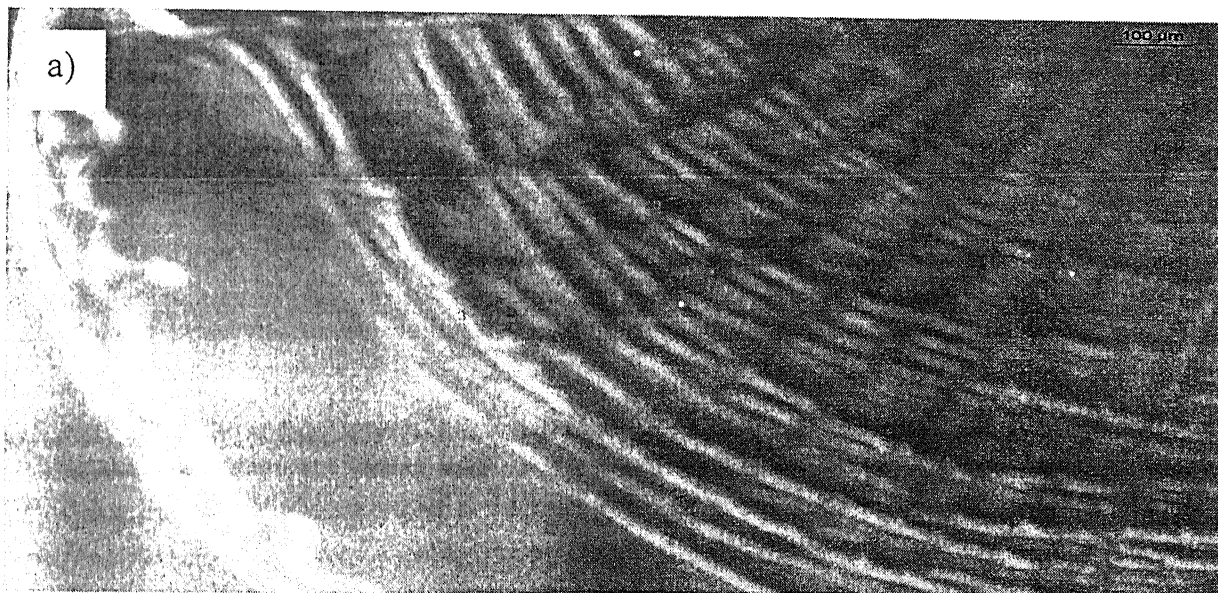


**Fig 3.22 a) image of final pattern when a drop of ethyl acetate evaporates, showing the distance between the concentric rings, magnification is 50x**



**Fig 3.22 b) image of final pattern when a drop of chloroform evaporates, showing the distance between the concentric rings, magnification is 50x**

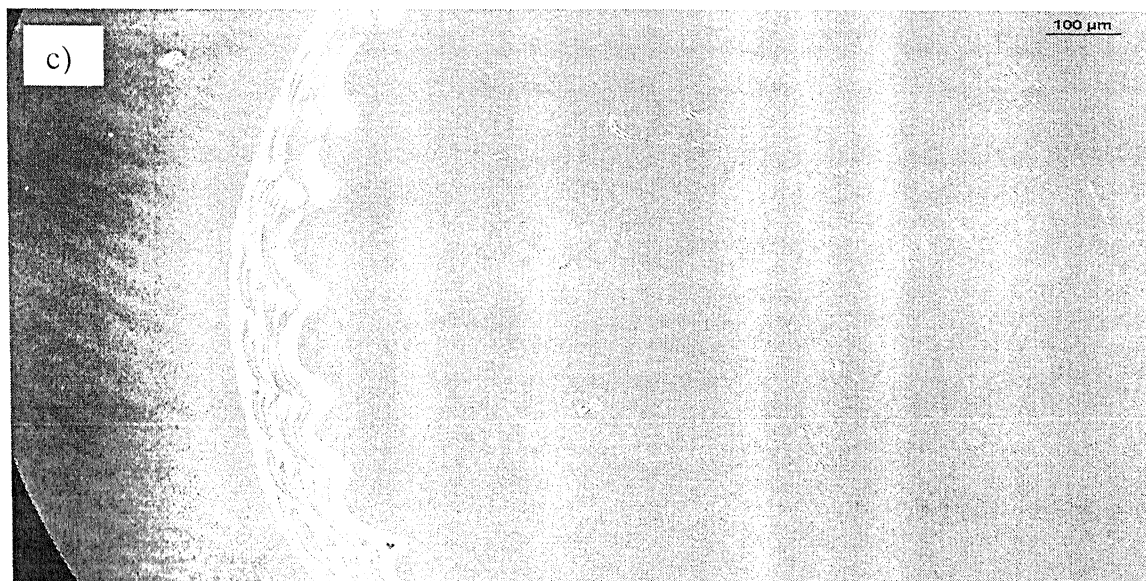


Fig 3.22 c) image of final pattern when a drop of toluene evaporates, showing the distance between the concentric rings, magnification is 50x

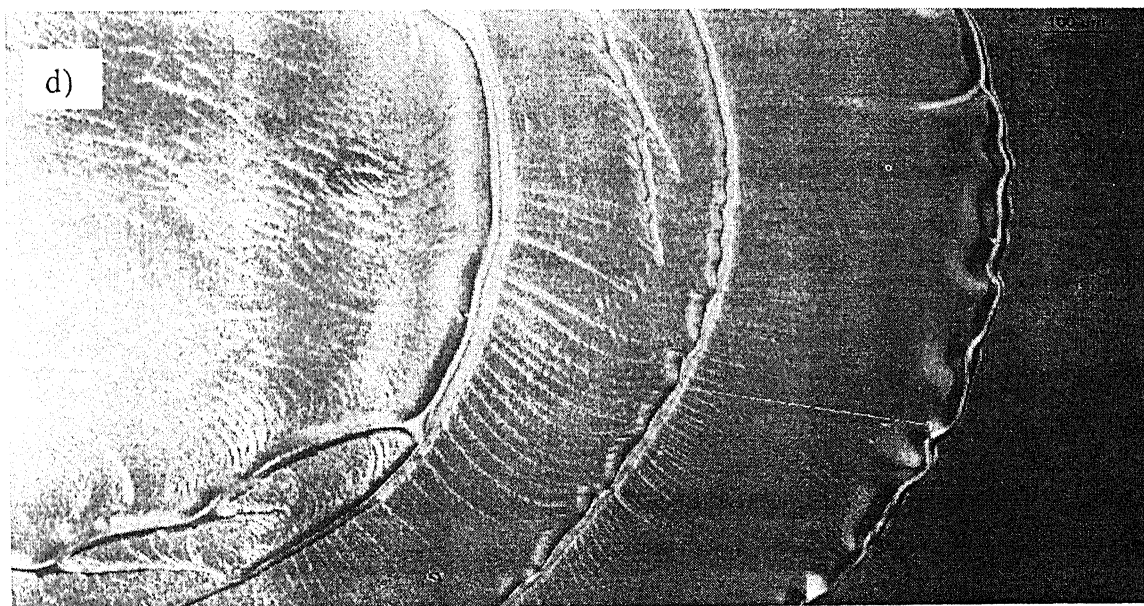


Fig 3.22 d) image of final pattern when a drop of dichloromethane evaporates, showing the distance between the concentric rings, magnification is 50x

The distance of the numbered line in Fig 3.22 a) – d) is presented as under.

**Figure 3.22 a)**

Object	Distance( $\mu\text{m}$ )	For the case of ethyl acetate the number of undulations is 8 for a specific length of 1125.74 $\mu\text{m}$ , along the outer ring.
1	34.38	
2	33.05	
3	56.88	
4	40.58	
5	41.41	
6	27.89	
7	15.99	
8	32.82	
9	35.75	
10	31.18	
11	19.88	
12	21.97	
13	17.80	
14	16.85	
15	21.01	
16	18.93	
17	21.97	

**Figure 3.22 b)**

Object	Distance( $\mu\text{m}$ )	For the case of chloroform the number of undulations is 6 for a specific length of 1127.4 $\mu\text{m}$ , along the outer ring
1	725.14	
2	80.44	
3	361.40	
4	69.23	
5	59.71	

**Figure 3.22 c)**

Object	Distance( $\mu\text{m}$ )	For the case of toluene the number of undulations is 7 for a specific length of 1126.8 $\mu\text{m}$ , along the outer ring.
1	14.78	
2	8.87	
3	20.69	
4	13.30	



**Figure 3.22 d)**

Object	Distance ( $\mu\text{m}$ )	
1	362.95	For the case of dichloromethane the number of undulations is
2	258.11	6 for a specific length of 1127.6 $\mu\text{m}$ , along the outer ring.
3	102.44	

The above data verify that with increasing solubility the distance between the concentric rings decreases. The number of undulations in along the outer ring is also given alongside the data.

The above observations can be explained as follows. In sec 3.2.1 we had stated that the depinning of contact line depends upon the balance of forces at the three phase contact line. Depinning occurs when the force pulling the contact line increases, as the contact angle ( $\theta_c$ ) decreases. Now if the suspension of the polymer is thick (highly dense) which is due to higher solubility, than the contact line resists the inward pulling force and the distance traveled by the contact line between depinning and subsequent pinning is less. Now the density of the of the polymer suspension in the drop of solvent can be increased by two methods.

- i) Polymer is highly soluble in the solvent.
- ii) If the polymer solubility in the solvent is moderate and the drop of solvent spends enough time on top of the substrate.

The above two points help in explaining our observations. Now the solubility of PMMA in ethyl acetate is higher than chloroform, which in turn is higher than toluene. Thus the suspension of polymer formed in the case of ethyl acetate drop is quite thick as compared to chloroform, followed by toluene for a given time scale. Therefore in the case of ethyl acetate the distance moved by the contact line between depinning and subsequent pinning is low, and the concentric rings are more closely spaced, where as the spacing of the concentric ring increases in the case of chloroform and for toluene the rings are restricted near the periphery in the form of a band.

Since dichloromethane is more volatile than toluene, the time scale for the evaporation of the drop is low for dichloromethane as compared to toluene. Thus in case

of dichloromethane the solution formed is less dense as compared to the one formed with toluene and therefore the distance traveled by the contact line between depinning and subsequent pinning is larger in the case of dichloromethane as compared to toluene.



## Conclusions

The formation of nanostructures is an emerging field of interest and calls in the attention of researchers from diverse background. Polymeric films have been chosen for study because of some inherent qualities of Polymeric films such as polymers are easy to handle, they are available in a wide variety having different characteristic properties like photoluminescence, fluorescence, electrical conductivity etc. Polymers are soluble in a variety of organic solvents, to form homogeneous solutions. In the present work an attempt has been made to qualitatively study the final patterns formed by an evaporating droplet on a Dissolving substrate. In the beginning we described the predominant mechanism of solute transfer in an evaporating drop of fluid, containing dissolved solute, taking a base case where a drop of polymer solution evaporates from the surface of a clean glass slide. Similar works has already been done, but our aim was to compare our results with the published work, in order to bring out a suitable mechanism.

After figuring out a suitable mechanism for solute transfer in an evaporating drop, an attempt was made to qualitatively understand the problem when a fluid drop evaporates from the surface of a dissolving substrate. The problem is typical in a sense that many competing mechanism plays their role in the formation of the final pattern of the redistributed solute. Analysis was based on the final pattern of the redistributed polymer, after the drop evaporates from the surface of the dissolving substrate. Experimental conditions were altered like, area exposed to evaporation, configuration of the drop (pendant drop), and the effect of solvent, to see their influence on the pattern formed by an evaporating drop on a dissolving substrate. We could qualitatively figure out the parameters, which controlled the transfer of solute in the present problem to the three phase contact line. The mechanism of solute transfer to the three phase contact line in an evaporating drop presents a simple yet effective method to from microstructures. The method of putting the liquid is very flexible since liquid can be drawn in any shape. We think that suitable alteration and proper control of physical and environmental conditions can lead to harnessing this method effectively to create microwells, microchannels and channels of any shape.

# Bibliography

- [1] P. G. de Gennes, Rev. Mod. Phys. **57**, 827(1985).
- [2] E. L. Decker and S. Garoff, Langmuir **13**, 6321 (1997).
- [3] R. D. Deegan, O. Bakajin, T. F. Dupont, G. Huber, S. R. Nagel, and T. A. Witten, Phys. Rev. E. **62**, 756(2000).
- [4] R. D. Deegan, Phys. Rev. E. **61**, 475(2000).
- [5] V. X. Nguyen, K. J. Stebe, Phys. Rev. Lett. **88**(16),164501/**88**(16)/164504 (2002).
- [6] T. Ondarchuhu and C. Joachim, Europhys. Lett. **42**, 215 (1998).
- [7] J. Boneberg, F. Burmeister, C. Shäfle, P. Leiderer, D.Reim, A. Fery, and S. Herminghaus, Langmuir **13**, 7080 (1997).
- [8] M. Srinivasarao, D. Collings, A. Phillips, S. Patel, Science **292**, 79 (2001).
- [9] N. maruyama, O. Karthaus, K. Ijio, M. Shimomura, T. Koito, S. Nishimura, T. Sawadaishi, N. Nishi and S. Tokura, Supramolecular Science **5**, Number 3-4, 331(1998).
- [10] T. cuk, S.M. Troian, C.M. hong and S. Wagner, applied phys. Lett.**77**, 2063(2000).
- [11] R.D. Deegan, O. Bakajin, T.F. Dupont, g. Huber, S.R. Nagel and T.A. Witten, Nature **389**, 827(1997).
- [12] G.D. Nadkarni and S. Garoff, Europhys. Lett. **20**, 523(1992).
- [13] “ Properties of Polymer” by D.W. Van Krevelen, Third edition, ELSEVIER.